



**WICHITA STATE  
UNIVERSITY**

**UNIVERSITY LIBRARIES**

**Operational usage and flight loads analysis  
of three king air models used as lead planes**

Item Type	Thesis
Authors	Menon, Alok N.
Publisher	Wichita State University
Rights	Copyright 2015 Alok Nath Menon
Download date	2026-05-21 01:03:18
Link to Item	<a href="http://hdl.handle.net/10057/11640">http://hdl.handle.net/10057/11640</a>

**OPERATIONAL USAGE AND FLIGHT LOADS ANALYSIS OF THREE  
KING AIR MODELS USED AS LEAD PLANES**

A Thesis by

Alok Nath Menon

Bachelor of Science, Embry-Riddle Aeronautical University, 2009

Submitted to the Department of Aerospace Engineering  
and the faculty of the Graduate School of  
Wichita State University  
in the partial fulfillment of  
the requirements for the degree of  
Master of Science

May 2015

©Copyright 2015 by Alok Nath Menon

All Rights Reserved

## OPERATIONAL USAGE AND FLIGHT LOADS ANALYSIS OF THREE KING AIR MODELS USED AS LEAD PLANES

The following faculty members have examined the final copy of this thesis for form and content, and recommend that it be accepted in partial fulfillment of the requirement for the degree of Master of Science, with a major in Aerospace Engineering.

---

Dr. Kamran Rokhsaz, Committee Chair

---

Dr. Linda Kliment, Committee Member

---

Dr. Alexander Bukhgeym, Committee Member

## ABSTRACT

Flight data from three models of the Beechcraft King Air aircraft has been used to perform operational usage and flight loads analysis. These aircraft have been flown mostly as lead planes during the 2009 through 2013 fire seasons accumulating 3094 useful flights from 4074 flight files. These flights account for nearly 5772 hours in flight time. The results have been presented in two forms; 1) for overall flights and 2) for six specific flight phases. The information in the overall section have been further split into Firefighting/Ferry and Extreme Attitude flights. The usage results presented include information about the maximum MSL altitudes, maximum indicated airspeeds, pitch and roll angles, and load factors presented in the form of V-n diagrams. In some cases, the maximum indicated airspeed is shown to be in excess of the published limits, but within 10% of the limit. In the case of one model, the vertical load factors have been shown to be larger than the operational limits.

The flight loads, due to gust and maneuver, and discrete gust velocities, have been presented in the form of exceedance charts, normalized in per 1000 hours and per nautical mile. The flight loads and discrete gust velocities have been shown to correlate better with AGL than MSL altitudes. The loads and the discrete gust velocities from Firefighting and Extreme Attitude flights have been demonstrated to have higher frequencies of occurrence compared to Ferry flights. The highest frequencies of occurrences of gust and maneuver loads and discrete gust velocities have been shown to be associated with the Lead phase, and the lowest with the Entry phase.

These aircraft were not designed for firefighting missions but now fly in a unique operating environment. Because of the mission-specific performance demands, the operators, manufacturers, and the regulators could use the statistical data from this investigation to understand their impact on the fatigue life of the aircraft.

## TABLE OF CONTENTS

Chapter	Page
1. INTRODUCTION . . . . .	1
1.1 Background . . . . .	1
1.2 Thesis Structure . . . . .	3
2. METHOD OF ANALYSIS . . . . .	4
2.1 Aircraft Description . . . . .	4
2.2 Recorded Data . . . . .	4
2.3 Derived and Added Parameters . . . . .	10
2.4 Takeoff and Landing Identification . . . . .	11
2.5 Flight Distance and Time . . . . .	13
2.6 Stall speed . . . . .	14
2.7 Aircraft Lift Curve Slope . . . . .	14
2.8 Derived Gust Velocity . . . . .	15
2.9 Mission Identification . . . . .	16
2.10 Phase Separation . . . . .	19
2.11 Loads Counting . . . . .	21
2.12 Altitude Bands . . . . .	22
3. RESULTS AND DISCUSSION - AIRCRAFT USAGE . . . . .	23
3.1 Overall Flight - Extreme Attitude . . . . .	24
3.2 Overall Flight - Firefighting/ Ferry . . . . .	28
3.3 Phase-Specific Results . . . . .	41
4. RESULTS AND DISCUSSION - AIRCRAFT LOADS . . . . .	67
4.1 Overall Results . . . . .	67
4.2 Phase-Specific Results . . . . .	86
5. CONCLUSION . . . . .	112
BIBLIOGRAPHY . . . . .	114
APPENDICES . . . . .	117

## LIST OF TABLES

<b>Table</b>		<b>Page</b>
2.1	Beechcraft King Air C90 Specifications . . . . .	4
2.2	Recorded and Derived Parameters . . . . .	5
2.3	Summary of Files Provided . . . . .	6
2.4	Summary of Files with Repeated Lines . . . . .	6
2.5	Summary of Files with Noisy Airspeed . . . . .	7
2.6	Summary of Files with Noisy Normal Acceleration . . . . .	7
2.7	Summary of Files with Aircraft Never Leaving the Ground . . . . .	8
2.8	Summary of Files with no Takeoff and Landings Identified . . . . .	8
2.9	Summary of Files with Incomplete Flight Data . . . . .	9
2.10	Summary of Files with Ground Phases . . . . .	9
2.11	Summary of Files without Ground Phases . . . . .	10
2.12	Squat Switch Availability in Files . . . . .	12
2.13	Squat-Switch-based Takeoff and Landing Criterion . . . . .	12
2.14	Known and Derived King Air C90 Parameters . . . . .	15
2.15	Summary of Lift Curve Slope . . . . .	15
2.16	Load Limits and Deadband . . . . .	21
2.17	Altitude Bands . . . . .	22
3.1	King Air Models Used for Analysis . . . . .	23
3.2	Files Containing Extreme Attitudes . . . . .	24
3.3	Summary of Pitch and Roll Angles for Extreme Attitude Flights . . . . .	26
3.4	Limit Load Factors for C90A, C90GT, and E90 . . . . .	35

## LIST OF TABLES (continued)

<b>Table</b>	<b>Page</b>
3.5 Summary of Pitch and Roll Angles . . . . .	38
3.6 Maximum and Minimum Pitch and Roll Angles for the Cruise-1 Phase . . . . .	44
3.7 Maximum and Minimum Pitch and Roll Angles for the Cruise-1 Phase . . . . .	44
3.8 Cruise Phase Distance and Duration . . . . .	47
3.9 Maximum and Minimum Pitch and Roll Angles for the Turns Phase . . . . .	51
3.10 Turns Phase Duration and Distance . . . . .	52
3.11 Entry Phase Duration and Distance . . . . .	55
3.12 Maximum and Minimum Pitch and Roll Angles for the Entry Phase . . . . .	55
3.13 Lead Phase Duration and Distance . . . . .	60
3.14 Maximum and Minimum Pitch and Roll Angles for the Lead Phase . . . . .	60
3.15 Exit Phase Duration and Distance . . . . .	64
3.16 Maximum and Minimum Pitch and Roll Angles for the Exit Phase . . . . .	64
4.1 Time in Altitude Band for Each Flight Type in Hours . . . . .	70
4.2 Distance Flown in Altitude Band for Each Flight Type in Nautical Miles . . . . .	71
4.3 Time in Altitude Band for Each Phase in Hours . . . . .	87
4.4 Distance Flown in Altitude Band for Each Phase in Nautical Miles . . . . .	87

## LIST OF FIGURES

Figure	Page
2.1 Typical Ferry Flight Profile . . . . .	18
2.2 Flight Profile for Entry, Lead, and Exit (Side View) . . . . .	19
2.3 Segment of Flight with Turns . . . . .	20
2.4 Peak-Valley Identification . . . . .	21
3.1 Maximum MSL Altitude and Coincident Indicated Airspeed for Extreme Attitude Flights . . . . .	25
3.2 Maximum Indicated Airspeed and Coincident MSL Altitude for Extreme Attitude Flights . . . . .	25
3.3 Maximum MSL Altitude and Coincident Indicated Airspeed for Extreme Attitude Flights . . . . .	26
3.4 Maximum Indicated Airspeed and Coincident MSL Altitude for Extreme Attitude Flights . . . . .	27
3.5 $V$ - $n$ Diagram for Extreme Attitude Flights . . . . .	28
3.6 Maximum MSL Altitude and Coincident Indicated Airspeed for Firefighting/-Ferry Flights . . . . .	29
3.7 Maximum MSL Altitude and Coincident Indicated Airspeed for C90A . . . . .	29
3.8 Maximum MSL Altitude and Coincident Indicated Airspeed for C90GT . . . . .	30
3.9 Maximum MSL Altitude and Coincident Indicated Airspeed for E90 . . . . .	30
3.10 Maximum Indicated Airspeed and Corresponding MSL Altitude for Firefighting/Ferry Flights for all Models . . . . .	31
3.11 Maximum Indicated Airspeed and Corresponding MSL Altitude for C90A . . . . .	32
3.12 Maximum Indicated Airspeed and Corresponding MSL Altitude for C90GT . . . . .	32
3.13 Maximum Indicated Airspeed and Corresponding MSL Altitude for E90 . . . . .	33
3.14 Number of Flights by Distance . . . . .	34

## LIST OF FIGURES (continued)

Figure	Page
3.15 Number of Flights by Duration . . . . .	34
3.16 <i>V-n</i> Diagram for King Air C90A . . . . .	36
3.17 <i>V-n</i> Diagram for King Air C90GT . . . . .	36
3.18 <i>V-n</i> Diagram for King Air E90 . . . . .	37
3.19 <i>V-n</i> Diagram for Firefighting/Ferry Flights . . . . .	37
3.20 Cumulative Probability of Pitch Angle for Overall Flights . . . . .	38
3.21 Cumulative Probability of Roll Angle for Overall Flights . . . . .	39
3.22 Maximum and Minimum Pitch Angle for Firefighting/Ferry Flights . . . . .	40
3.23 Maximum and Minimum Roll Angle for Firefighting/Ferry Flights . . . . .	40
3.24 Flight Distance Correlated with Maximum MSL Altitude for Cruise-1 Phase .	42
3.25 Flight Distance Correlated with Maximum MSL Altitude for Cruise-2 Phase .	42
3.26 Maximum Indicated Airspeed Correlated with MSL Altitude for Cruise-1 Phase	43
3.27 Maximum Indicated Airspeed Correlated with MSL Altitude for Cruise-1 Phase	43
3.28 Cumulative Probability of Maximum and Minimum Pitch Angle for Cruise-1 Phase . . . . .	45
3.29 Cumulative Probability of Maximum and Minimum Roll Angle for Cruise-1 Phase	45
3.30 Cumulative Probability of Maximum and Minimum Pitch Angle for Cruise-2 Phase . . . . .	46
3.31 Cumulative Probability of Maximum and Minimum Roll Angle for Cruise-2 Phase	46
3.32 <i>V-n</i> Diagram for Cruise-1 Phase . . . . .	48
3.33 <i>V-n</i> Diagram for Cruise-2 Phase . . . . .	48
3.34 Flight Distance Correlated with Maximum MSL Altitude for Turns Phase . .	50

## LIST OF FIGURES (continued)

Figure	Page
3.35 Maximum Indicated Airspeed Correlated with MSL Altitude for Turns Phase .	50
3.36 Cumulative Probability of Maximum and Minimum Pitch Angle for Turns Phase	51
3.37 Cumulative Probability of Maximum and Minimum Roll Angle for Turns Phase	52
3.38 <i>V-n</i> Diagram for Turns Phase . . . . .	53
3.39 Flight Distance Correlated with Maximum MSL Altitude for Entry Phase . . .	54
3.40 Maximum Indicated Airspeed Correlated with MSL Altitude for Entry Phase .	54
3.41 Cumulative Probability of Maximum and Minimum Pitch Angle for Entry Phase	56
3.42 Cumulative Probability of Maximum and Minimum Roll Angle for Entry Phase	56
3.43 <i>V-n</i> Diagram for Entry Phase . . . . .	57
3.44 Flight Distance Correlated with Maximum MSL Altitude for Lead Phase . . .	58
3.45 Maximum Indicated Airspeed Correlated with MSL Altitude for Lead Phase .	59
3.46 Maximum MSL Altitude correlated with Flight Distance for Lead Phase . . .	59
3.47 Cumulative Probability of Maximum and Minimum Pitch Angle for Lead Phase	61
3.48 Cumulative Probability of Maximum and Minimum Roll Angle for Lead Phase	61
3.49 <i>V-n</i> Diagram for Lead Phase . . . . .	62
3.50 Flight Distance Correlated with Maximum MSL Altitude for Exit Phase . . .	63
3.51 Maximum Indicated Airspeed Correlated with MSL Altitude for Exit Phase .	63
3.52 Cumulative Probability of Maximum and Minimum Pitch Angle for Exit Phase	65
3.53 Cumulative Probability of Maximum and Minimum Roll Angle for Exit Phase	65
3.54 <i>V-n</i> Diagram for Exit Phase . . . . .	66
4.1 Cumulative Occurrences of Incremental Vertical Gust Load Factor per 1000 Hours - Overall (AGL Altitude) . . . . .	68

## LIST OF FIGURES (continued)

Figure	Page
4.2 Cumulative Occurrences of Incremental Vertical Gust Load Factor per 1000 Hours - Overall (MSL Altitude) . . . . .	68
4.3 Cumulative Occurrences of Incremental Vertical Maneuver Load Factor per 1000 Hours - Overall (AGL Altitude) . . . . .	69
4.4 Cumulative Occurrences of Incremental Vertical Maneuver Load Factor per 1000 Hours - Overall (MSL Altitude) . . . . .	69
4.5 Cumulative Occurrences of Incremental Vertical Gust Load Factor per 1000 Hours	72
4.6 Cumulative Occurrences of Incremental Vertical Gust Load Factor per Nautical Mile . . . . .	72
4.7 Cumulative Occurrences of Incremental Vertical Maneuver Load Factor per 1000 Hours . . . . .	73
4.8 Cumulative Occurrences of Incremental Vertical Maneuver Load Factor per Nautical Mile . . . . .	74
4.9 Cumulative Occurrences of Incremental Vertical Gust Load Factor per 1000 Hours - Extreme Attitudes . . . . .	75
4.10 Cumulative Occurrences of Incremental Vertical Gust Load Factor per Nautical Mile - Extreme Attitudes . . . . .	75
4.11 Cumulative Occurrences of Incremental Vertical Gust Load Factor per 1000 Hours - Firefighting . . . . .	76
4.12 Cumulative Occurrences of Incremental Vertical Gust Load Factor per Nautical Mile - Firefighting . . . . .	76
4.13 Cumulative Occurrences of Incremental Vertical Gust Load Factor per 1000 Hours - Ferry . . . . .	77
4.14 Cumulative Occurrences of Incremental Vertical Gust Load Factor per Nautical Mile - Ferry . . . . .	77
4.15 Cumulative Occurrences of Incremental Vertical Maneuver Load Factor per 1000 Hours - Extreme Attitudes . . . . .	78

## LIST OF FIGURES (continued)

Figure	Page
4.16 Cumulative Occurrences of Incremental Vertical Maneuver Load Factor per Nautical Mile - Extreme Attitudes . . . . .	79
4.17 Cumulative Occurrences of Incremental Vertical Maneuver Load Factor per 1000 Hours - Firefighting . . . . .	79
4.18 Cumulative Occurrences of Incremental Vertical Maneuver Load Factor per Nautical Mile - Firefighting . . . . .	80
4.19 Cumulative Occurrences of Incremental Vertical Maneuver Load Factor per 1000 Hours - Ferry . . . . .	80
4.20 Cumulative Occurrences of Incremental Vertical Maneuver Load Factor per Nautical Mile - Ferry . . . . .	81
4.21 Cumulative Occurrences of Derived Gust Velocity per 1000 Hours . . . . .	82
4.22 Cumulative Occurrences of Derived Gust Velocity per Nautical Mile . . . . .	82
4.23 Cumulative Occurrences of Derived Gust Velocity per 1000 Hours - Extreme Attitudes . . . . .	83
4.24 Cumulative Occurrences of Derived Gust Velocity per Nautical Mile - Extreme Attitudes . . . . .	84
4.25 Cumulative Occurrences of Derived Gust Velocity per 1000 Hours - Firefighting	84
4.26 Cumulative Occurrences of Derived Gust Velocity per Nautical Mile - Firefighting	85
4.27 Cumulative Occurrences of Derived Gust Velocity per 1000 Hours - Ferry . . .	85
4.28 Cumulative Occurrences of Derived Gust Velocity per Nautical Mile - Ferry . .	86
4.29 Cumulative Occurrences of Incremental Vertical Gust Load Factor per 1000 Hours - All Phases . . . . .	88
4.30 Cumulative Occurrences of Incremental Vertical Gust Load Factor per Nautical Mile - All Phases . . . . .	89
4.31 Cumulative Occurrences of Incremental Vertical Gust Load Factor per 1000 Hours - Cruise-1 Phase . . . . .	90

## LIST OF FIGURES (continued)

Figure		Page
4.32	Cumulative Occurrences of Incremental Vertical Gust Load Factor per Nautical Mile - Cruise-1 Phase . . . . .	90
4.33	Cumulative Occurrences of Incremental Vertical Gust Load Factor per 1000 Hours - Cruise-2 Phase . . . . .	91
4.34	Cumulative Occurrences of Incremental Vertical Gust Load Factor per Nautical Mile - Cruise-2 Phase . . . . .	91
4.35	Cumulative Occurrences of Incremental Vertical Gust Load Factor per 1000 Hours - Entry Phase . . . . .	92
4.36	Cumulative Occurrences of Incremental Vertical Gust Load Factor per Nautical Mile - Entry Phase . . . . .	92
4.37	Cumulative Occurrences of Incremental Vertical Gust Load Factor per 1000 Hours - Lead Phase . . . . .	93
4.38	Cumulative Occurrences of Incremental Vertical Gust Load Factor per Nautical Mile - Lead Phase . . . . .	93
4.39	Cumulative Occurrences of Incremental Vertical Gust Load Factor per 1000 Hours - Exit Phase . . . . .	94
4.40	Cumulative Occurrences of Incremental Vertical Gust Load Factor per Nautical Mile - Exit Phase . . . . .	94
4.41	Cumulative Occurrences of Incremental Vertical Gust Load Factor per 1000 Hours - Turns Phase . . . . .	95
4.42	Cumulative Occurrences of Incremental Vertical Gust Load Factor per Nautical Mile - Turns Phase . . . . .	95
4.43	Cumulative Occurrences of Incremental Vertical Maneuver Load Factor per 1000 Hours - All Phases . . . . .	96
4.44	Cumulative Occurrences of Incremental Vertical Maneuver Load Factor per Nautical Mile - All Phases . . . . .	97
4.45	Cumulative Occurrences of Incremental Vertical Maneuver Load Factor per 1000 Hours - Cruise-1 Phase . . . . .	98

## LIST OF FIGURES (continued)

Figure	Page
4.46	Cumulative Occurrences of Incremental Vertical Maneuver Load Factor per Nautical Mile - Cruise-1 Phase . . . . . 99
4.47	Cumulative Occurrences of Incremental Vertical Maneuver Load Factor per 1000 Hours - Cruise-2 Phase . . . . . 99
4.48	Cumulative Occurrences of Incremental Vertical Maneuver Load Factor per Nautical Mile - Cruise-2 Phase . . . . . 100
4.49	Cumulative Occurrences of Incremental Vertical Maneuver Load Factor per 1000 Hours - Entry Phase . . . . . 100
4.50	Cumulative Occurrences of Incremental Vertical Maneuver Load Factor per Nautical Mile - Entry Phase . . . . . 101
4.51	Cumulative Occurrences of Incremental Vertical Maneuver Load Factor per 1000 Hours - Lead Phase . . . . . 101
4.52	Cumulative Occurrences of Incremental Vertical Maneuver Load Factor per Nautical Mile - Lead Phase . . . . . 102
4.53	Cumulative Occurrences of Incremental Vertical Maneuver Load Factor per 1000 Hours - Exit Phase . . . . . 102
4.54	Cumulative Occurrences of Incremental Vertical Maneuver Load Factor per Nautical Mile - Exit Phase . . . . . 103
4.55	Cumulative Occurrences of Incremental Vertical Maneuver Load Factor per 1000 Hours - Turns Phase . . . . . 103
4.56	Cumulative Occurrences of Incremental Vertical Maneuver Load Factor per Nautical Mile - Turns Phase . . . . . 104
4.57	Cumulative Occurrences of Incremental Gust Velocity per 1000 Hours - All Phases 105
4.58	Cumulative Occurrences of Incremental Gust Velocity per Nautical Mile - All Phases . . . . . 105
4.59	Cumulative Occurrences of Incremental Gust Velocity per 1000 Hours - Cruise-1 Phase . . . . . 106

**LIST OF FIGURES** (continued)

<b>Figure</b>	<b>Page</b>
4.60 Cumulative Occurrences of Incremental Gust Velocity per Nautical Mile - Cruise-1 Phase . . . . .	106
4.61 Cumulative Occurrences of Incremental Gust Velocity per 1000 Hours - Cruise-2 Phase . . . . .	107
4.62 Cumulative Occurrences of Incremental Gust Velocity per Nautical Mile - Cruise-2 Phase . . . . .	107
4.63 Cumulative Occurrences of Incremental Gust Velocity per 1000 Hours - Entry Phase . . . . .	108
4.64 Cumulative Occurrences of Incremental Gust Velocity per Nautical Mile - Entry Phase . . . . .	108
4.65 Cumulative Occurrences of Incremental Gust Velocity per 1000 Hours - Lead Phase . . . . .	109
4.66 Cumulative Occurrences of Incremental Gust Velocity per Nautical Mile - Lead Phase . . . . .	109
4.67 Cumulative Occurrences of Incremental Gust Velocity per 1000 Hours - Exit Phase . . . . .	110
4.68 Cumulative Occurrences of Incremental Gust Velocity per Nautical Mile - Exit Phase . . . . .	110
4.69 Cumulative Occurrences of Incremental Gust Velocity per 1000 Hours - Turns Phase . . . . .	111
4.70 Cumulative Occurrences of Incremental Gust Velocity per Nautical Mile - Turns Phase . . . . .	111

## NOMENCLATURE

### ACRONYMS

AGL	Above Ground Level
API	Application Programming Interface
ASM	Aerial Supervision Module
ATGS	Air Tactical Group Supervisor
BLM	Bureau of Land Management
CSV	Comma-Separated-Values
DFDR	Digital Flight Data Recorders
FAA	Federal Aviation Administration
FTA	Fire Traffic Area
IAS	Indicated Airspeed
KIAS	Knots Indicated Airspeed
MSL	Mean Sea Level
NED	National Elevation Dataset
OLM	Operational Load Monitoring
ROC	Rate of Climb
UDRI	University of Dayton Research Institute
USFS	United States Forest Service
USGS	United States Geological Survey

### GREEK SYMBOLS

$\Delta\lambda$	Difference in longitude
$\Delta\phi$	Difference in latitude
$\mu$	Non-dimensional mass parameter
$\phi$	Latitude
$\rho$	Air density at altitude

$\rho_0$  Standard sea level air density

## OTHER SYMBOLS

$\bar{C}$  Aircraft response factor

$\Delta n_z$  Incremental normal acceleration

$\Delta t$  Flight Data Sample Time

$g$  Gravitational acceleration

$K_g$  Gust alleviation factor

$R$  Radius of Earth

$t_{land}$  Time at Landing

$t_{takeoff}$  Time at Takeoff

$U_{de}$  Derived Gust Velocity

$V_e$  Equivalent airspeed

$V_{stall_1}$  Stall speed at full flaps and gross weight

$V_{stall}$  Stall speed at full flaps and  $W_2$

$V_{true}$  True Airspeed

$W_2$  Aircraft weight with 30% fuel and two passengers

$W_{30\%Fuel}$  Weight of 30% fuel

$W_{EmptyWeight}$  Empty weight of the aircraft

$W_{GW}$  Total weight of all passengers

$W_{PAX}$  Gross weight of the aircraft

$\bar{c}$  Wing mean geometric chord

$\beta$  Prandtl-Glauret compressibility factor,  $\sqrt{1 - M^2}$

$\frac{\partial \epsilon}{\partial \alpha}$  Derivative of downwash angle with respect to angle of attack

$\lambda$  Taper Ratio

$\Lambda_{c/2}$   $c/2$  Chord Line Sweep

$\Lambda_{LE}$  Leading Edge Sweep

$a_o$  Airfoil lift curve slope

$AR$	Aspect Ratio
$b$	Span
$C_{L\alpha_{HT}}$	Horizontal Tail Lift Curve Slope
$C_{L\alpha_{WB}}$	Wing-Body Lift Curve Slope
$C_{L\alpha}$	Aircraft Lift Curve Slope
$c_{root}$	Root Chord
$c_{tip}$	Tip Chord
$K$	an Emperical Factor
$S$	Planform Area
$S_t$	Horizontal Tail Planform Area
$S_w$	Wing Planform Area

# CHAPTER 1

## INTRODUCTION

### 1.1 Background

Aerial firefighting has been a crucial part of fighting wildfires in the United States for decades. This method is often used to combat large fires or those where land-based firefighting is not possible due to treacherous or unreachable terrain. It is considered as one of the most dangerous flying missions because of the conditions in which they are flown. The dangers associated with aerial firefighting are partly due to the extreme loads experienced by the aircraft structure due to the high temperature, unpredictable flying conditions, and harsh maneuvers conducted because of uneven terrain [1]. It was found in 1974 by NASA [2] and in 1987 by the United States Forest Service [3] that air tankers frequently exceeded the operational limits during these firefighting missions.

After fatal accidents that were caused by mechanical and structural failures during the 2002 fire season, the United States Forest Service (USFS) and Bureau of Land Management (BLM) established an independent commission, the Blue Ribbon Panel, to determine the steps to ensure safety of the aerial firefighting program. The assessment found many reasons for the accidents. The reasons for the catastrophic structural failures were attributed to inadequate inspections to monitor the deterioration, extreme loads experienced by the aircraft atypical of the normal operations for which they were designed, and lack of an “engineering basis” to certify the safety of the aircraft that had been operating under these adverse conditions [4].

To tackle these problems, USFS embarked on an Operational Load Monitoring (OLM) program for the aircraft fleet. In the first phase, heavy air tankers were addressed, as they were the ones that had the most fatalities due to structural failures. It was envisioned that the data from the OLM program would be used to determine a severity factor for each mission flown by an aircraft. Since the maintenance for each part of the aircraft is scheduled usually

based on its accumulated hours, this severity factor would be used to determine “true” hours accumulated by the part. This would result in more frequent maintenance checks to crucial structural components.

In addition, the loads experienced and their occurrences during the flight due to maneuvers and gusts had to be estimated to determine the aircraft gust response. Extensive research was performed by Press et.al. in the 1950s to determine the atmospheric turbulence and gust loads [5][6]. The Federal Aviation Administration (FAA) has also conducted research in the same field because of their involvement in OLM focusing on monitoring life and safety of aging aircraft. To determine the gust velocities from the loads, it was first necessary to separate the flight loads into those due to gust and maneuvers. After some experimentation, the FAA adopted a technique developed by the U.S. Air Force to separate the gust and maneuver loads using durations [7]. Research conducted by Rustenburg et.al. at University of Dayton Research Institute (UDRI) led to using a two-second rule to separate the gust and maneuver loads [8].

This approach was used for the analysis of operational loads on lead aircraft. The lead aircraft were fitted with a recording system and sensors. For the purpose of the analysis, since the aircraft were relatively small compared to large tankers, they were assumed to be rigid bodies. The resulting load counts would be assumed to represent the fatigue spectrum of the whole aircraft. The lead planes have significantly different loading cycles compared to air tankers. While the air tankers are used to conduct, at most two “drop” runs in a single flight, the lead planes are flown in multiple “lead” runs during a single flight, which sometimes lasts as long as two hours. The lead run is conducted at low altitudes close to the fire zone at low speeds, which is followed by the exit phase where the aircraft peels off to give the following tanker space to safely exit the drop zone. This set of phases is repeated multiple times during a single Aerial Supervision Module/Lead (ASM/Lead) mission. In some cases, these low altitude flights are also combined with higher altitude surveillance and communication missions that require the aircraft to be flown in repeated circular patterns.

These missions, typical of a lead aircraft, results in cyclic loading of the airframe more frequently than an air tanker.

The focus of the present research was to use in-flight recorded data to examine the usage of these airframes and to quantify the flight loads experienced by maneuvering the airframes and those due to the atmosphere in which they are flown. The aircraft's acceleration response to a discrete gust was used to predict the gust velocities. The two-second rule was used to separate the gust and maneuver loads. The gust and maneuver load and derived gust velocity exceedance spectra were developed. It is understood that this type of information can be used by the operators, the manufacturers, and the regulatory agencies to better understand the factors that impact fatigue life of aircraft.

## **1.2 Thesis Structure**

Chapter 2 contains the flight data files, the data analysis methods, and the phase separation criterion. Aircraft statistical usage data, which includes those of the overall flight as well as individual phases, are presented in Chapter 3. Chapter 4 is comprised of the aircraft loads data, also shown in terms of the overall flight and individual phases. The conclusions, derived from the analysis and results of Chapter 3 and 4, are presented in Chapter 5.

## CHAPTER 2

### METHOD OF ANALYSIS

#### 2.1 Aircraft Description

The statistical aircraft usage and flight loads were extracted from the flight data obtained on a fleet of the Beechcraft King Air models used by the USFS. The fleet consisted of three each of the C90A and C90GT models and one of the E90.

For the analysis, the values shown in Table 2.1 [9][10][11] were used if no model is listed by the parameter. The values for the C90A were used for the analysis of all the aircraft because there were no major differences among the three models.

Table 2.1: Beechcraft King Air C90 Specifications

Parameter and Units	Value
Maximum Takeoff Weight (C90A) (lb)	9,650
Maximum Takeoff Weight (C90GT/E90) (lb)	10,100
Fuel Capacity (C90A) (gallons)	384
Fuel Capacity (C90GT/E90) (gallons)	392
Wing Area (ft <sup>2</sup> )	293.94
Wing Span (ft)	50.25
Mean Aerodynamic Chord (ft)	6.513
Maximum Operating Speed (KIAS)	226
Limit Load Factor with Flaps Up (C90A/GT) (g)	+3.29/-1.33
Limit Load Factor with Flaps Up (E90) (g)	3.7/-1.68
Limit Load Factor with Flaps Down (C90A/GT) (g)	+2/0

#### 2.2 Recorded Data

##### 2.2.1 General Description

All aircraft were equipped with Digital Flight Data Recorders (DFDRs) made and supported by the Appareo Systems. The raw data from the recorders were post-processed by the USFS and placed in a central depository. The post-processed files were provided in

a Comma-Separated-Values (CSV) format containing all data at 8 Hz. There were a few differences in the number of parameters recorded for various aircraft, but those available for all aircraft are listed in Table 2.2. Some of the parameters shown in this table were obtained through post processing and some contained no information.

Table 2.2: Recorded and Derived Parameters

<b>Channel #</b>	<b>Parameter</b>	<b>Unit</b>
1	Line Number	-
2	Elapsed Time	seconds
3	Latitude	degrees
4	Elevation	feet
5	Longitude	degrees
6	Pitch	degrees
7	Roll	degrees
8	Speed	knots
9	Vertical Speed	feet per minute
10	Heading	degrees
11	Pitch Rate	degrees per second
12	Roll Rate	degrees per second
13	Yaw Rate	degrees per second
14	Longitudinal Acceleration	g
15	Lateral Acceleration	g
16	Normal Acceleration	g
17	True Airspeed	knots
18	Equivalent Airspeed	knots
19	Indicated Airspeed	knots
20	Course Direction	degrees
21	Pitot Pressure	in Hg
22	Static Pressure	in Hg
23	Outside Air Temperature	degrees C
27	Weight On Wheels	discrete
28	Discrete1	discrete
29	Discrete2	discrete
30	Discrete3	discrete
31	Discrete4	discrete

Some files did not contain any information about ground operations because the segments of file that contained recordings while the aircraft were on the ground were removed in the post-processing. This did not pose a problem because the focus of the present investigation was only on the airborne phases.

### 2.2.2 Data Quality Control

The data in the central depository was for three models of the King Air family spanning seven aircraft. The dataset consisted of 4074 total flight files. Table 2.3 shows the tally of files for each aircraft available for each year.

Table 2.3: Summary of Files Provided

<b>Aircraft/Year</b>	<b>1</b>	<b>2</b>	<b>3</b>	<b>4</b>	<b>5</b>	<b>6</b>	<b>7</b>	<b>Total</b>
2009	160	195	152	240	250	205	8	1210
2010	150	122	148	177	133	0	107	837
2011	161	20	150	197	115	0	72	715
2012	161	71	137	153	187	0	0	709
2013	147	51	152	109	144	0	0	603
Total	779	459	739	876	829	205	187	4074

Among the data provided, some files did not contain useful information or had obvious errors. These files were not used in the analysis. The files that were not used could be categorized into the following:

#### Repeated Lines:

In the 2009-year data, some files had lines of data that were repeated at specific intervals. These repeated lines duplicated all parameters with the exception of “line number” and “elapsed time”. This fact indicated the problem was with the post-processing while converting the raw data into CSV files. A summary of the prevalence of the problem for each airplane in year 2009 is shown in Table 2.4.

Table 2.4: Summary of Files with Repeated Lines

<b>Aircraft/Year</b>	<b>1</b>	<b>2</b>	<b>3</b>	<b>4</b>	<b>5</b>	<b>6</b>	<b>7</b>	<b>Total</b>
2009	76	107	88	130	87	111	7	606

### Noise in Airspeed:

Some files had consecutive lines in which the recorded airspeed changed by over 20 knots. Taking into account the sample rate of 8 Hz, this would indicate a change in airspeed of over 20 knots in a span of 1/8th of a second. This would be physically impossible in the middle of a flight. This appeared to be an installation problem because it was limited to a single aircraft and seemed consistent for all the recorded types of airspeeds i.e. calibrated, indicated, and equivalent. A tabulated summary of the problem by year is shown in Table 2.5.

Table 2.5: Summary of Files with Noisy Airspeed

<b>Aircraft/Year</b>	<b>7</b>
2010	21
2011	3
Total	24

### Noise in Normal Acceleration:

A few files had a line of data where the normal acceleration recorded unrealistically high magnitudes. These values were significantly larger than those preceding and following them. Oddly, this erratic behavior was limited to a single instance in the file thus making it hard to determine the cause of the problem. As seen in Table 2.6, the problem was present in nearly all aircraft over all years.

Table 2.6: Summary of Files with Noisy Normal Acceleration

<b>Aircraft/Year</b>	<b>1</b>	<b>2</b>	<b>3</b>	<b>4</b>	<b>5</b>	<b>6</b>	<b>7</b>	<b>Total</b>
2009	0	0	1	2	0	1	0	4
2010	0	0	0	0	1	0	0	1
2011	0	0	1	0	0	0	0	1
2012	0	3	0	2	0	0	0	5
2013	0	0	1	0	0	0	0	1
Total	0	3	3	4	1	1	0	12

No Flight Data:

The data in this group of files suggested that the aircraft remained on the ground for the complete duration of the recording. Since the scope of the analysis only dealt with the airborne phase of the operation, these files were not used. Table 2.7 shows that nearly fifty percent of the files within this category were from the 2009 fire season.

Table 2.7: Summary of Files with Aircraft Never Leaving the Ground

<b>Aircraft/Year</b>	<b>1</b>	<b>2</b>	<b>3</b>	<b>4</b>	<b>5</b>	<b>6</b>	<b>7</b>	<b>Total</b>
2009	34	46	15	40	13	21	0	169
2010	3	21	10	11	9	0	4	58
2011	1	1	10	8	4	0	0	24
2012	7	2	16	15	9	0	0	49
2013	6	0	14	6	3	0	0	29
Total	51	70	65	80	38	21	4	329

Takeoff/Landing Not Found:

A few files were eliminated because no takeoff or landing point could be identified. The main reason for this was that the Above Ground Level (AGL) altitude indicated the aircraft as being several hundred feet above the ground although the airspeed showed it had landed. Since the number of files affected was not significant, it was concluded that changing the landing and takeoff criteria to accommodate them was not warranted. There were no patterns to the problem's occurrence since it was present on almost all aircraft and all years. The files with this problem are listed in Table 2.8 below.

Table 2.8: Summary of Files with no Takeoff and Landings Identified

<b>Aircraft/Year</b>	<b>1</b>	<b>2</b>	<b>3</b>	<b>4</b>	<b>5</b>	<b>6</b>	<b>7</b>	<b>Total</b>
2009	0	2	0	1	1	1	0	5
2010	3	0	0	0	0	0	0	3
2011	2	3	5	2	1	0	3	16
2012	3	6	1	1	0	0	0	11
2013	1	1	2	0	3	0	0	7
Total	9	12	8	4	5	1	3	42

### Incomplete Files:

These files were a direct result of incorrect splitting of flight files during the initial post-processing when they were placed in the central depository. This incorrect splitting caused the file to be broken in the middle of the flight, resulting in flights that ended at airspeeds close to the cruise speed. Table 2.9 shows the rarity of the problem, with cases belonging to the aircraft 1, 2, and 7.

Table 2.9: Summary of Files with Incomplete Flight Data

<b>Aircraft/Year</b>	<b>1</b>	<b>2</b>	<b>3</b>	<b>4</b>	<b>5</b>	<b>6</b>	<b>7</b>	<b>Total</b>
2009	0	1	0	0	0	0	0	1
2010	2	0	0	0	0	0	0	2
2011	0	0	0	0	0	0	2	2
2012	1	2	0	0	0	0	0	3
2013	0	0	0	0	0	0	0	0
Total	3	3	0	0	0	0	2	8

The good files that were used for the analysis were of two types, those with ground phases and those without.

### Good Files with Ground Phases:

Most flight files contained ground phases. This meant that the data in the files included periods when the aircraft was on the ground before takeoff and after landing. Table 2.10 shows the number of flights with ground phases for each year and aircraft. None of the data files from aircraft 6 contained ground data from any of the years.

Table 2.10: Summary of Files with Ground Phases

<b>Aircraft/Year</b>	<b>1</b>	<b>2</b>	<b>3</b>	<b>4</b>	<b>5</b>	<b>6</b>	<b>7</b>	<b>Total</b>
2009	1	0	6	2	115	0	0	124
2010	142	101	138	166	123	0	82	752
2011	159	16	134	187	110	0	64	669
2012	150	58	120	135	178	0	0	641
2013	140	50	135	103	138	0	0	566
Total	592	225	533	593	664	0	146	2752

## Good Files without Ground Phases:

Some of the files were initially post-processed to eliminate the ground phases before placing them in the archives. As seen in Table 2.11 the post processing was done only on the data from 2009 and for all aircraft.

Table 2.11: Summary of Files without Ground Phases

<b>Aircraft/Year</b>	<b>1</b>	<b>2</b>	<b>3</b>	<b>4</b>	<b>5</b>	<b>6</b>	<b>7</b>	<b>Total</b>
2009	49	39	42	65	34	71	1	301

## **2.3 Derived and Added Parameters**

### **2.3.1 AGL Altitude**

The squat switch data was recorded in either the “weight\_on\_wheels” or the “discrete1” channel. To identify Lead phases and takeoff/landing in case of unreliable squat switch data, there was a need to obtain AGL altitudes. The AGL altitudes were also required to identify lead phases that were characterized by a low-altitude flight profile. The first and the most reliable choice was the Google Elevation Application Programming Interface (Google Elevation API) but it was limited to 2,500 queries per day. The average number of lines in the flight data files was more than 50,000. By sampling the ground elevation data from Google Elevation API at 1 Hz, it would take 2.5 days to obtain the ground elevations for a single file. Since this speed was unreasonable, given the total number of files was 4074, a free and unrestricted service provided by the U.S. Geological Survey (USGS) called the National Elevation Dataset (NED) was used.

Due to the large number of total data points for all the files combined, it was decided to obtain the AGL altitudes at a sample rate of 1 Hz. The obtained altitudes were then linearly interpolated for the points in between to accommodate the recorded 8-Hz data.

The resolution of the data from NED varied from 1/9 arc-second in heavily populated areas, to 1 arc-seconds in very remote areas of North America. This corresponded to resolutions ranging from 10 feet for the former to 90 feet for the latter. For most of the United

States, data was available at 1/3 arc-seconds with a 30-foot resolution [12]. Further detail concerning this database is provided in Appendix A.

### 2.3.2 MSL/Pressure Altitude

Due to the presence of noise in the Mean Sea Level (MSL) altitude in the CSV files, this parameter had to be filtered. The noise in pressure altitude was filtered using a two-second running average. The recorded pressure altitude was replaced by the filtered values for the remainder of the analysis.

### 2.3.3 Rate of Climb

The rate of climb parameter was derived from the filtered MSL altitude using the equation below.

$$\text{ROC} = (\text{MSL}_i - \text{MSL}_{i-1}) \cdot \text{SampleRate} \cdot 60 \quad (2.1)$$

where,

ROC = rate of climb in feet/minute

MSL<sub>*i*</sub> = MSL altitude in feet at *i*<sup>th</sup> point in the file

SampleRate = sample rate in hertz at which the data was recorded in the file

## 2.4 Takeoff and Landing Identification

### 2.4.1 Squat Switch

The presence of the “weight\_on\_wheels” channel in some of the files aided in the identification of the takeoff and landing points. The squat switch data, when available, were in three different formats as shown in Table 2.12. This parameter, which toggled between '0' and '1', was either recorded in the “weight\_on\_wheels” or “discretel” channel.

Table 2.12: Squat Switch Availability in Files

<b>Format</b>	<b>Available Channels</b>	<b>Squat Switch Data</b>
I	weight_on_wheels	Yes
	discrete1	No
II	weight_on_wheels	No
	discrete1	Yes
III	weight_on_wheels	Channel Absent
	discrete1	Yes

Takeoff was identified if simultaneously the squat-switch indicated “in air” and the indicated airspeed was between 95 knots and 120 knots. Likewise, landing was identified if the indicated airspeed was between 70 knots and 90 knots and the squat-switch showed the aircraft was on ground. If the squat switch signal indicated a takeoff or landing at airspeeds greater than 120 knots or less than 70 knots, respectively, the event was ignored and was instead passed over to the next method of identification. In some cases, the squat-switch indication flipped a number of times when the aircraft was close to the ground, possibly due to bouncing on the runway. Therefore, the squat-switch reading was required to remain in the same value (“sustain” criterion) for five seconds to be counted as being valid. Table 2.13 shows the summary of the criteria used to identify takeoff and landing using the squat switch data.

Table 2.13: Squat-Switch-based Takeoff and Landing Criterion

	<b>IAS Limits</b>	<b>File Limits</b>	<b>Sustain</b>
Takeoff	$95 < \text{KIAS} < 120$	-	5 sec
Landing	$70 < \text{KIAS} < 90$	End of File	5 sec

Obviously, in those cases where the data file was void of ground phases, the squat-switch could not be used for identification of takeoff and landing. In such cases, landing was assumed to coincide with the end of the file, if it also satisfied the defined airspeed limits. If the airspeed limits were not met at the end of file, the file was marked as incomplete. In

those same cases, the first line of the file was marked as the takeoff point, if it also satisfied the airspeed limits defined for takeoff.

### 2.4.2 Indicated Airspeed and AGL Altitude

A different approach was taken either when no squat switch data was available or when no takeoffs and landings were found using the previous criteria.

The aircraft takeoff was marked at the point when the indicated airspeed reached or first exceeded 95 knots. It was understood that this would eliminate part of the data from the analysis, but it was also important to ensure no ground data was mixed with flight loads.

If the file started with an indicated airspeed greater than 120 knots, it was assumed that the file was the product of an incorrect splitting during post-processing. These files were marked as incomplete because a portion of the flight was missing.

The identification of landing started only once a takeoff was found. An additional altitude requirement was introduced to eliminate other low speed flights from being erroneously identified as landing. In addition to the airspeed lower than 80 knots, the AGL altitude was required to remain under 100 feet for five consecutive seconds for the landing to be marked.

## 2.5 Flight Distance and Time

The flight distance was calculated by integrating the true airspeed from takeoff to landing.

$$D = \sum_{t_{takeoff}}^{t_{land}} V_{true} \cdot \Delta t \quad (2.2)$$

where,

$$\begin{aligned} V_{true} &= \text{true airspeed from the flight file in knots} \\ t_{takeoff} &= \text{time at takeoff in seconds} \\ t_{land} &= \text{time at landing in seconds} \\ \Delta t &= \text{flight data sample time in seconds} \end{aligned}$$

The flight time was calculated as the time between takeoff and touchdown.

$$T = t_{land} - t_{takeoff} \quad (2.3)$$

## 2.6 Stall speed

The stall speed was determined to ensure the landing never occurred below the stall speed. For the Beechcraft King Air C90A's idle power condition, the lowest possible stall speed for 100% flaps is 76 KIAS [7] at 0-degree bank angle and maximum landing weight. For the flight without payload, 2 passengers, and 30% fuel, a rough estimate of the stall speed was determined from the following equations:

$$W_{30\%Fuel} = 0.3 \times \text{Max Fuel Weight} = 737.4 \text{ lb} \quad (2.4)$$

$$W_2 = W_{EmptyWeight} + W_{30\%Fuel} + W_{PAX} = 6902.4 \text{ lb} \quad (2.5)$$

$$V_{stall} = V_{stall_1} \times \sqrt{\frac{W_2}{W_{GW}}} = 64.27 \text{ KIAS} \quad (2.6)$$

where,

$W_{30\%Fuel}$	=	weight of 30% fuel in pounds
$W_{EmptyWeight}$	=	empty weight of the aircraft in pounds
$W_{PAX}$	=	gross weight of the aircraft in pounds
$W_{GW}$	=	total weight of all passengers in pounds
$V_{stall_1}$	=	stall speed at full flaps and gross weight
$W_2$	=	aircraft weight with 30% fuel and two passengers
$V_{stall}$	=	stall speed at full flaps and $W_2$

## 2.7 Aircraft Lift Curve Slope

The aircraft lift curve slope was estimated by combining the lift curve slope of the wing and the horizontal tail. To calculate these components, some of the required parameters were measured from the aircraft drawings. The estimated and known aircraft parameters are listed in Table 2.14.

Table 2.14: Known and Derived King Air C90 Parameters

Geometry	Symbol	Wing	Horizontal Tail
Span	$b$	50.25 ft	17.25 ft
Planform Area	$S$	293.94 ft <sup>2</sup>	79.875 ft <sup>2</sup>
Aspect Ratio	$AR$	8.59	3.725
Tip Chord	$c_{tip}$	3.087 ft	3.473 ft
Root Chord	$c_{root}$	9.647 ft	5.788 ft
Taper Ratio	$\lambda$	0.32	0.6
Leading Edge Sweep	$\tan(\Lambda_{LE})$	0.055	0.157
$c/2$ Chord Line Sweep	$\tan(\Lambda_{c/2})$	-0.063	0

Using the parameters listed in Table 2.14, the lift curve slopes of the wing and the horizontal tail were estimated using the following formula. They were then used to estimate the aircraft lift curve slope.

$$\mathcal{K} = \frac{a_o}{2\pi} = 1 \quad (2.7)$$

$$C_{L_\alpha} = \frac{2\pi \cdot AR}{2 + \sqrt{\frac{AR^2 \beta^2}{\mathcal{K}} \left( 1 + \frac{(\tan \Lambda_{c/2})^2}{\beta^2} \right) + 4}} \quad (2.8)$$

$$C_{L_\alpha} = C_{L_{\alpha_{WB}}} + C_{L_{\alpha_{HT}}} \cdot \frac{S_t}{S_w} \cdot \left( 1 - \frac{\partial \epsilon}{\partial \alpha} \right) \quad (2.9)$$

The lift curve slope of wing-body, tail and aircraft are summarized in Table 2.15.

Table 2.15: Summary of Lift Curve Slope

	( $C_{L_\alpha}$ per radian)
Wing-Body	5.12
Tail	3.829
Aircraft	5.765

## 2.8 Derived Gust Velocity

Derived gust velocity was determined using various aircraft and flight parameters.

$$U_{de} = \frac{\Delta n_z}{\bar{C}} \quad (2.10)$$

where,

$$\begin{aligned} \Delta n_z &= n_z - 1 &&= \text{incremental normal acceleration} \\ \bar{C} &= \frac{\rho_0 V_e C_{L\alpha} S}{2W} K_g &&= \text{aircraft response factor} \\ \rho_0 &= 0.002377 \text{ slugs/ft}^3 &&= \text{standard sea level air density} \\ V_e &= \text{ft/sec} &&= \text{equivalent airspeed} \\ C_{L\alpha} &= 5.7654 &&= \text{aircraft lift-curve slope per radian} \\ S &= 293.94 \text{ ft}^2 &&= \text{wing reference area} \\ W &= 7639.8 \text{ lb} &&= \text{gross weight} \\ K_g &= \frac{0.88\mu}{5.3 + \mu} &&= \text{gust alleviation factor} \\ \mu &= \frac{2W}{\rho g \bar{c} C_{L\alpha} S} &&= \text{non-dimensional mass parameter} \\ \rho &= \text{slugs/ft}^3 &&= \text{air density at altitude} \\ g &= 32.17 \text{ ft/sec}^2 &&= \text{gravitational acceleration} \\ \bar{c} &= 6.513 \text{ ft} &&= \text{wing mean geometric chord} \end{aligned}$$

Since the weight of the aircraft was not a recorded parameter, it was assumed to be that of the empty aircraft, thirty percent fuel, and two passengers. The weight was calculated as shown in Equation 2.5.

## 2.9 Mission Identification

### 2.9.1 Ferry

Flights which originated from one airport followed by cruise and landing at another airport were characterized as Ferry flights. These flights were identified by calculating their average speed.

The average speed was determined by calculating the great-circle distance between the takeoff and landing point and dividing it by the flight time. The great-circle distance

(point-to-point distance) was calculated using the Haversine formula shown below [13].

$$a = \sin^2\left(\frac{\Delta\phi}{2}\right) + \cos\phi_1 \cdot \cos\phi_2 \cdot \sin^2\left(\frac{\Delta\lambda}{2}\right) \quad (2.11)$$

$$c = 2 \cdot \operatorname{atan2}\left(\sqrt{a}, \sqrt{1-a}\right) \quad (2.12)$$

$$d = R \cdot c \quad (2.13)$$

where,

$\phi$  = latitude

$\Delta\phi$  = difference in latitude

$\Delta\lambda$  = difference in longitude

$R$  = Radius of Earth = 3959 miles

A typical ferry flight consists of mostly cruising at higher altitudes. The only times spent below cruise speeds are during climbs and descents for takeoff and landing. Hence, if the calculated average speed for a flight was greater than 150 knots, then the flight was categorized as a ferry mission. The average of 150 KIAS was chosen based on the average speeds of a few known ferry flights. Figure 2.1 shows the typical ferry flight with distinct climb, cruise and descent phases. The figure shows that the majority of the flight time was spent in the cruise phase resulting in a high average speed.

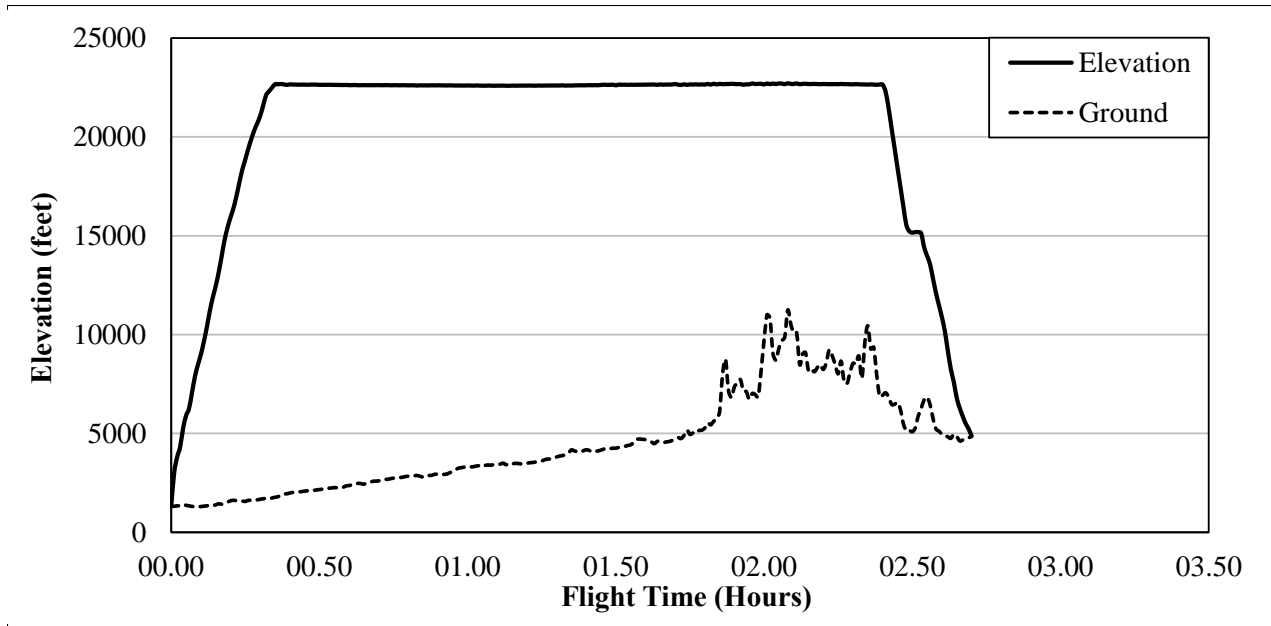


Figure 2.1: Typical Ferry Flight Profile

### 2.9.2 Air Tactical Group Supervisor (ATGS)

The ATGS missions are usually conducted at AGL altitudes between 2,000 and 2,500 feet [14]. Their constant right-hand circular flight paths also characterize the mission. The purpose of the ATGS mission is to supervise the air traffic within the Fire Traffic Area (FTA). In order to monitor the fire-fighting operations, the aircraft loiters conducting right-hand turns, enabling the observer in the right seat to monitor the operation below. The turns and circles phases are used along with the above criteria to categorize the mission as ATGS.

### 2.9.3 Aerial Supervision Module (ASM)/Lead

During an ASM/Lead mission, the aircraft is used to conduct surveillance as in an ATGS, in addition to leading the air tankers to the drop zone. These lead missions are conducted at very low altitudes and are usually characterized by left hand turns. In those cases when a combination of low altitude left hand turns and high-altitude, right-hand turns were detected in a flight, it was categorized as an ASM/Lead mission.

## 2.10 Phase Separation

### 2.10.1 Leads

Lead phases were characterized by a low altitude level flight profile. Hence, the segments of the flight when the rate of climb was less than  $|250|$  feet per minute at AGL altitudes consistently less than 300 feet lasting a minimum of two seconds were identified as lead phases. If the time between two lead phases was less than 2 minutes, they were combined into one single phase. If the rate of climb or the AGL altitude exited their bounds for less than two seconds, the lead phase was not terminated. This was utilized to prevent legitimate leads from being terminated early due to possible noise in the data or the terrain features below the flight path.

Flight segments 60 seconds before the start and after the end of a lead were categorized as Entry and Exit phases, respectively. Figure 2.2 shows a schematic of a typical flight profile including the Entry, the Lead, and the Exit phases.

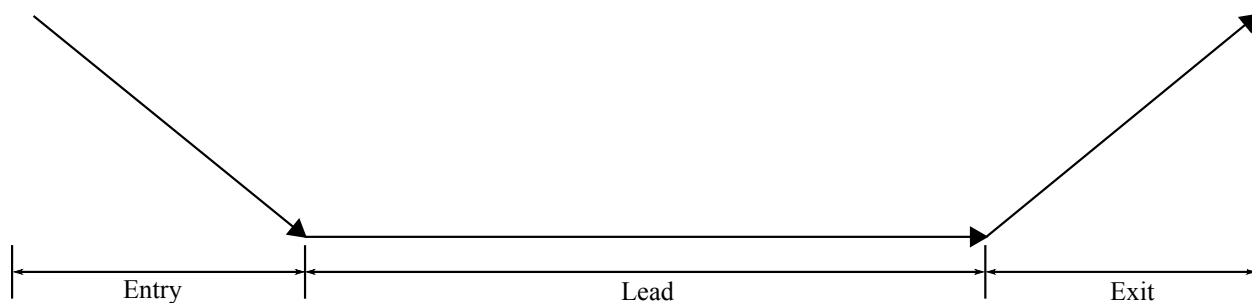


Figure 2.2: Flight Profile for Entry, Lead, and Exit (Side View)

### 2.10.2 Turns

The Air Tactical Group Supervisor (ATGS) and Aerial Supervision Module (ASM)/Lead missions have flight profiles with numerous circular turns. To distinguish these missions from others, it was necessary to identify these Turn phases. The Turn phases were identified by a continuous change in heading in one direction until the total change became greater than 360 degrees (i.e. one complete turn). Changes in the direction of the turn were allowed as long

as they lasted less than two seconds. A top profile of a segment of flight from a file including turns is shown in Figure 2.3. In this case, ten complete circular turns were identified.

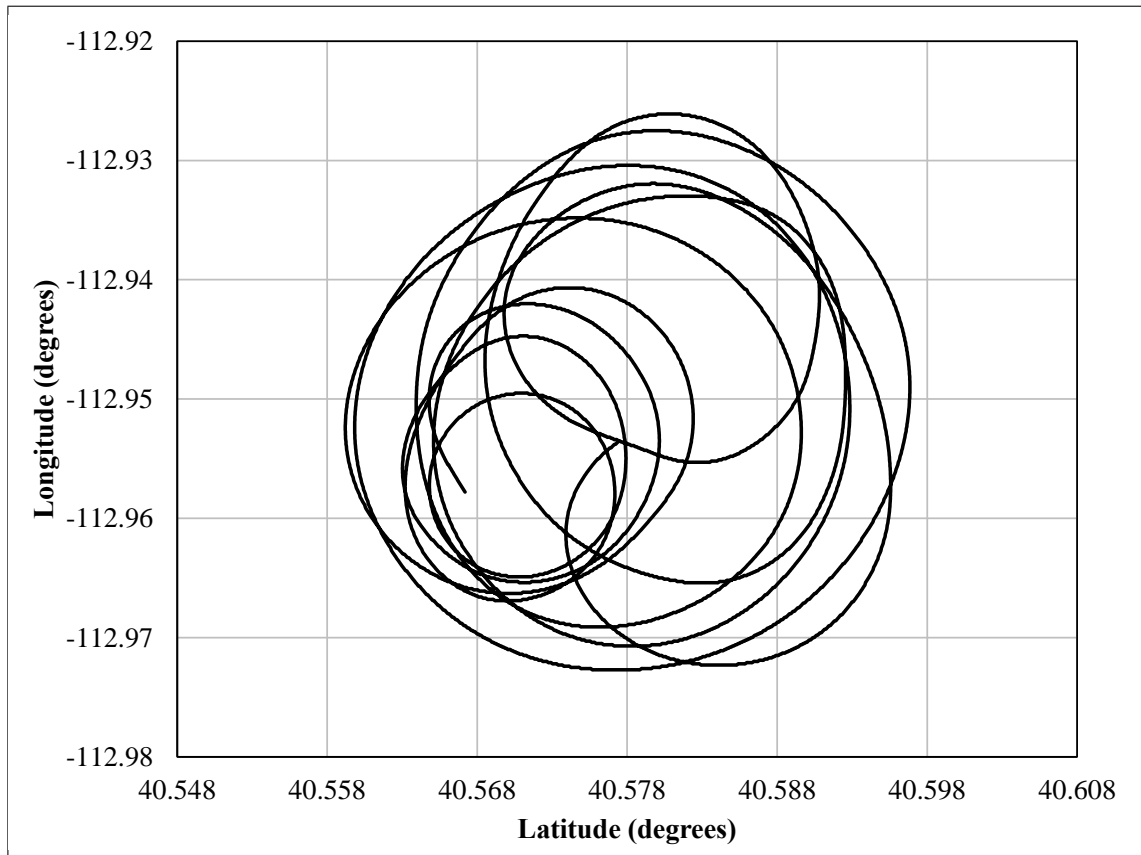


Figure 2.3: Segment of Flight with Turns

### 2.10.3 Cruise-1 and Cruise-2

The flight segment between takeoff and reaching the fire site was called the Cruise-1 phase. The return to base until landing was called the Cruise-2 phase. These two phases consisted of rectilinear flights combined with some maneuvering to approach the fire area. The beginning of the Cruise-1 phase was set to be at takeoff and its end as the beginning of the first Turn or an Entry phase. The beginning of the Cruise-2 phase was set to be the end of the last Turn or an Exit and its end at the landing point.

## 2.11 Loads Counting

### 2.11.1 Peaks and Valleys

The method of peak between means was used to count the number of occurrences of vertical loads and derived gust velocities. The largest magnitude of loads between consecutive crossings of the deadband was classified as either a peak or a valley. A deadband is a range of loads about the zero that is defined to avoid the loads associated with small structurally insignificant vibrations from being included in the analysis. The crossing of the deadband was counted regardless of the crossing being into or through the deadband. A graphical representation of the Peak and Valley identification is shown in Figure 2.4. The upper and lower limits and deadband width used for this analysis are listed in Table 2.16.

Table 2.16: Load Limits and Deadband

	<b>Upper Limit</b>	<b>Lower Limit</b>	<b>Deadband</b>
Normal Acceleration (g)	+2.5	-2.5	$\pm 0.05$
Derived Gust (ft/sec)	+50	-50	$\pm 2$

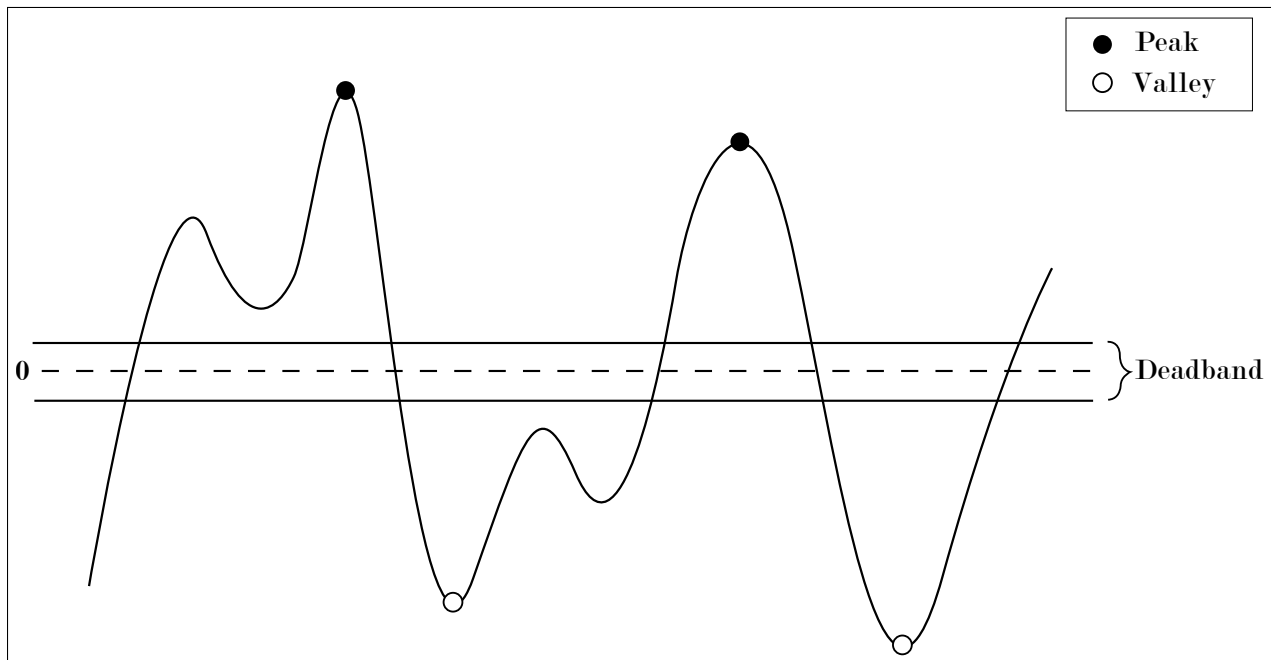


Figure 2.4: Peak-Valley Identification

### 2.11.2 Gust and Maneuver Separation

Vertical load factors could be the result of either a gust or a maneuver. The 2-second criterion [8], which suggests that load factor peaks with crossing greater than 2 seconds be counted as maneuver was used for gust and maneuver separation. Consequently, all load factor peaks less than 2 seconds were identified as gusts. These loads for each individual phase and for the overall flights were plotted as cumulative occurrence per 1000 flight hours as well as per nautical mile. The load counts were also separated into altitude bands to provide a better understanding of the effect of altitude.

### 2.12 Altitude Bands

The altitude bands established for the analysis are shown in Table 2.17. The same limits of the bands was used for AGL and MSL altitudes.

Table 2.17: Altitude Bands

<b>Band #</b>	<b>Altitude</b>
1	< 500 ft
2	500-1500 ft
3	1500-4500 ft
4	4500-9500 ft
5	9500-14500 ft
6	14500-19500 ft
7	19500-24500 ft
8	> 24500 ft

## CHAPTER 3

### RESULTS AND DISCUSSION - AIRCRAFT USAGE

This section contains statistical usage results. Since the dataset consisted of information from three models of King Air, C90A, C90GT, and E90, a comparison and summary of results for each model is also presented along with the results for the entire dataset. The statistical usage results includes distance and duration information for complete flights as well as for individual phases.

As discussed in Chapter 2, the dataset included 4074 flight data files for years 2009 through 2013. Of these, 1021 files could not be used for the analysis for a variety of reasons. In the remaining 3053 flight files, 3094 flights were identified using the criteria discussed in section 2.4. A summary of the files used for the analysis by aircraft model is shown in Table 3.1. The majority of the data files were from the C90GT (63.25%), followed by the C90A (31.94%). The least amount of data was available for the E90 model.

Table 3.1: King Air Models Used for Analysis

Model/Year	C90A	C90GT	E90	Total
2009	160	264	1	425
2010	243	427	82	752
2011	174	431	64	669
2012	208	433	0	641
2013	190	376	0	566
Total	975	1931	147	3053

Some of the data files contained pitch angles in excess of  $\pm 30$  degrees and/or roll angles beyond  $\pm 80$  degrees. Since these extreme attitudes are not considered part of the normal operation, they were separated and categorized as Extreme Attitude flights. The remaining flights were categorized as Firefighting and Ferry missions. Table 3.2 shows the number of Extreme Attitude flight files by model and year. As seen in the table, the model

with largest number of Extreme Attitude flights was the C90GT, accounting for 73.6% of the cases.

Table 3.2: Files Containing Extreme Attitudes

<b>Model/Year</b>	<b>C90A</b>	<b>C90GT</b>	<b>E90</b>	<b>Total</b>
2009	10	15	0	25
2010	5	6	5	16
2011	4	17	2	23
2012	6	23	0	29
2013	2	32	0	34
Total	27	93	7	127

The overall flight is defined as the total airborne phase from takeoff to landing. The statistical analysis of the overall flights was split into two sets, Extreme Attitude and Fire-fighting/Ferry.

### 3.1 Overall Flight - Extreme Attitude

Again, the reader is reminded that Extreme Attitudes were cases where the pitch angle was in excess of  $\pm 30$  degrees or roll angle reached beyond  $\pm 80$  degrees. For flights with extreme attitudes, the relationship between the maximum MSL altitude and the corresponding indicated airspeed is shown in Figure 3.1. The figure shows that in these cases, the aircraft did not exceed the maximum MSL altitude of 30,000 feet but the majority of the flights occurred at relatively higher altitudes. The correlation between maximum indicated airspeed and the coincident MSL altitude is shown in Figure 3.2. It can be seen from the figure that in a small number of flights the maximum airspeed of 226 KIAS was exceeded slightly, but never reached 250 KIAS. It is evident that these high-speed flights took place well below the cruise altitude, 60% of which occurred in the 5,000-10,000 feet MSL altitude band while never exceeding 7,600 feet. Absence of flap information did not allow examination of flap dependent airspeed limits.

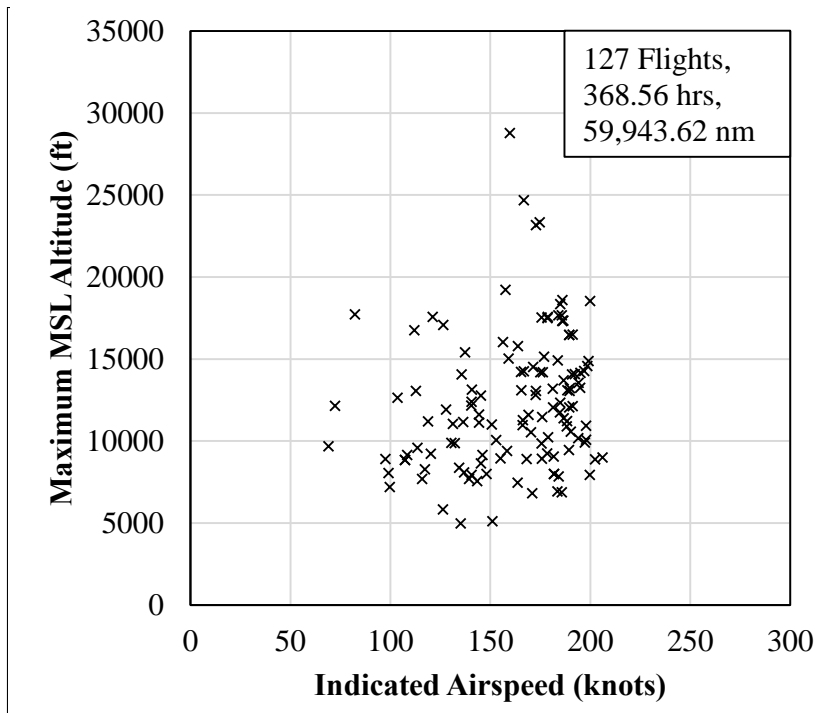


Figure 3.1: Maximum MSL Altitude and Coincident Indicated Airspeed for Extreme Attitude Flights

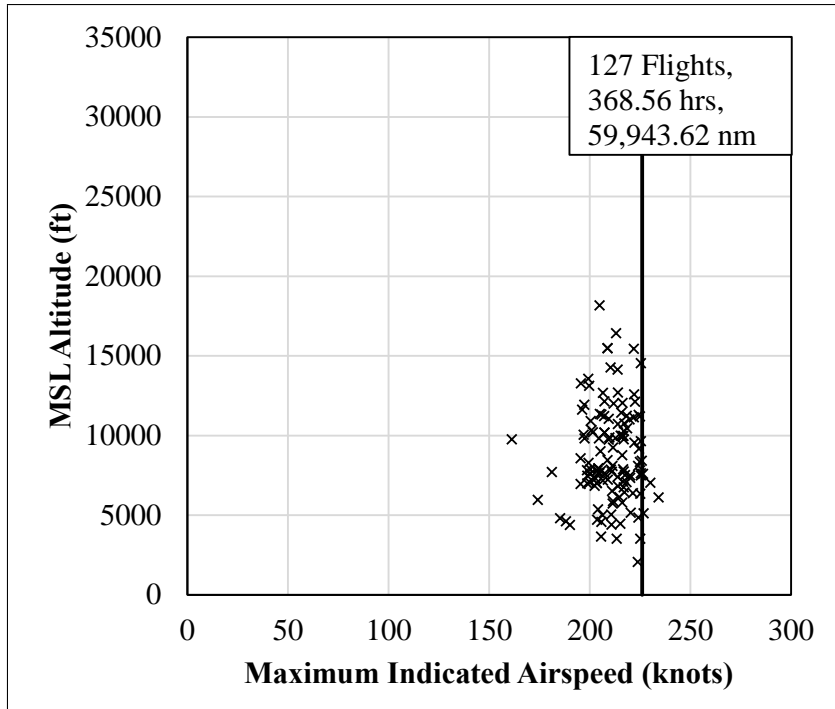


Figure 3.2: Maximum Indicated Airspeed and Coincident MSL Altitude for Extreme Attitude Flights

The statistical summaries of the pitch and roll angles for the Extreme Attitude flights are shown in Table 3.3. According to the table, the average attitude for the roll angle was +67 and -82.7 degrees.

Table 3.3: Summary of Pitch and Roll Angles for Extreme Attitude Flights

	Pitch Angle (deg)		Roll Angle (deg)	
	Positive	Negative	Positive	Negative
Maximum	55.8	-6.2	177.8	-28.4
Minimum	10.7	-64.8	22.6	-179.8
Average	24.4	-19.0	67.1	-82.7
Standard Deviation	6.4	7.2	16.4	14.2

Figures 3.3 and 3.4 show the maximum and minimum pitch and roll angles. These figures show a few cases where the aircraft was flown at unusually high pitch and roll angles. In one specific case, marked on the figures, the aircraft was flown through a steep dive coupled with a complete roll. Since this maneuver occurred at airspeed around 150 KIAS, it could be associated with a firefighting simulation-training flight.

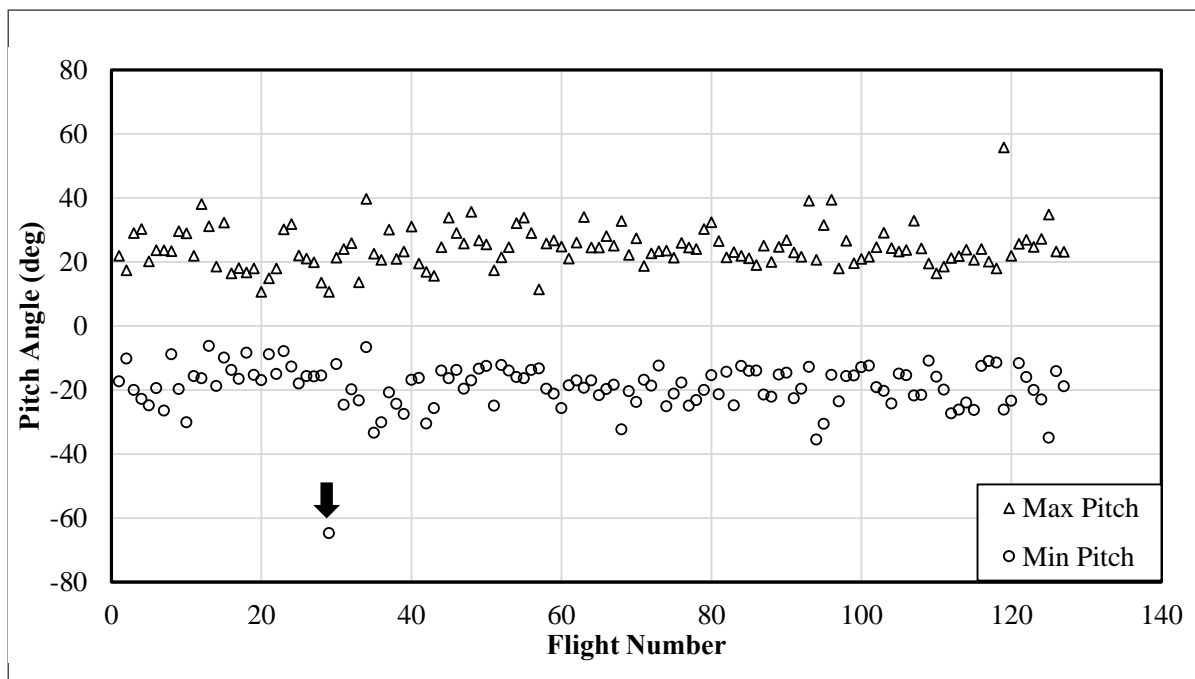


Figure 3.3: Maximum MSL Altitude and Coincident Indicated Airspeed for Extreme Attitude Flights

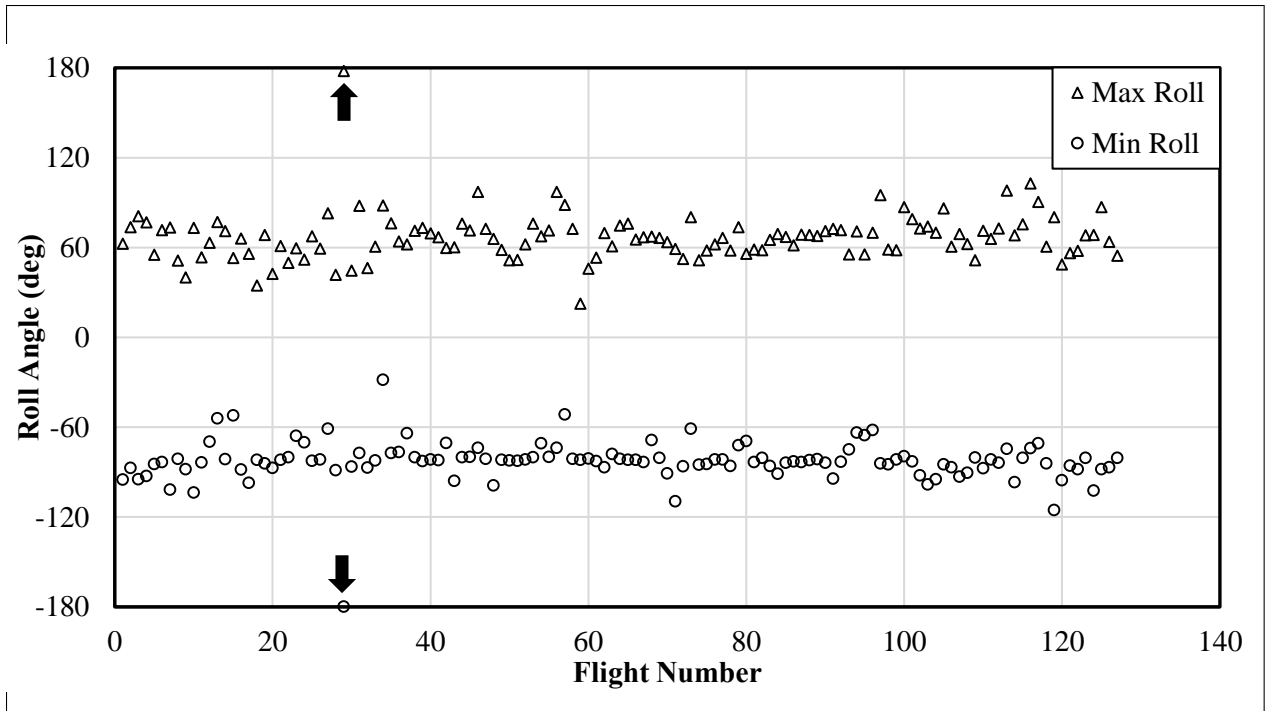


Figure 3.4: Maximum Indicated Airspeed and Coincident MSL Altitude for Extreme Attitude Flights

Figure 3.5 represents the  $V-n$  diagram of the Extreme Attitude flights. As expected from these unusual attitudes, these maneuvers resulted in high vertical load factors. The unusual case with large roll and pitch angle mentioned earlier appears in the  $V-n$  diagram as the point with the load factor of 3.6 g. Except for this case, the vertical load factors were below 3.29 g limit. Since the aircraft weight was not known, it is unclear if the structural limit load factors were indeed exceeded.

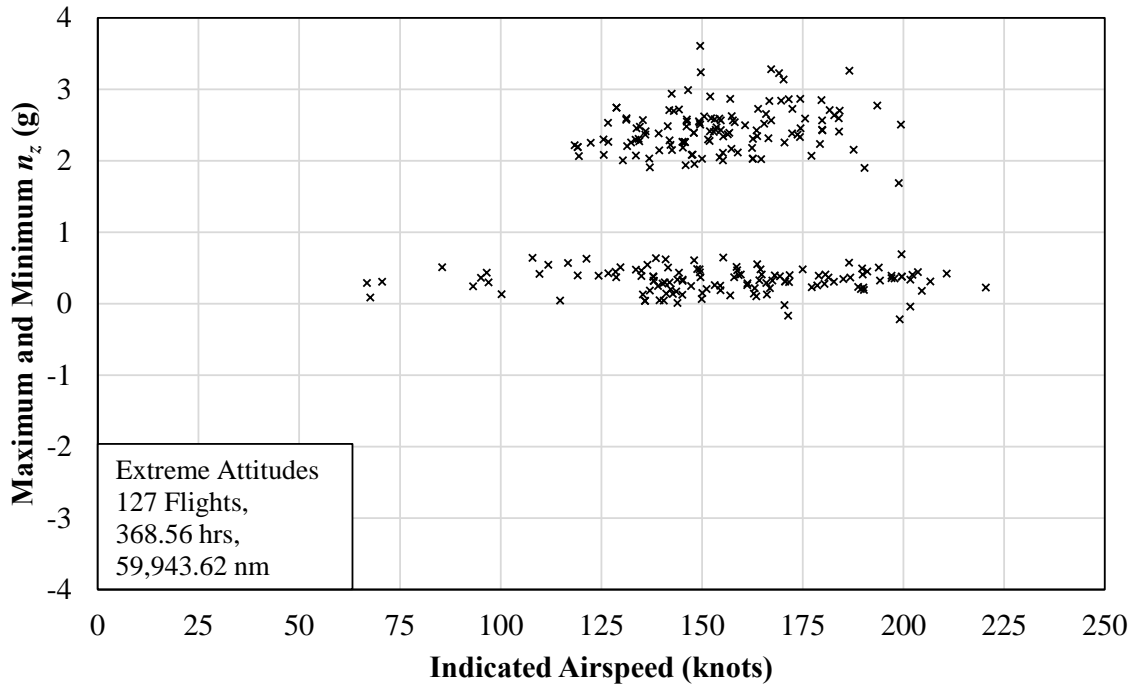


Figure 3.5:  $V$ - $n$  Diagram for Extreme Attitude Flights

### 3.2 Overall Flight - Firefighting/ Ferry

The correlation between the indicated airspeed and MSL altitude for Firefighting/-Ferry flights for all aircraft is presented in Figure 3.6 whereas Figures 3.7 through 3.9 shows the same information for individual models. These figures also show the limits on the indicated airspeed and altitude, as given in the operating handbooks [9][10][11]. All but two flights were within the maximum operational altitude limits. In the two cases when this limit was exceeded, the exceedance was only 17 and 53 feet each, and well within the range of accuracy of the recordings.

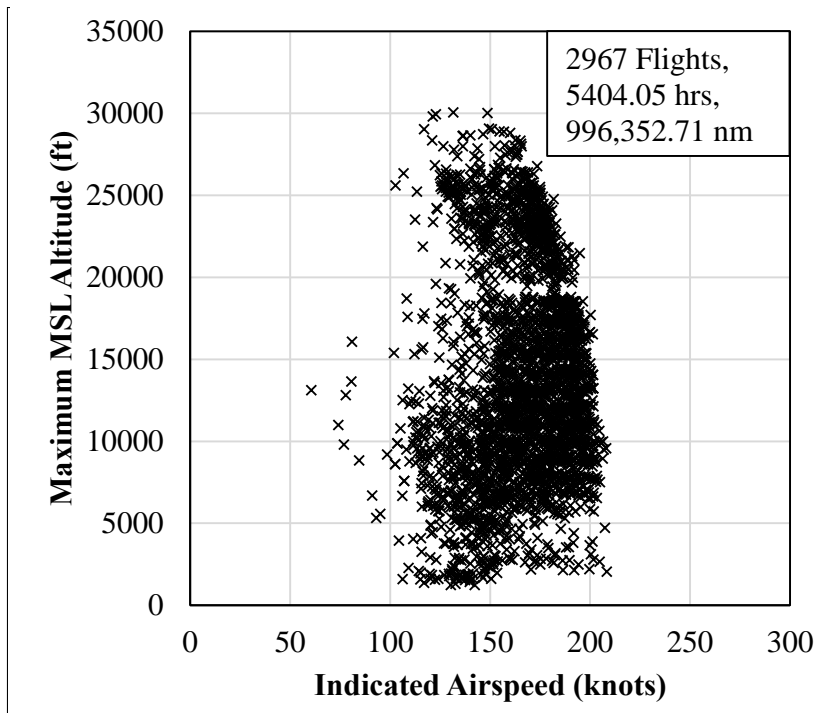


Figure 3.6: Maximum MSL Altitude and Coincident Indicated Airspeed for Firefighting/Ferry Flights

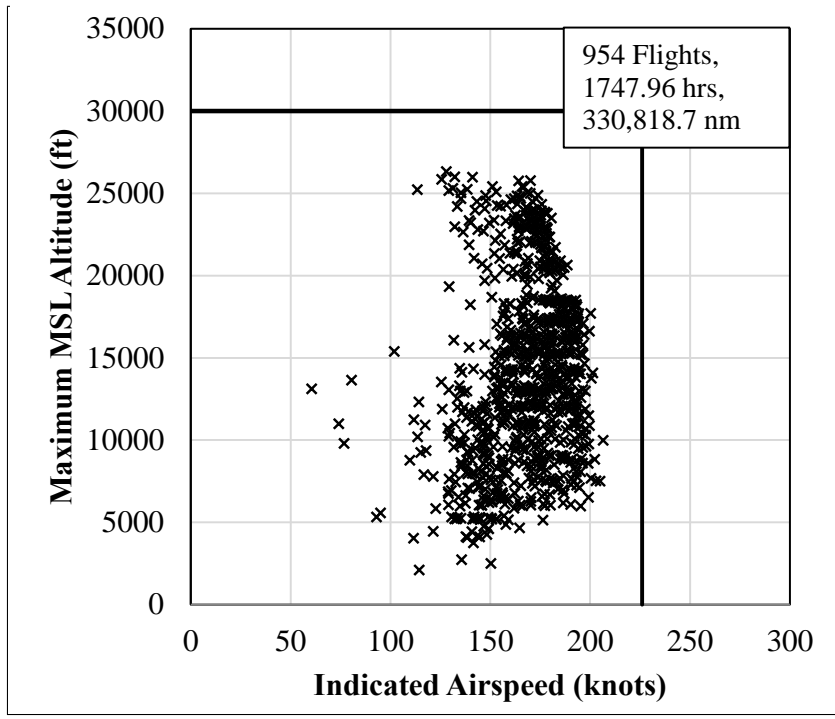


Figure 3.7: Maximum MSL Altitude and Coincident Indicated Airspeed for C90A

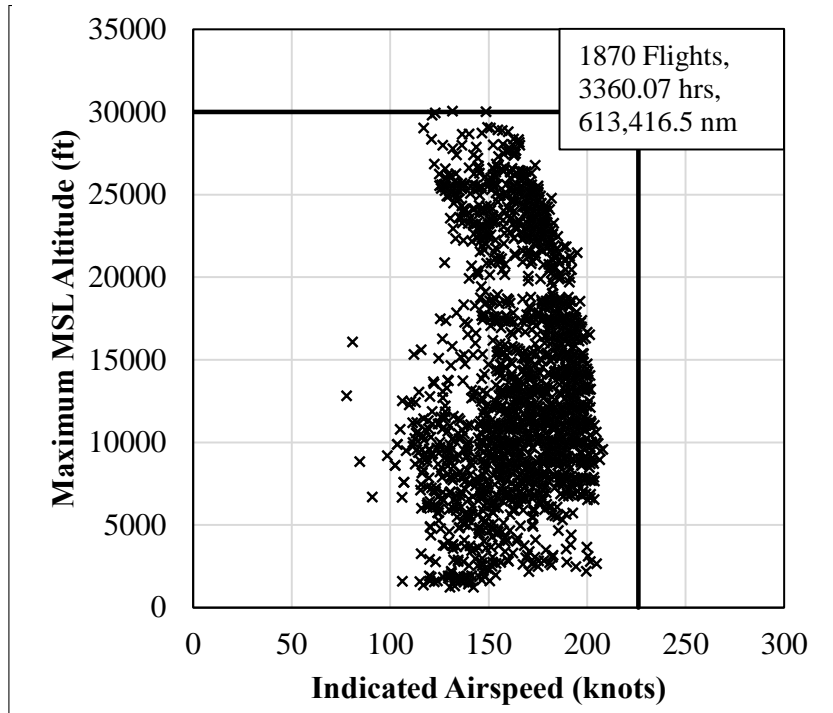


Figure 3.8: Maximum MSL Altitude and Coincident Indicated Airspeed for C90GT

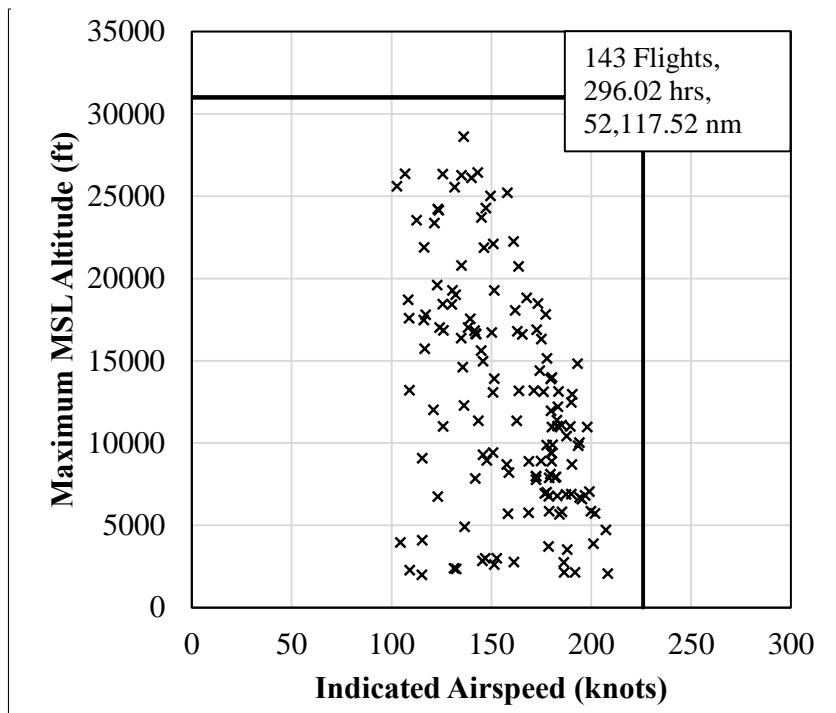


Figure 3.9: Maximum MSL Altitude and Coincident Indicated Airspeed for E90

Figure 3.10 shows the correlation between maximum indicated airspeed and the coincident MSL altitude for all aircraft, while the same results are presented for each model in Figures 3.11 through 3.13. In these figures, the limit indicated airspeed is shown with a solid line, while a value 10% above that is shown with a dashed line. As seen in Figures 3.11 through 3.13, in a few cases the indicated airspeed exceeded the maximum operating limits at or below 16,000 feet MSL. The percentage of flights when the indicated airspeed reached beyond the maximum operational limits was extremely low, accounting for 1.1% C90A, 4% for C90GT, and 7.3% for the E90 model. Since the number of data files available for the E90 was significantly smaller compared to the C90A and C90GT variants, this percentage may not hold statistical significance. Nonetheless, in every case, the indicated airspeeds remained within 10% of the published never-exceed limitations, which meant that the airspeeds never exceeded the dive velocity.

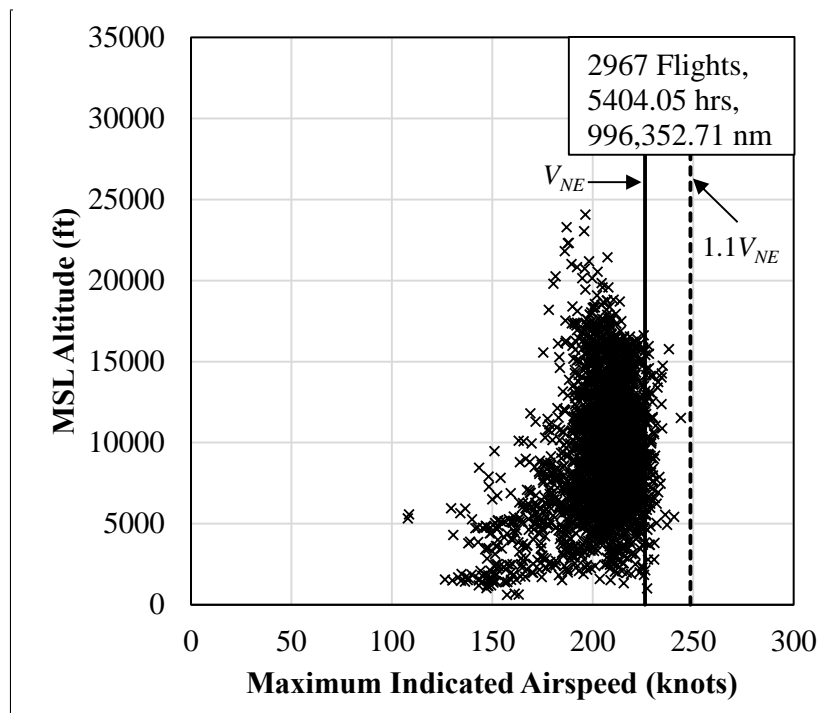


Figure 3.10: Maximum Indicated Airspeed and Corresponding MSL Altitude for Firefighting/Ferry Flights for all Models

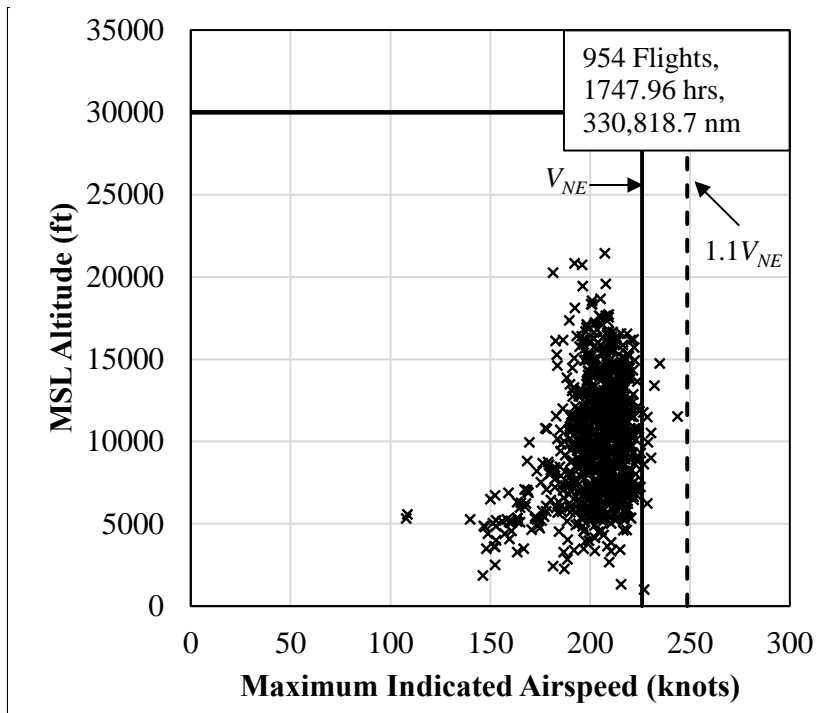


Figure 3.11: Maximum Indicated Airspeed and Corresponding MSL Altitude for C90A

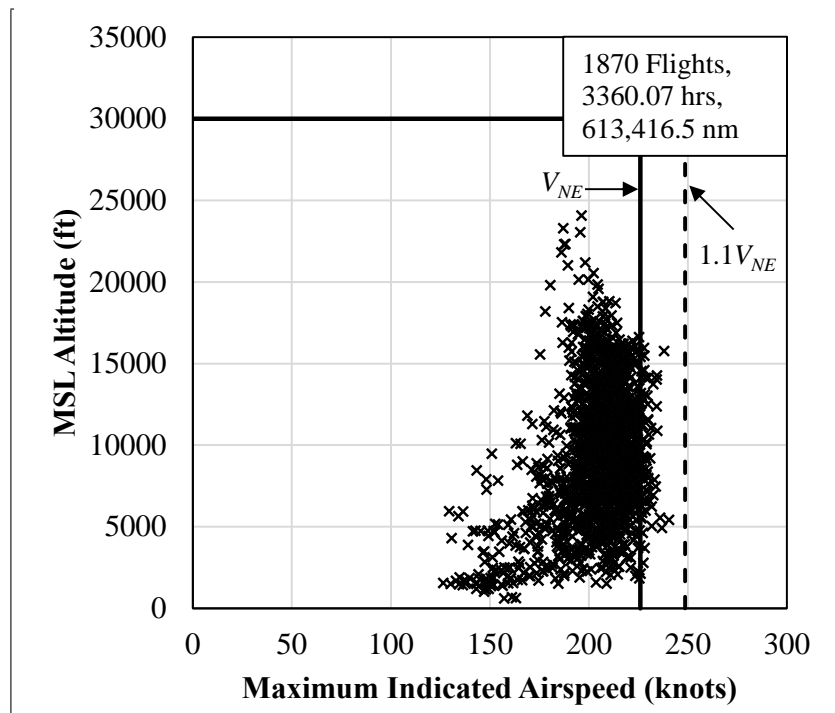


Figure 3.12: Maximum Indicated Airspeed and Corresponding MSL Altitude for C90GT

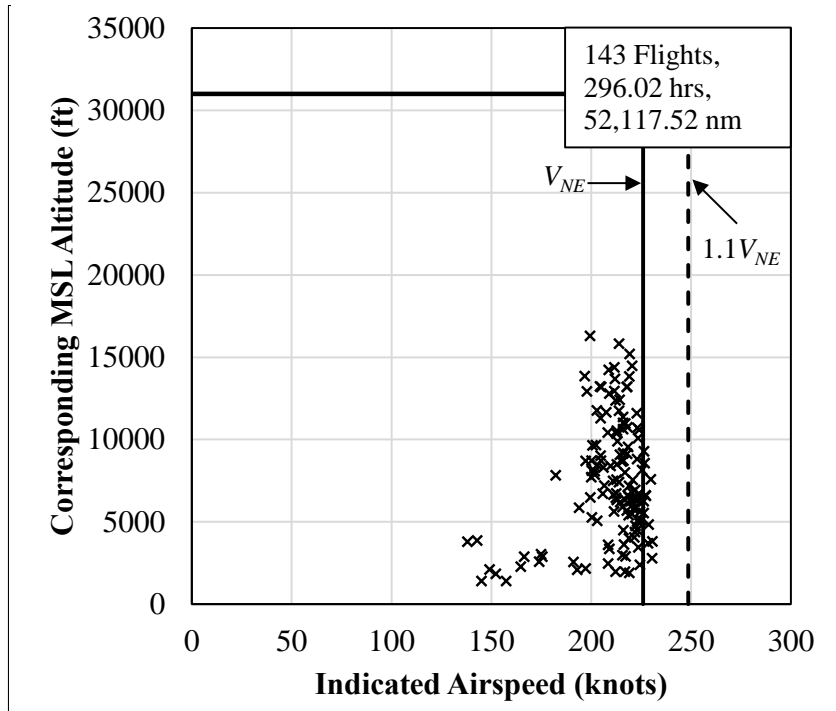


Figure 3.13: Maximum Indicated Airspeed and Corresponding MSL Altitude for E90

The flight distance was calculated by integrating the true airspeed. Figure 3.14 shows the number of flights grouped by flight distance for Firefighting/Ferry flights. As seen in the figure, more than half of the flights were flown over distances shorter than 350 nautical miles while the majority (90%) were under 650 nautical miles. The average distance flown during the Firefighting and Ferry flights was 335.8 nautical miles with a standard deviation of 217.1 nautical miles.

Figure 3.15 shows the number of flights sorted by duration. Almost half (49.3%) the flights lasted less than 90 minutes and the majority (93.8%) were shorter than 4 hours. The average flight time was 109.3 minutes with a standard deviation of 75.7 minutes.

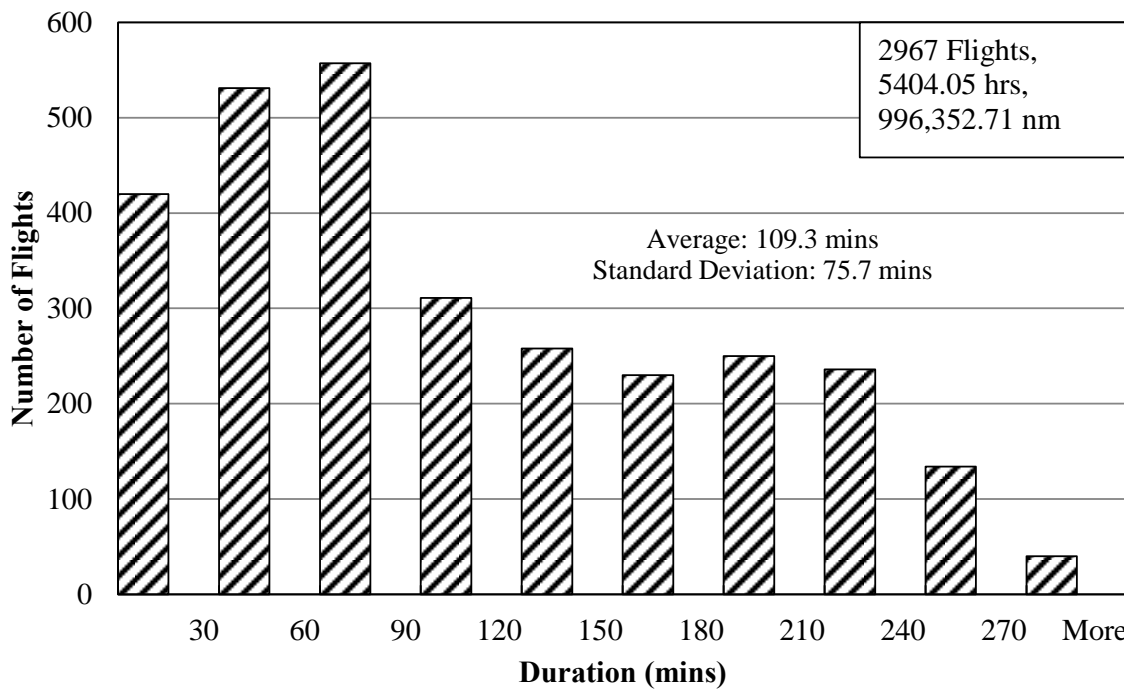
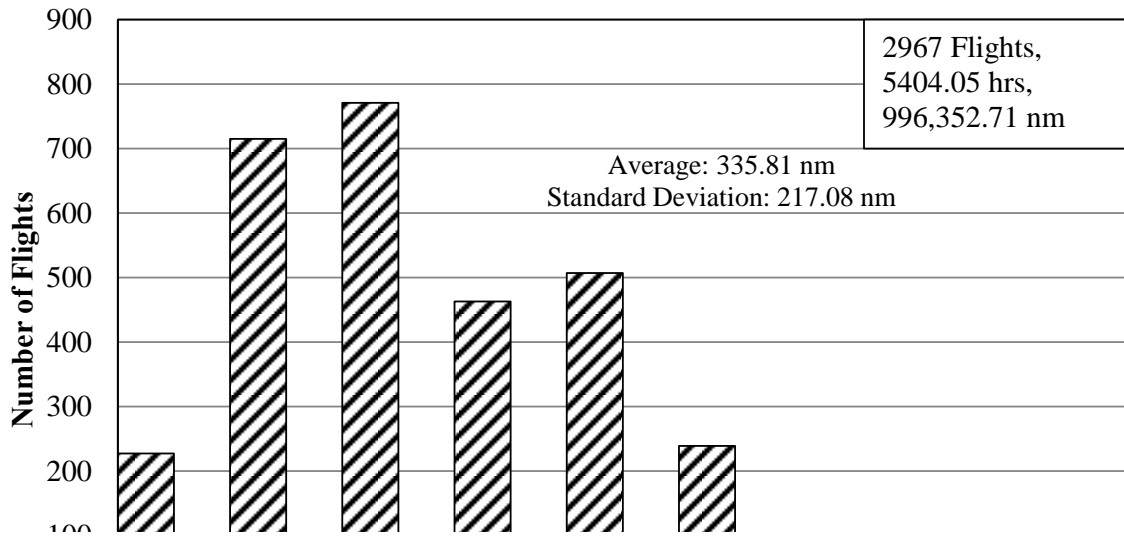


Figure 3.15: Number of Flights by Duration

### 3.2.1 *V-n* Diagram

The maximum and minimum limit load factors for all models are summarized in Table 3.4. The King Air E90 has a higher limit load factor than the C90A and the C90GT variants, which have the same limits.

Table 3.4: Limit Load Factors for C90A, C90GT, and E90

	<b>C90A</b>	<b>C90GT</b>	<b>E90</b>
No Flaps	+3.29/ - 1.33	+3.29/ - 1.33	+3.7/ - 1.68

The *V-n* diagram was constructed for each model separately due to variations in their limits. The stall speed at 1g, derived in Section 2.6 as 64.27 KIAS for aircraft weight of 6902.4 pounds with flaps fully deflected, was used for the construction. The relationship between the velocity and normal load from zero to maximum  $n_z$  was derived as:

$$V = \sqrt{n} \times V_{stall} \quad (3.1)$$

where,

$V$  = indicated airspeed in knots

$n$  = limit load factor in g

$V_{stall}$  = stall speed of the aircraft derived in Section 2.6

The negative part of the *V-n* diagram could not be constructed because the maximum negative lift stall speed was not known.

The *V-n* diagrams of the C90A, C90GT, and E90 are shown in Figures 3.16 through 3.18 respectively. Almost all of the data points were within the bounds defined by the operational limits for the E90 and C90A, except in one case each. Upon inspection, it was found that both cases were the result of a pull-up maneuver following a dive. In the case of the C90GT model, the results from a handful of flights were outside of the envelope. However, as the aircraft weight was not known, it was not possible to determine if these represented exceedance of the load factors or stalls. The *V-n* diagram of all the models combined is shown in Figure 3.19.

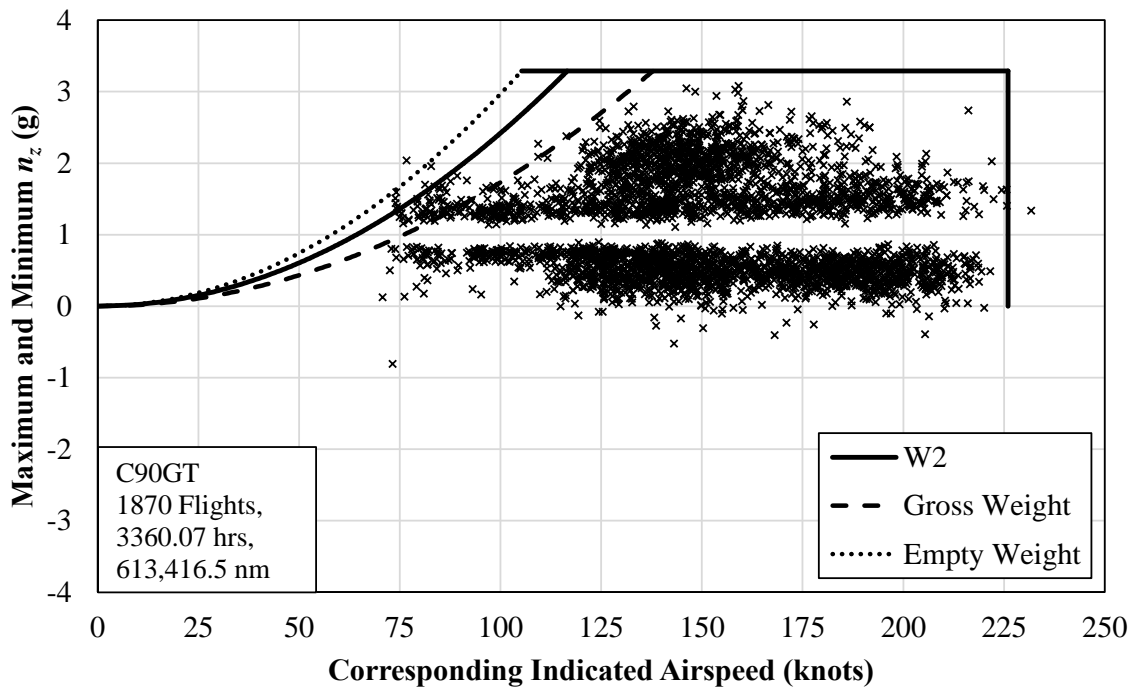
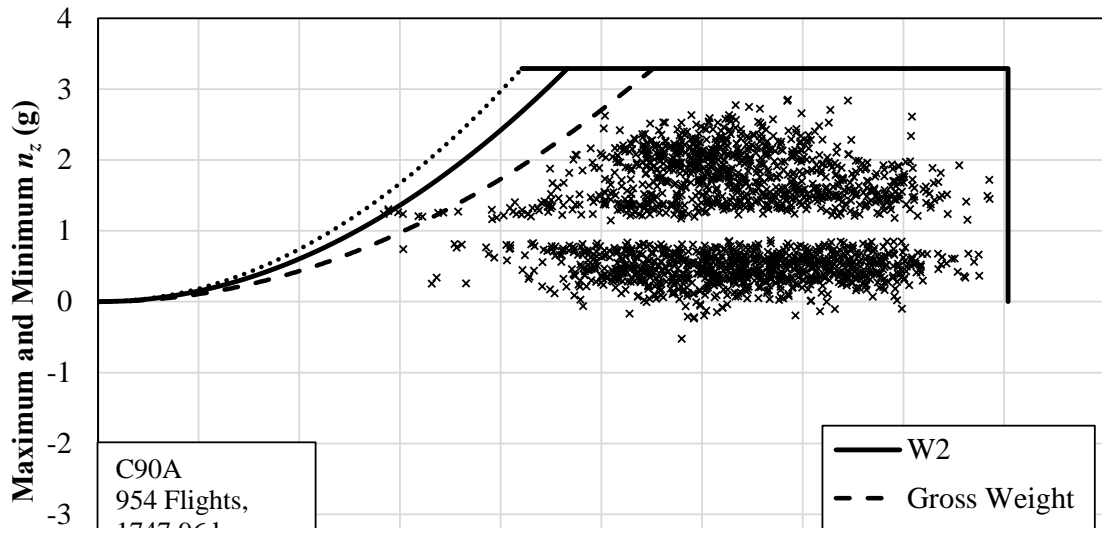


Figure 3.17:  $V-n$  Diagram for King Air C90GT

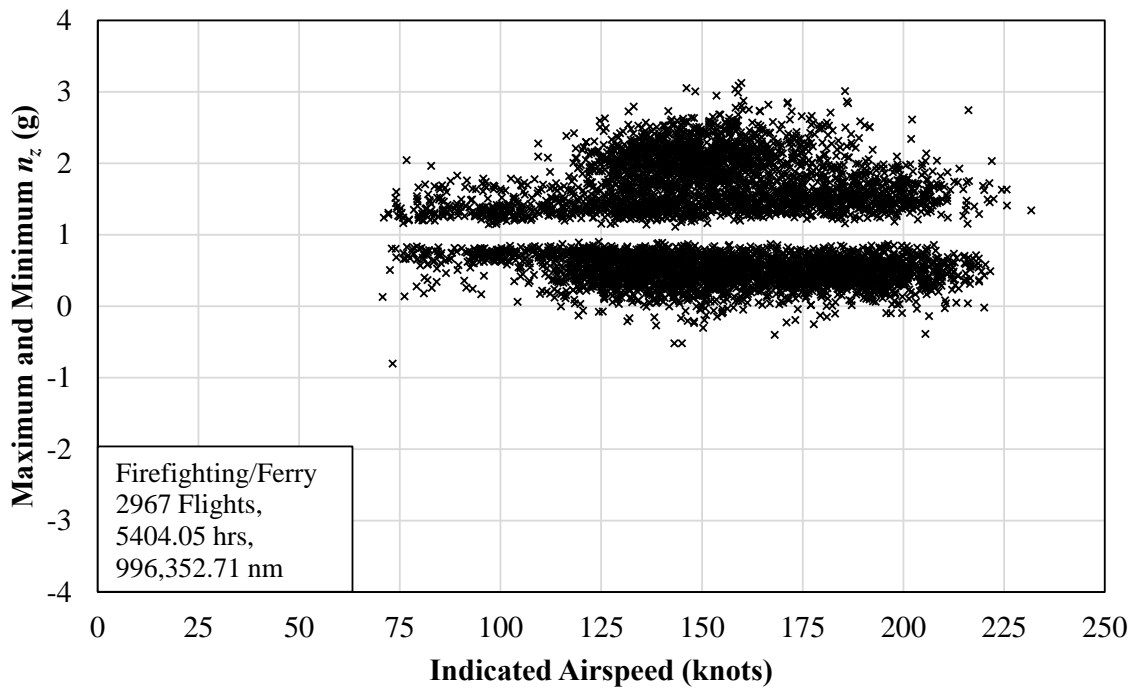
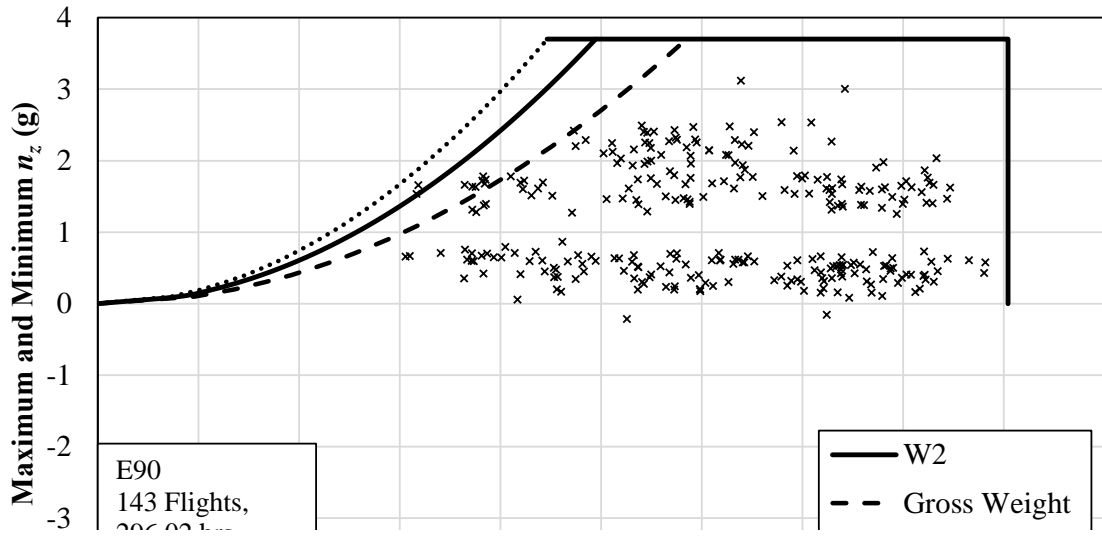


Figure 3.19:  $V$ - $n$  Diagram for Firefighting/Ferry Flights

A summary of the recorded maximum and minimum pitch and roll angles is shown in Table 3.5. The reader is reminded that  $\pm 30$  degrees in pitch and  $\pm 80$  degrees in roll were the limits used to separate the Extreme Attitude flights.

Table 3.5: Summary of Pitch and Roll Angles

	Pitch Angle (deg)		Roll Angle (deg)	
	Positive	Negative	Positive	Negative
Maximum	29.9	0.6	78.3	-1.8
Minimum	0.9	-29.1	1.3	-79.8
Average	15.1	-9.7	39.2	-44.1
Standard Deviation	4.6	4.9	17.4	19.4

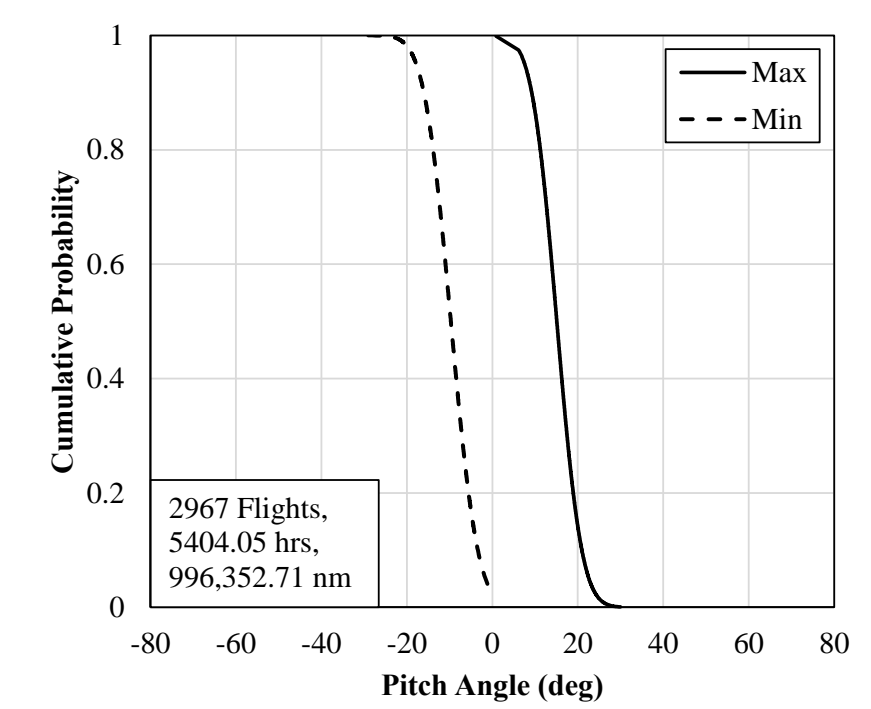


Figure 3.20: Cumulative Probability of Pitch Angle for Overall Flights

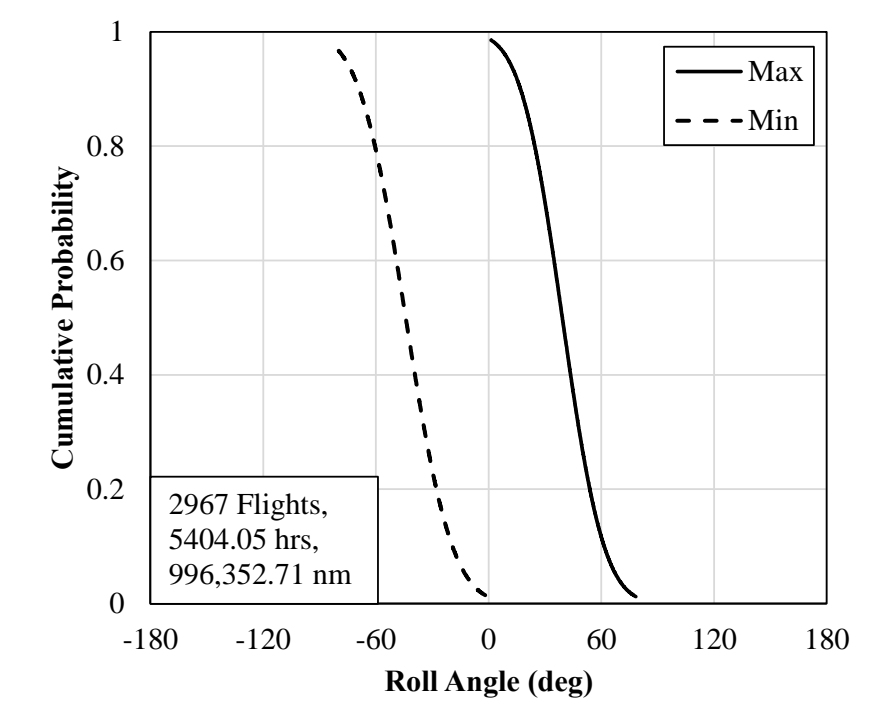


Figure 3.21: Cumulative Probability of Roll Angle for Overall Flights

Figures 3.22 and 3.23 show the maximum and minimum pitch and roll angles for the Firefighting and Ferry flights. The former shows that majority of the flights (89.6%) had pitch angles less than  $\pm 20$  degrees. The latter figure shows no trend in the roll angles. In these figures, the dashed lines depict the limits separating Extreme Attitude flights.

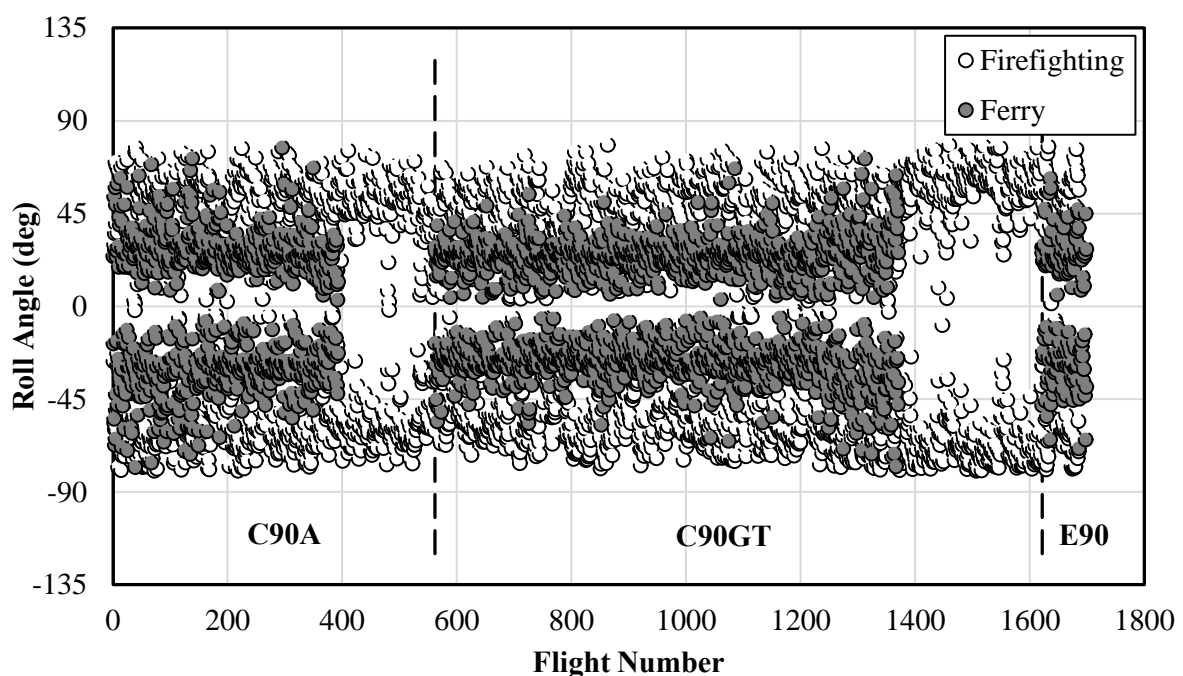
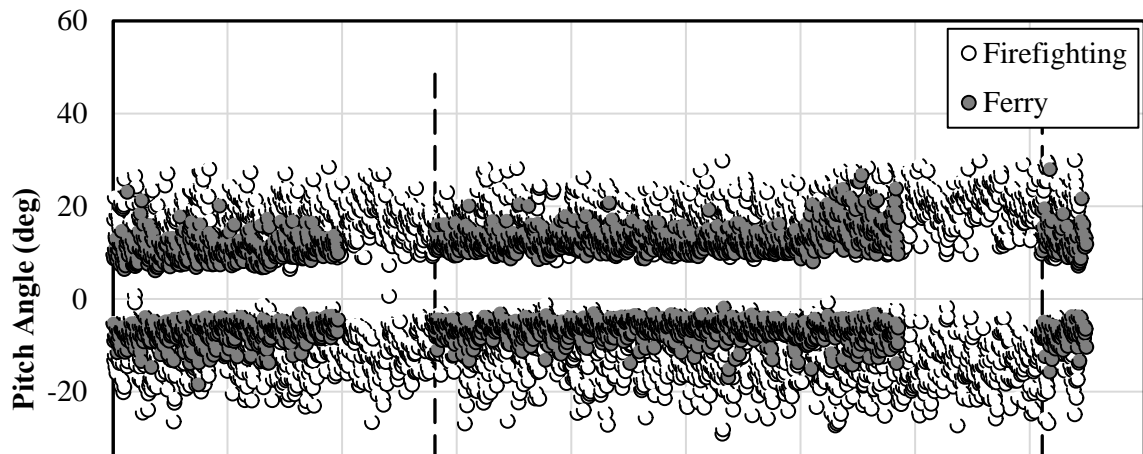


Figure 3.23: Maximum and Minimum Roll Angle for Firefighting/Ferry Flights

### 3.3 Phase-Specific Results

#### 3.3.1 Cruise Phases

The cruise phases were categorized as Cruise-1 and Cruise-2. As discussed in Section 2.9.3, the flight segment from takeoff to the first Entry or Turn was defined as Cruise-1 and that from the last Exit or the last Turn to landing was defined as Cruise-2. In the entire dataset, 1478 occurrences of Cruise-1 and Cruise-2 each were identified. Since Extreme Attitude flights were not part of a typical firefighting mission, cruises that were part of these flights were not included in the analysis. This reduced the number of cruises to 1361.

The correlations between the indicated airspeed and MSL altitude for Cruise-1 and Cruise-2 are shown in Figures 3.24 and 3.25 respectively. Both cruise phases showed nearly identical scatter of data with the maximum MSL altitude largely concentrated between 5000 to 15,000 feet MSL altitude, with very few flights exceeding 25,000 feet and none above 30,000 feet. Figures 3.26 and 3.27 show that at their maximum indicated airspeed, the aircraft were never flown above 20,000 feet MSL altitude. These figures also show the published VNE and a value 10% above that. Again, it is obvious from these figures that the maximum indicated airspeeds were exceeded in a number of cases, but remained below 10% above the published limits.

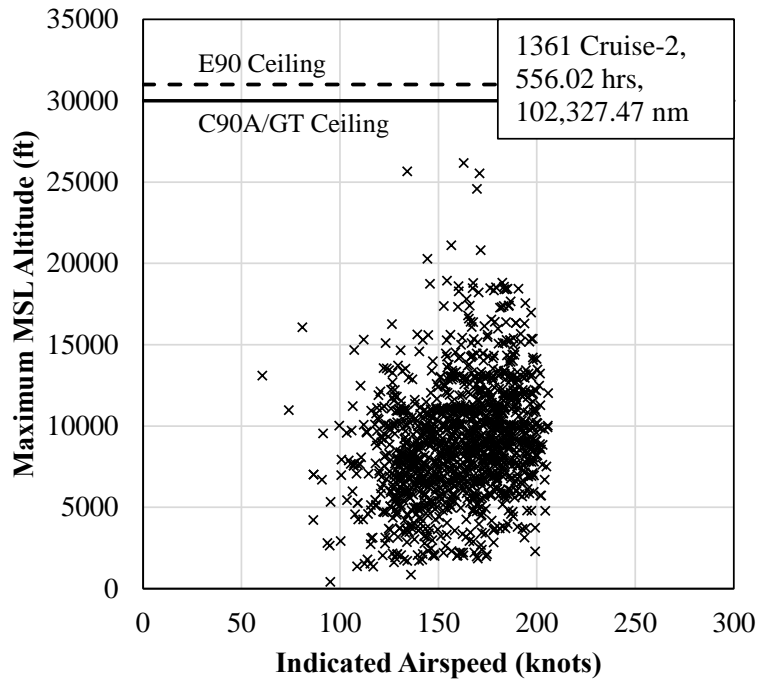
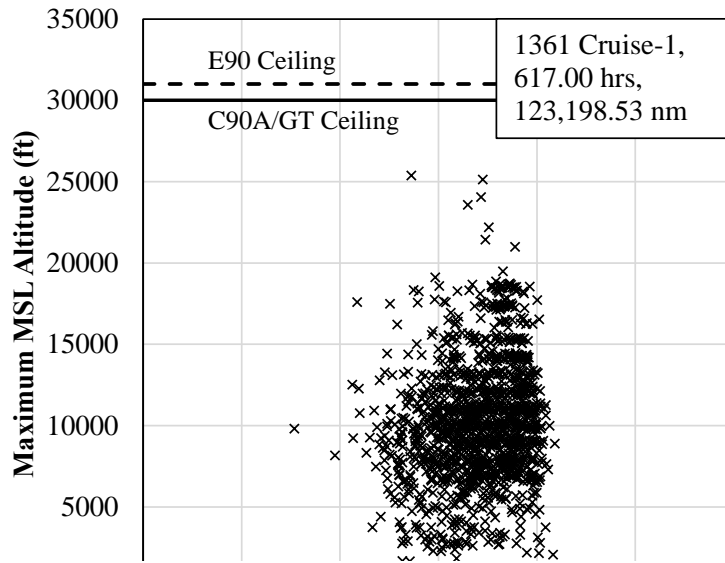


Figure 3.25: Flight Distance Correlated with Maximum MSL Altitude for Cruise-2 Phase

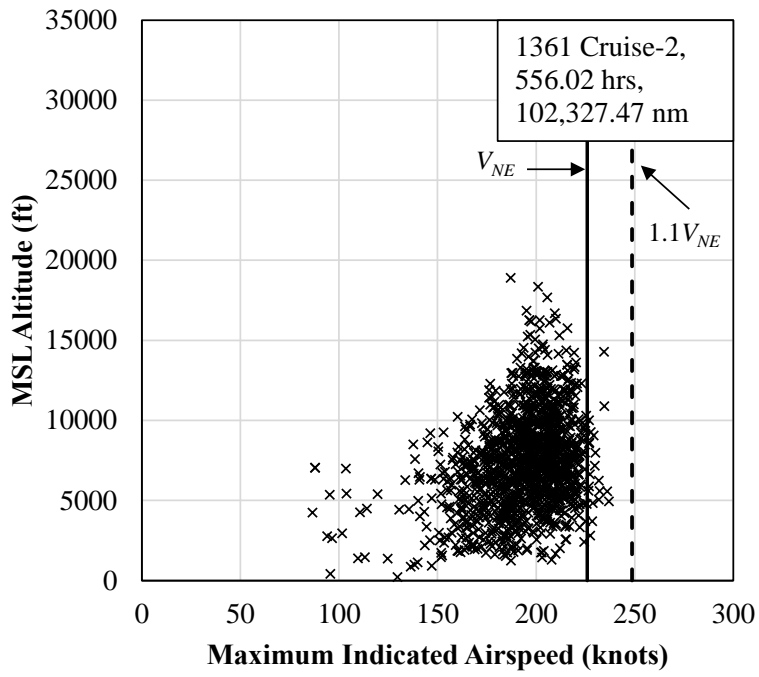
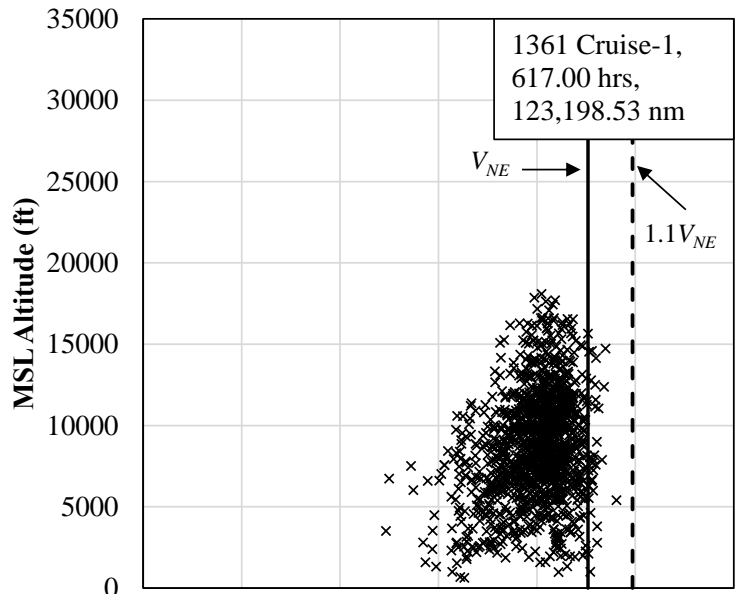


Figure 3.27: Maximum Indicated Airspeed Correlated with MSL Altitude for Cruise-1 Phase

The absolute maximum and minimum values of the pitch and the roll angles for the Cruise-1 and Cruise-2 phases are summarized in Tables 3.6 and 3.7 respectively. In general, average maximum pitch angle during Cruise-1 were slightly smaller than Cruise-2, perhaps due to the difference in weight during the two phases.

Table 3.6: Maximum and Minimum Pitch and Roll Angles for the Cruise-1 Phase

	<b>Pitch Angle (deg)</b>		<b>Roll Angle (deg)</b>	
	<b>Max</b>	<b>Min</b>	<b>Max</b>	<b>Min</b>
Maximum	28.8	4.8	76.7	-3
Minimum	6	-23.9	0.8	-76.4
Average	12.8	-5.2	31.1	-36.8
Standard Deviation	3.1	3.9	15.4	16

Table 3.7: Maximum and Minimum Pitch and Roll Angles for the Cruise-1 Phase

	<b>Pitch Angle (deg)</b>		<b>Roll Angle (deg)</b>	
	<b>Max</b>	<b>Min</b>	<b>Max</b>	<b>Min</b>
Maximum	27.4	3.6	76.7	-0.8
Minimum	2.4	-24.7	1.1	-79.2
Average	10.8	-7.7	33.4	-39.3
Standard Deviation	4.3	3.4	14.1	14.6

Figures 3.28 through 3.31 show the cumulative probabilities for maximum and minimum pitch and roll angles for Cruise-1 and Cruise-2 respectively. Since, the averages of the maximum roll angles for the two phases were very similar, both the figures show equal probability of left and right turns.

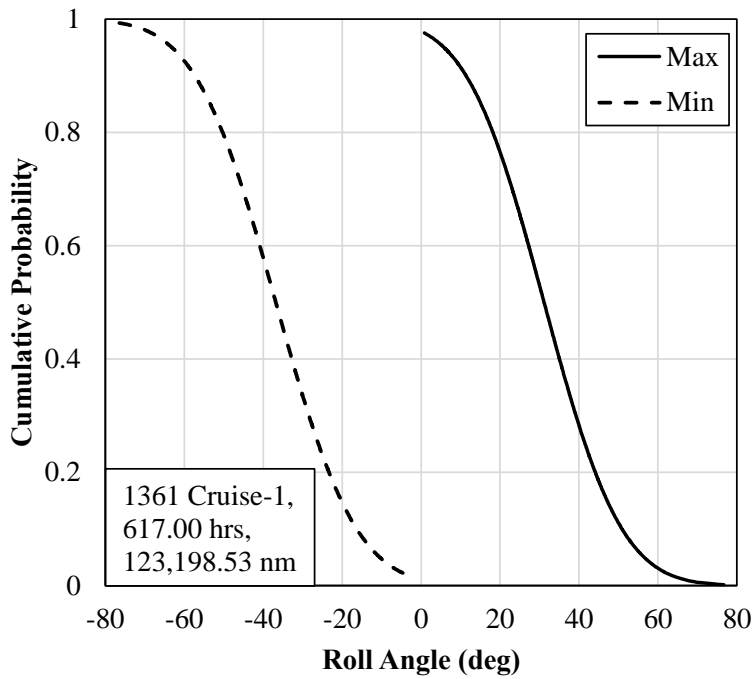
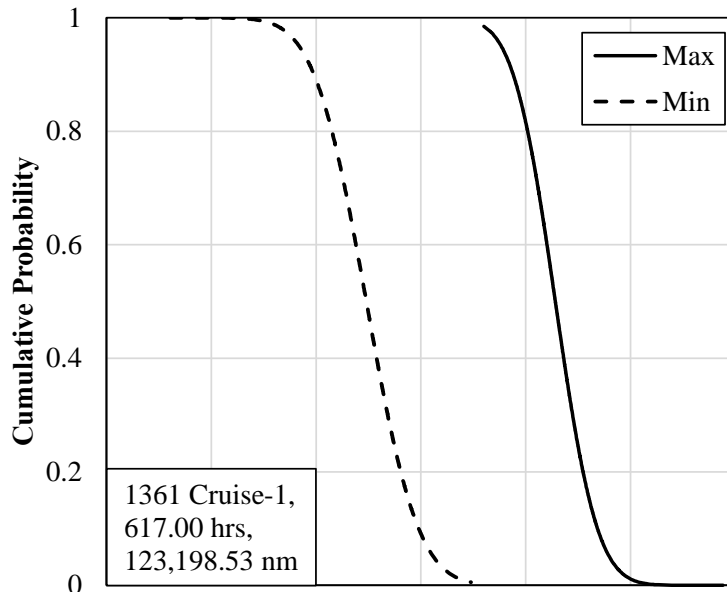


Figure 3.29: Cumulative Probability of Maximum and Minimum Roll Angle for Cruise-1 Phase

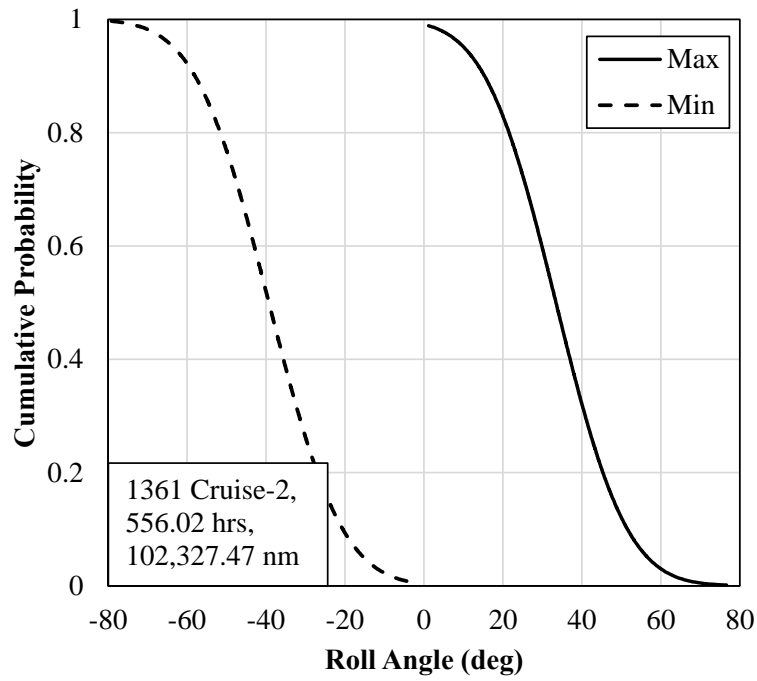
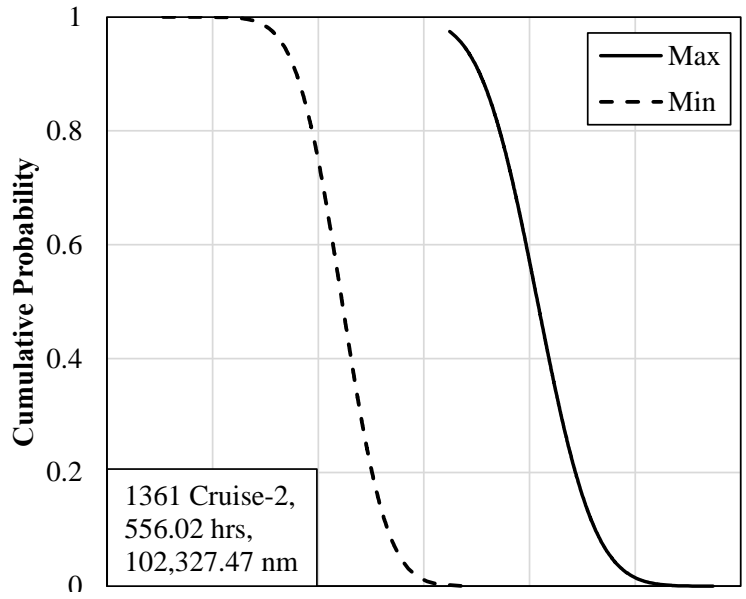


Figure 3.31: Cumulative Probability of Maximum and Minimum Roll Angle for Cruise-2 Phase

Cruise-1 and Cruise-2 distances and durations are shown in Table 3.8. The average times in both cruise phases were very similar but the distance flown during Cruise-2 was shorter than in Cruise-1. The average durations of Cruise-1 and Cruise-2 were 27.2 minutes and 24.5 minutes, respectively. The average distances of Cruise-1 and Cruise-2 were 90.5 nm and 75.2 nm, respectively.

Table 3.8: Cruise Phase Distance and Duration

	<b>Cruise-1</b> <b>1361 cases</b>		<b>Cruise-2</b> <b>1361 cases</b>	
	<b>Duration</b> <b>(min)</b>	<b>Distance</b> <b>(nm)</b>	<b>Duration</b> <b>(min)</b>	<b>Distance</b> <b>(nm)</b>
Maximum	240.2	636.3	173.6	476.3
Average	27.2	90.5	24.5	75.2
Standard Deviation	23.2	83.1	18.8	58.2
Total	37,020.10	123,198.50	33,361.20	102,327.50

The  $V-n$  diagrams for the Cruise-1 and Cruise-2 phases are shown in Figures 3.32 and 3.33. As expected, at no time during the Cruise-1 did the aircraft exceed the limit loads. However, in the case of Cruise-2, a few cases appeared outside of the boundaries shown in these figures. This could be attributed to the rough estimate of the aircraft weight in construction of the stall boundaries. At higher airspeeds, typical of a cruise, the loads were well below the operational limits.

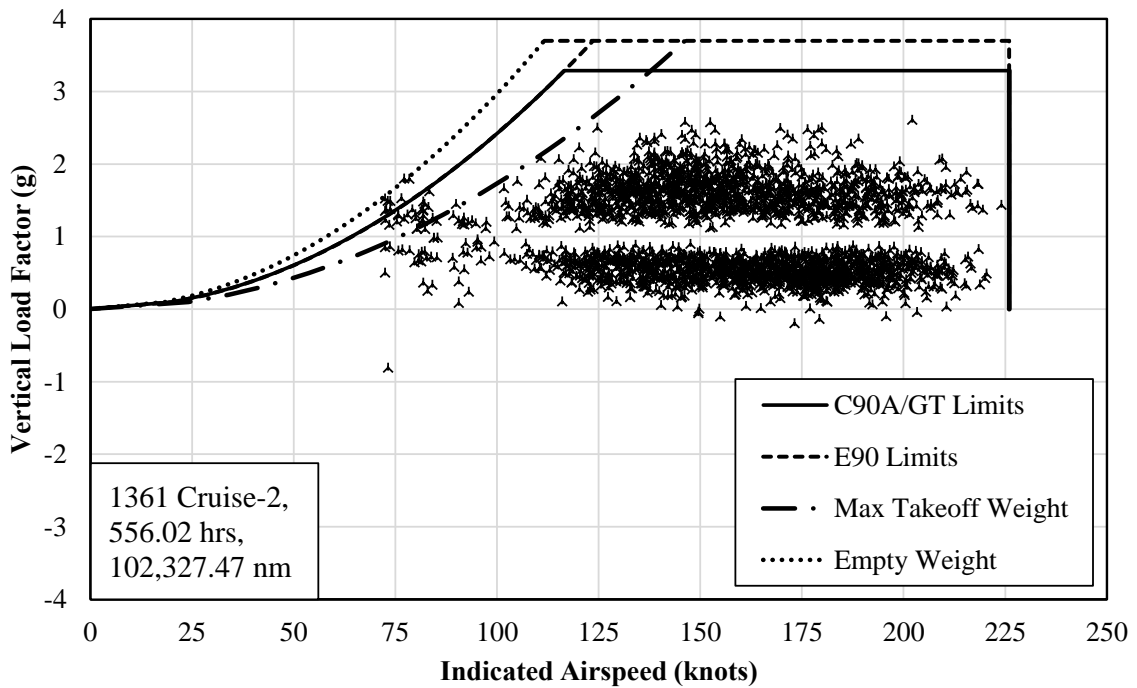
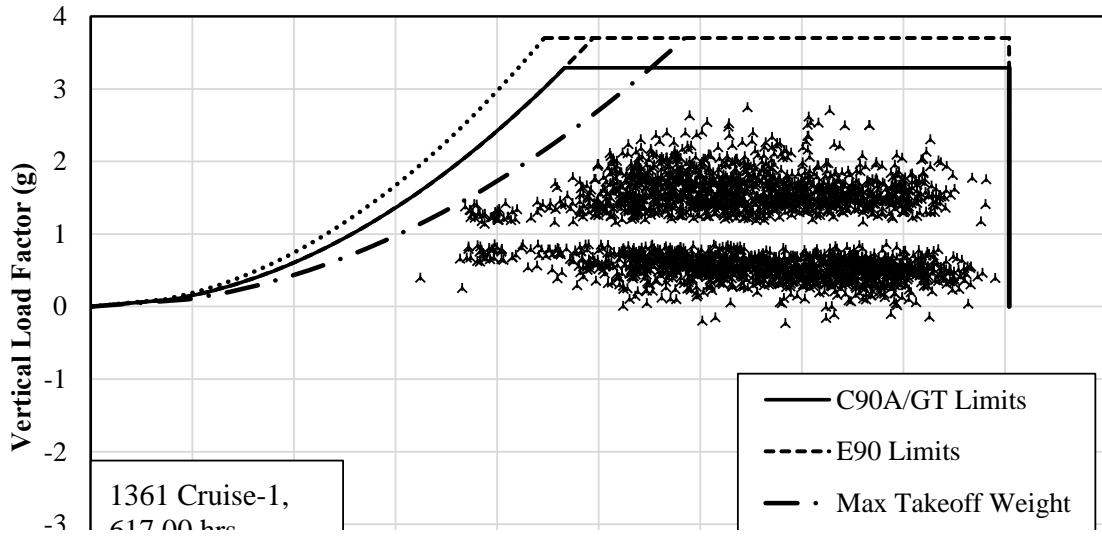


Figure 3.33: *V-n* Diagram for Cruise-2 Phase

### 3.3.2 Turns Phase

The Turn phases were defined in Section 2.9.2 as those when the data indicated continuous change in heading totaling to greater than 360 degrees. Using this criterion, 14,935 turns were identified within the dataset excluding the extreme attitude files.

The correlation between the indicated airspeed and MSL altitude for this phase is shown in Figures 3.34 and 3.35. During this phase, the MSL altitude never exceeded 20,000 feet. The maximum operating indicated airspeed was never exceeded. The largest airspeed during a Turn phase was 221 KIAS that occurred at 950 feet MSL. These two figures show that the MSL altitudes for the Turns ranged from 400 feet to about 15,000 feet with the majority (99%) being below 12,000-foot MSL. This distribution of altitudes was consistent with ATGS and ASM/Lead missions. Generally, ATGS missions include Turns at around 2500 feet AGL during surveillance and tactical operations. On the other hand, Turns associated with ASM/Leads missions are flown at much lower altitudes. Turns at altitudes lower than 300 feet were included in the Lead phases and were not included in these results.

Although there were Turns at indicated airspeed greater than 180 knots, they only accounted for two percent of the cases. This meant that nearly 98% of the Turns were flown at maximum indicated airspeed between 100 knots and 180 knots.

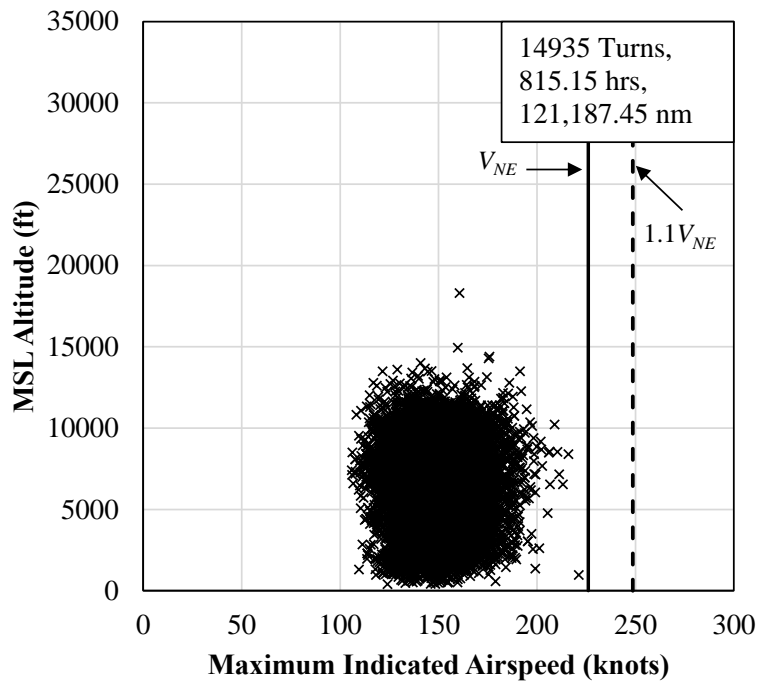
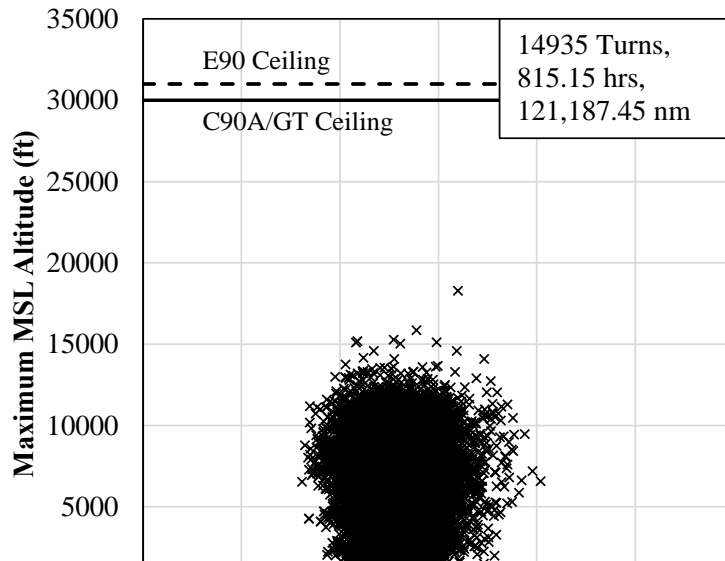


Figure 3.35: Maximum Indicated Airspeed Correlated with MSL Altitude for Turns Phase

The maximum and minimum pitch and the roll angles for this phase are summarized in Table 3.9. The maximum and minimum roll angles varied over a wide range of values. However, left turns showed a higher probability of occurrence since the probability of occurrence of maximum roll was high for negative values.

Table 3.9: Maximum and Minimum Pitch and Roll Angles for the Turns Phase

	Pitch Angle (deg)		Roll Angle (deg)	
	Max	Min	Max	Min
Maximum	30	6	78.3	26.3
Minimum	0.8	-28.1	-24.6	-79.8
Average	11.8	-4.9	14.8	-40.3

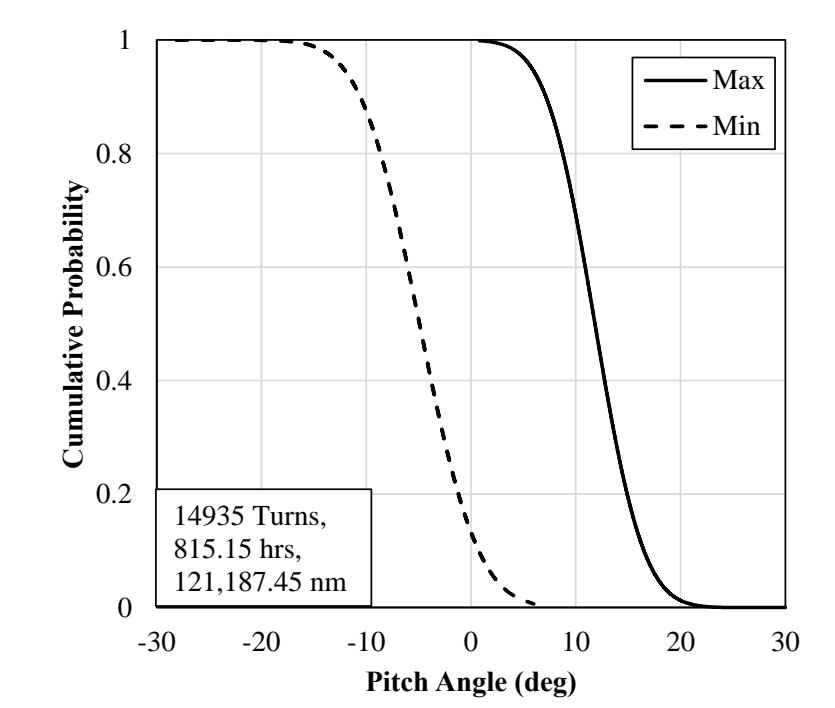


Figure 3.36: Cumulative Probability of Maximum and Minimum Pitch Angle for Turns Phase

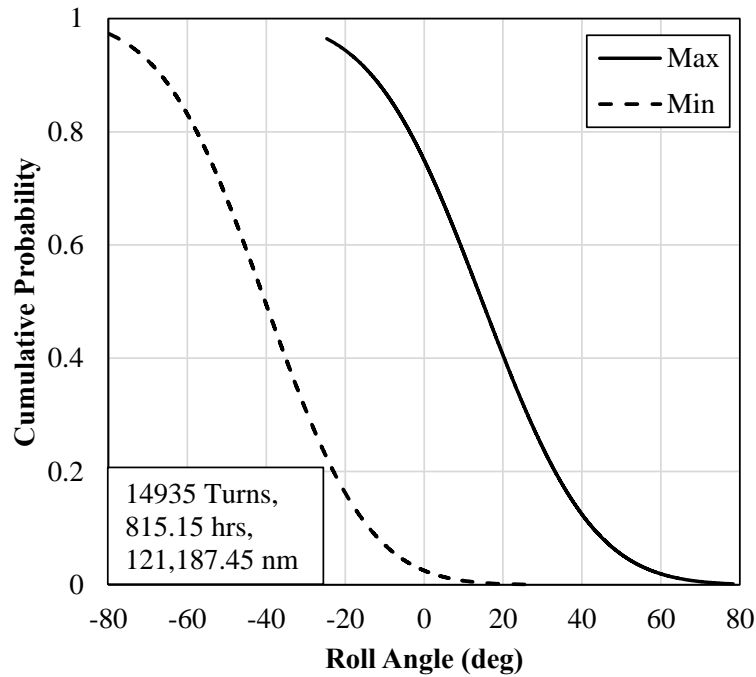


Figure 3.37: Cumulative Probability of Maximum and Minimum Roll Angle for Turns Phase

The Turn phase total duration and distance are summarized in Table 3.10. An average Turn phase was 3.3 minutes long and traversed just more than eight nautical miles.

Table 3.10: Turns Phase Duration and Distance

	<b>Turns</b>	
	<b>14935 Cases</b>	
	<b>Duration (min)</b>	<b>Distance (nm)</b>
Maximum	95.6	243.6
Average	3.3	8.1
Standard Deviation	2.5	6.2
Total	48909	121187.5

The  $V-n$  diagram for the Turn phases is shown in Figure 3.38. The loads recorded during the Turn phases varied over a wide range of values. In a few cases, the loads greater than 3 g were detected but limits were never exceeded.

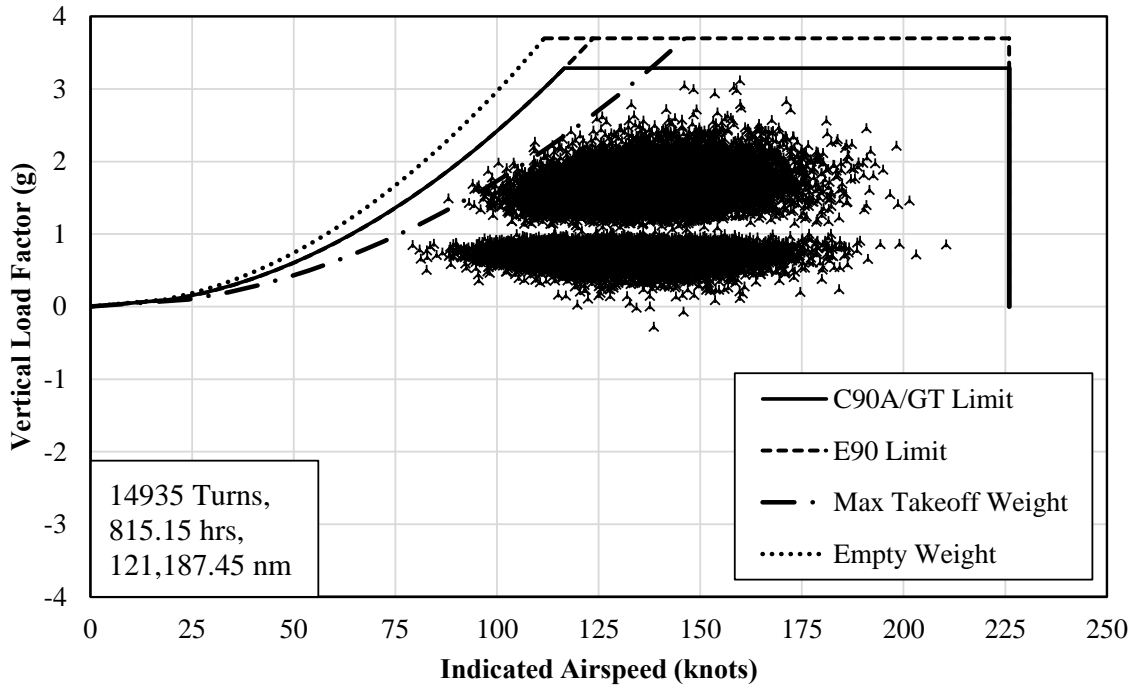


Figure 3.38: *V-n* Diagram for Turns Phase

### 3.3.3 Entry

Entry phases were chosen to have a duration of one minute before the start of the Lead phase. Entry phases are characterized by descending to a low altitude at airspeeds around 100 to 150 knots. The airspeeds are chosen to match the performance of the following air tankers.

There were 3659 Entry phases found in Firefighting flights. The correlation between the indicated airspeed and MSL altitude for Entry phase is shown in Figures 3.39 and 3.40. The majority (97.9%) of the entry phases had the maximum MSL altitudes between 600 feet and 10,000 feet. The higher MSL altitudes were due to the high-elevation terrain. Similarly, the majority (98.4%) of the phases had a maximum indicated airspeed between 110 and 180 KIAS. The average maximum airspeed during the Entry phase was 142.8 KIAS.

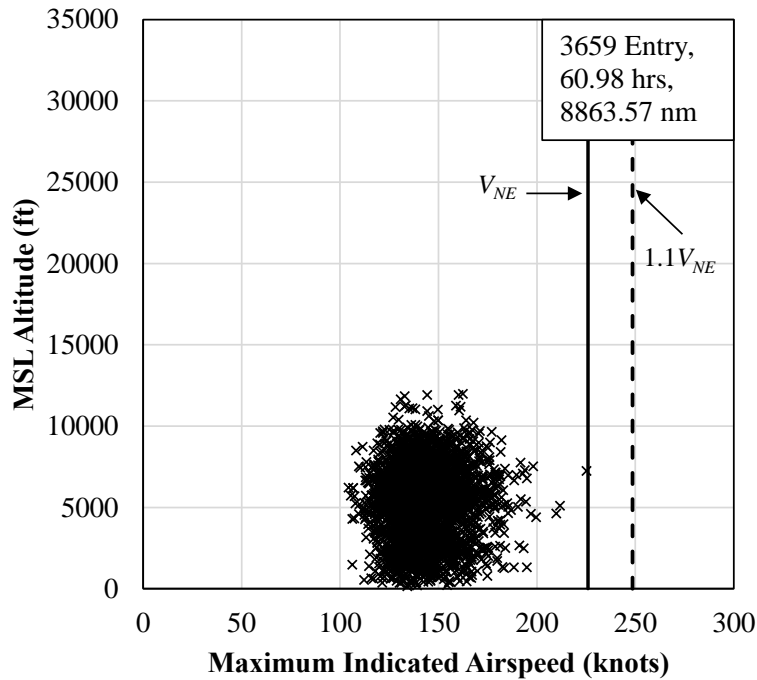
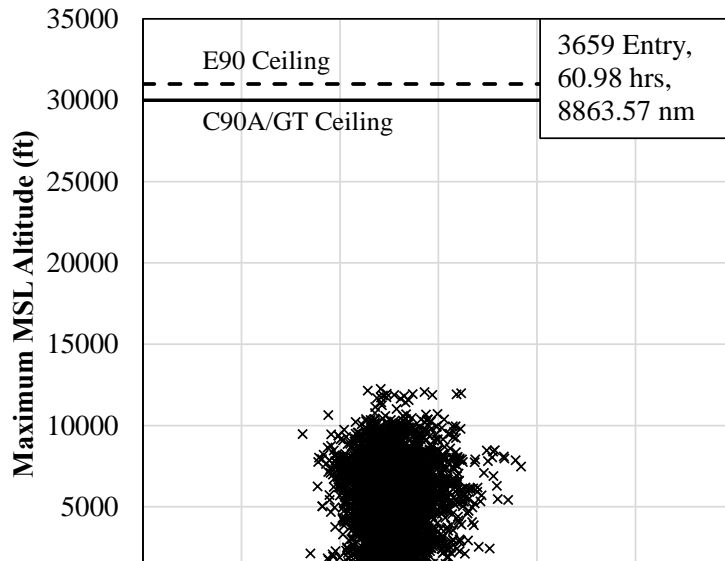


Figure 3.40: Maximum Indicated Airspeed Correlated with MSL Altitude for Entry Phase

Entry phase distance and duration statistics is shown in Table 3.11. The average distance flown during an Entry was 2.42 nautical miles.

Table 3.11: Entry Phase Duration and Distance

	<b>Entry 3659 Cases</b>	
	<b>Duration (min)</b>	<b>Distance (nm)</b>
Maximum	1	3.98
Average	1	2.42
Standard Deviation	0	0.26
Total	3659	8863.6

Table 3.12 shows the maximum and minimum pitch and roll angle statistics for the Entry phase. As expected, the average maximum roll angles were low compared to the average minimum.

Table 3.12: Maximum and Minimum Pitch and Roll Angles for the Entry Phase

	<b>Pitch Angle (deg)</b>		<b>Roll Angle (deg)</b>	
	<b>Max</b>	<b>Min</b>	<b>Max</b>	<b>Min</b>
Maximum	23.5	3	70.8	18.5
Minimum	-0.5	-22.7	-29.5	-78.9
Average	6.1	-5.6	13.6	-33.1
Standard Deviation	3.1	3.1	16.7	17.3

Figures 3.41 and 3.42 show the cumulative probabilities for maximum and minimum pitch and roll angles for the Entry phase. Since Entry phases are usually a left turning downward trajectory towards the drop area, the figures show higher probabilities of negative pitch and negative roll angles.

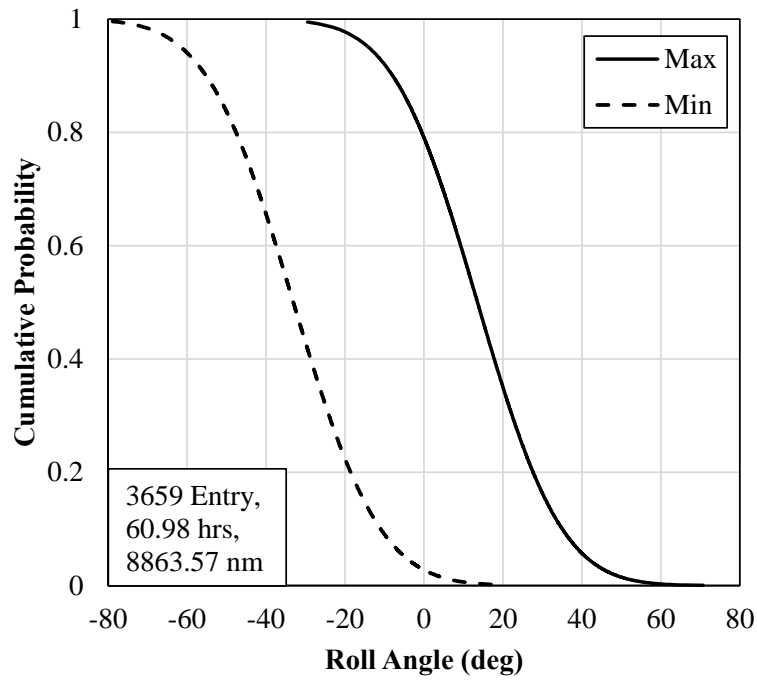
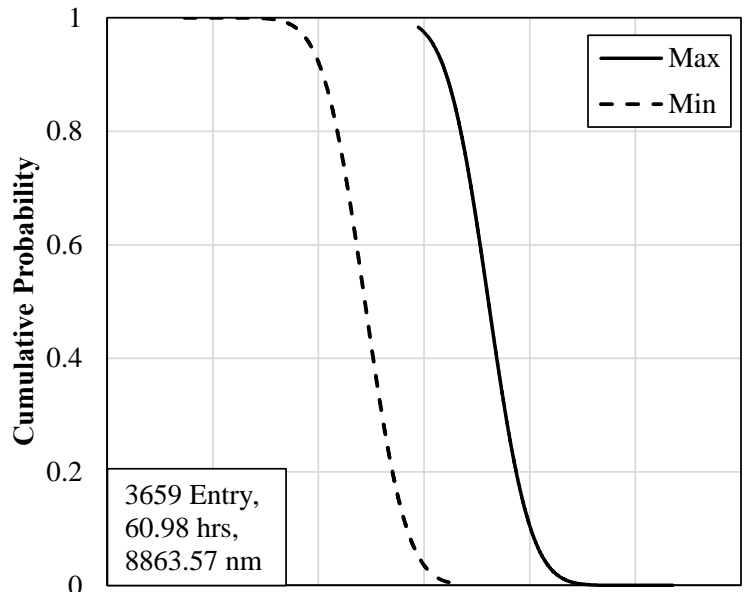


Figure 3.42: Cumulative Probability of Maximum and Minimum Roll Angle for Entry Phase

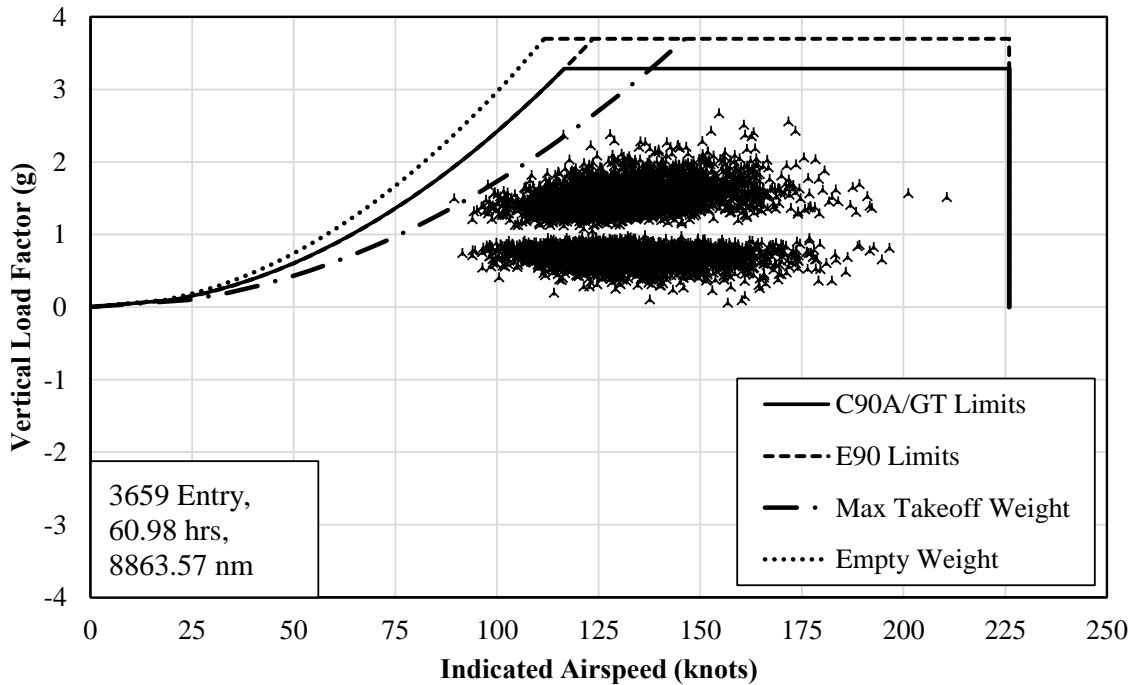


Figure 3.43:  $V$ - $n$  Diagram for Entry Phase

### 3.3.4 Lead

The Lead phase is characterized by low altitude (less than 300 feet AGL) level flights as they are used to lead the air tankers to the drop zone. During a typical ASM/Lead mission, while leading a tanker, the lead pilot releases a short smoke trail to mark the location of the start of the drop as well as showing the wind drift above the drop zone. The lead phase is also a low speed phase (100-140 KIAS) to allow the fully loaded air tankers to follow at pace. Since the available data did not have any indication for the smoke, all low altitude flights that fell within the criteria defined in 2.9.1 were tagged as Lead phases. As a result, some Lead phases showed relatively high indicated airspeeds, suggesting that they were misidentified.

There were 3659 Lead phases found. The correlation between the indicated airspeed and MSL altitude for Lead phases is shown in Figures 3.44 and 3.45. Only thirty-nine (0.9%) Lead phases had airspeeds above 180 KIAS and fewer than one percent were flown below 100 KIAS. The maximum MSL altitude was 11,845 feet and the minimum was 93 feet. The Leads with less than two minutes separating them were combined together. Therefore, some of the combined Leads included pull-ups and dives at higher than 300-foot AGL altitude.

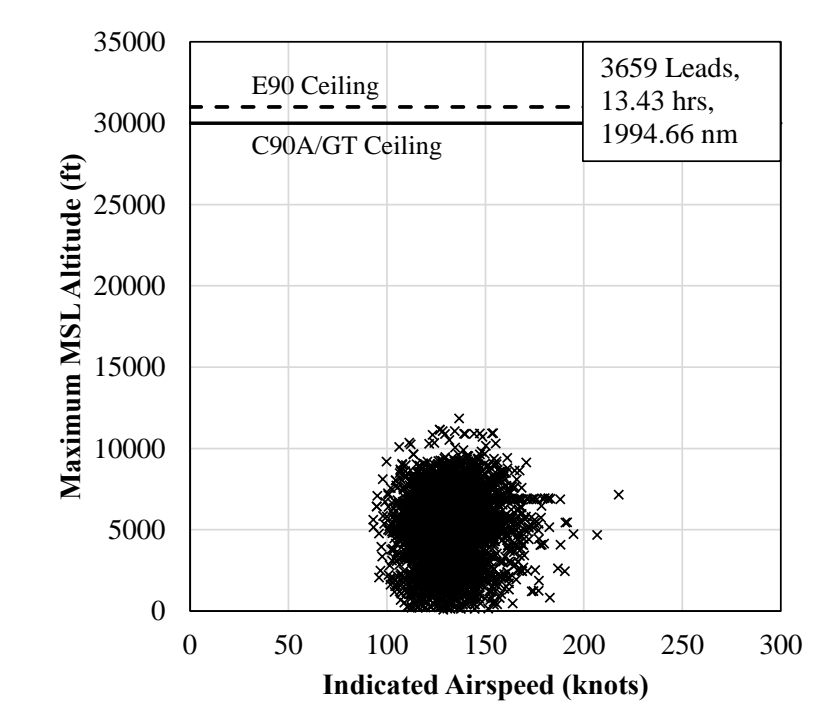


Figure 3.44: Flight Distance Correlated with Maximum MSL Altitude for Lead Phase

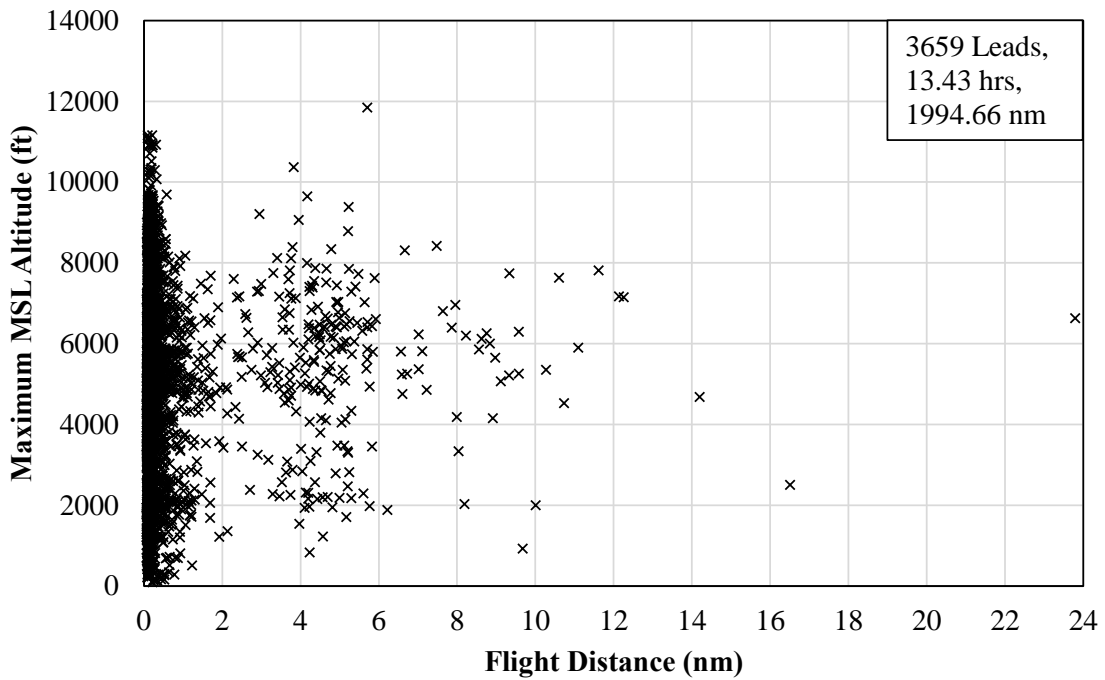
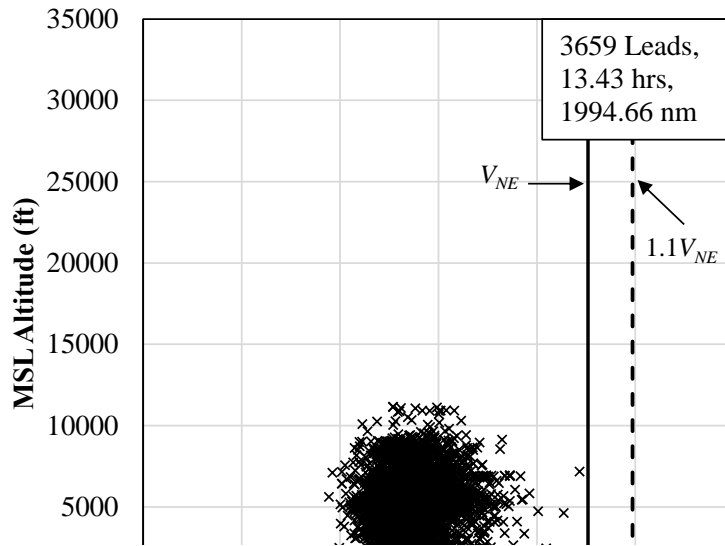


Figure 3.46: Maximum MSL Altitude correlated with Flight Distance for Lead Phase

Table 3.13 shows the Lead duration and distance statistics. According to this data, the average Lead phase lasted 12 seconds and the longest was 8.4 minutes. A typical Lead phase lasts only a few seconds, but the process of combining Leads resulted in longer times. The average distance flown is quite short.

Table 3.13: Lead Phase Duration and Distance

	<b>Lead 3659 Cases</b>	
	<b>Duration (min)</b>	<b>Distance (nm)</b>
Maximum	8.4	23.8
Average	0.2	0.55
Standard Deviation	0.5	1.36
Total	806	1994.7

Table 3.14 shows the maximum, minimum, average and standard deviation of the maximum and minimum pitch and roll angles during the Lead phase.

Table 3.14: Maximum and Minimum Pitch and Roll Angles for the Lead Phase

	<b>Pitch Angle (deg)</b>		<b>Roll Angle (deg)</b>	
	<b>Max</b>	<b>Min</b>	<b>Max</b>	<b>Min</b>
Maximum	18.7	12.3	66.3	49.2
Minimum	-4.5	-21	-49.8	-72.5
Average	5.9	1.6	4.2	-14.6
Standard Deviation	2.8	2.8	18.4	19.4

Figures 3.47 and 3.48 represent the cumulative probabilities for maximum and minimum pitch and roll angles for Lead phases. Examining these figures along with the data in Table 3.13, it is evident that the Leads were almost level flights with small variations in pitch and roll angles

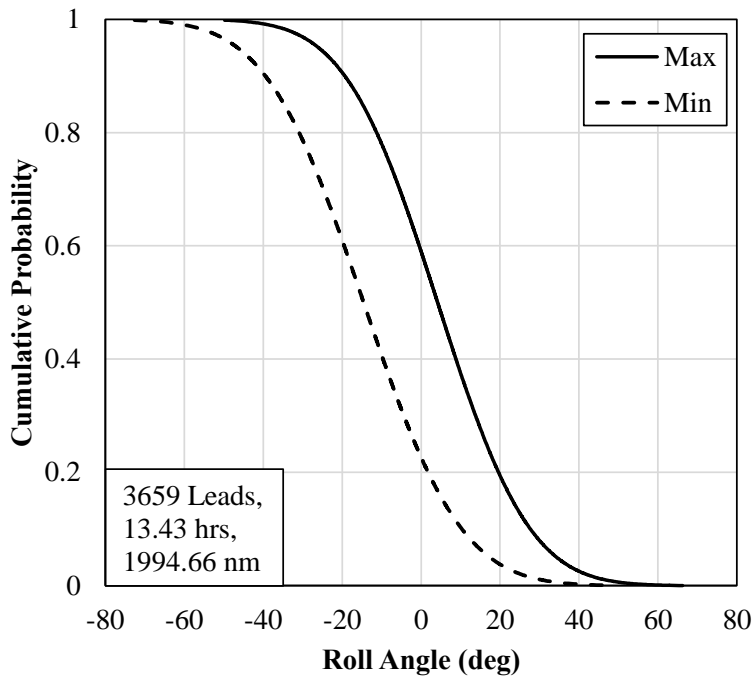
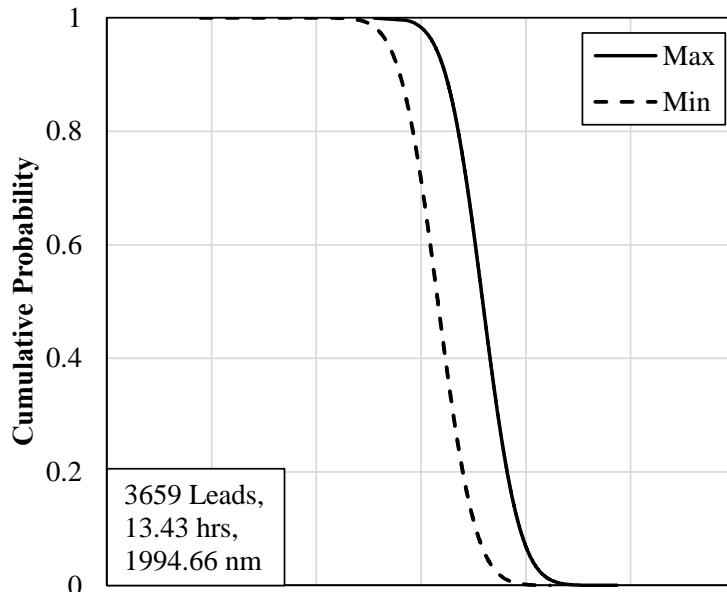


Figure 3.48: Cumulative Probability of Maximum and Minimum Roll Angle for Lead Phase

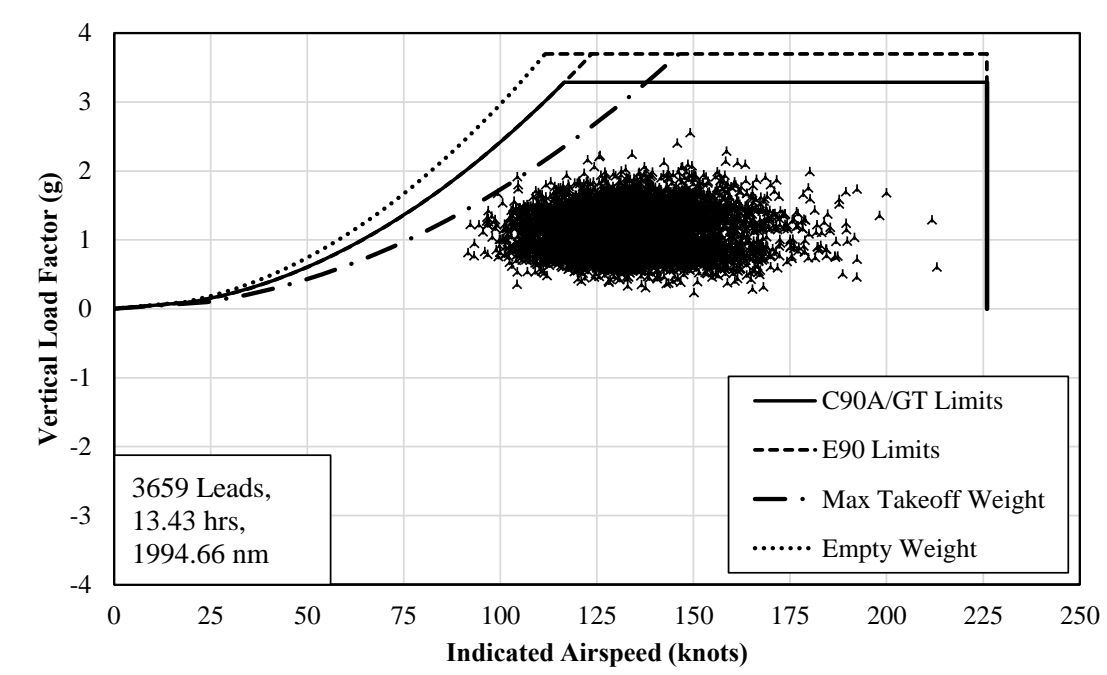


Figure 3.49:  $V-n$  Diagram for Lead Phase

### 3.3.5 Exit

The Exit phases were also chosen to have a fixed duration after the Lead. There were 3659 Exit phases found. Figures 3.50 and 3.51 show the correlation between the indicated airspeed and MSL altitude for the Exit phase.

The grouping of the data points in airspeed and altitude correlation for the Entry and Exit phases are nearly identical. For the Exit phases, the majority (98.8%) of the cases had indicated airspeeds between 110 and 180 KIAS. In addition, the majority (98.3%) of the cases had the maximum MSL altitudes between 600 feet and 10,000 feet. During a routine Exit after Lead, the lead plane would accelerate and pull-up to the left or right to ensure that the following air tanker would have enough space to exit the drop zone safely. This suggests that Exit phases involves more aggressive maneuvering. The Entry phase had an average maximum airspeed of 142.8 KIAS and that of Exit phase was 144.8 KIAS.

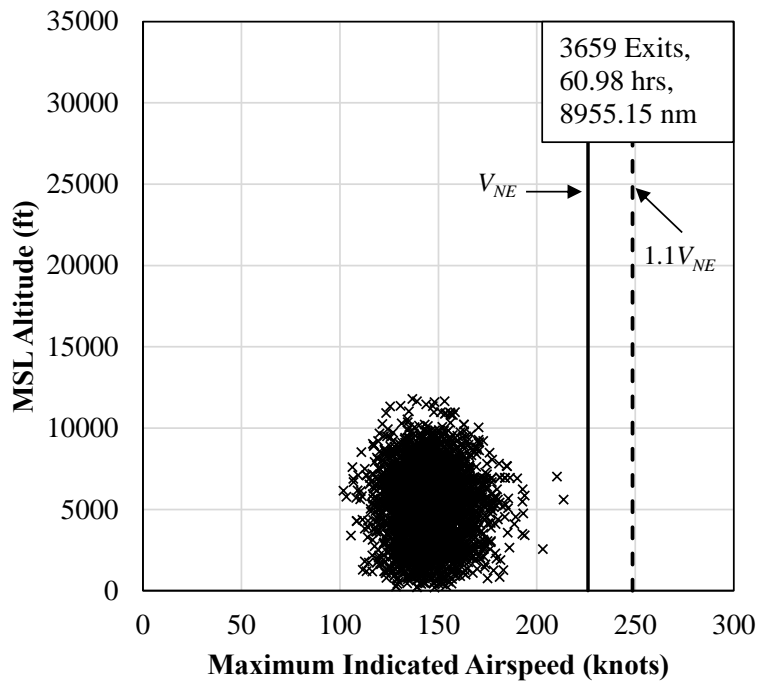
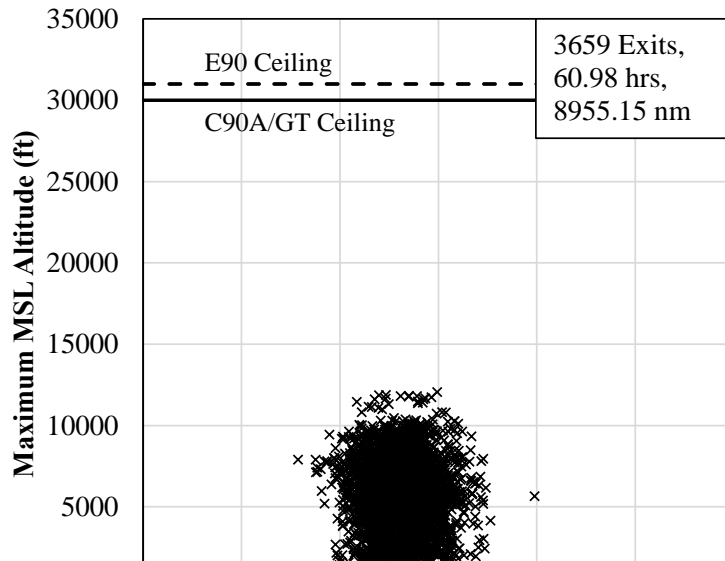


Figure 3.51: Maximum Indicated Airspeed Correlated with MSL Altitude for Exit Phase

Table 3.15 summarizes the usage statistics of the Exit phase. The average distance of the Exit phase was 2.45 nautical miles, which is slightly higher than that of the Entry phase. The total distance flown in the Exit phase being longer than the Entry suggests a higher average speed during the Exit phase.

Table 3.15: Exit Phase Duration and Distance

	<b>Exit 3659 Cases</b>	
	<b>Duration (min)</b>	<b>Distance (nm)</b>
Maximum	1	3.83
Average	1	2.45
Standard Deviation	0	0.24
Total	3659	8955.2

The maximum and minimum pitch and the roll angles for the Exit phase are summarized in Table 3.16. The magnitude of the average minimum roll angle was significantly higher than the average maximum suggesting a higher occurrence of negative roll.

Table 3.16: Maximum and Minimum Pitch and Roll Angles for the Exit Phase

	<b>Pitch Angle (deg)</b>		<b>Roll Angle (deg)</b>	
	<b>Max</b>	<b>Min</b>	<b>Max</b>	<b>Min</b>
Maximum	28.5	8	75.6	30.1
Minimum	1.3	-20.4	-44.1	-78.9
Average	12.1	0.2	11.8	-35.1
Standard Deviation	3.2	2.8	21.7	18.3

Figures 3.52 and 3.53 show the cumulative probabilities for maximum pitch and roll angles for Exit phases. These figures show a higher probability of positive pitch and negative roll angles. This would suggest that most common exit maneuver was a pull-up to the left.

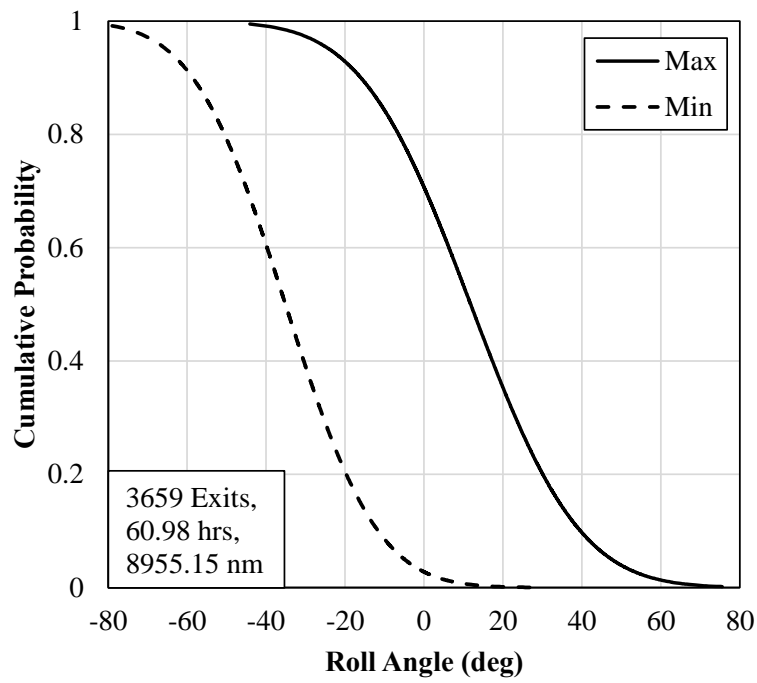
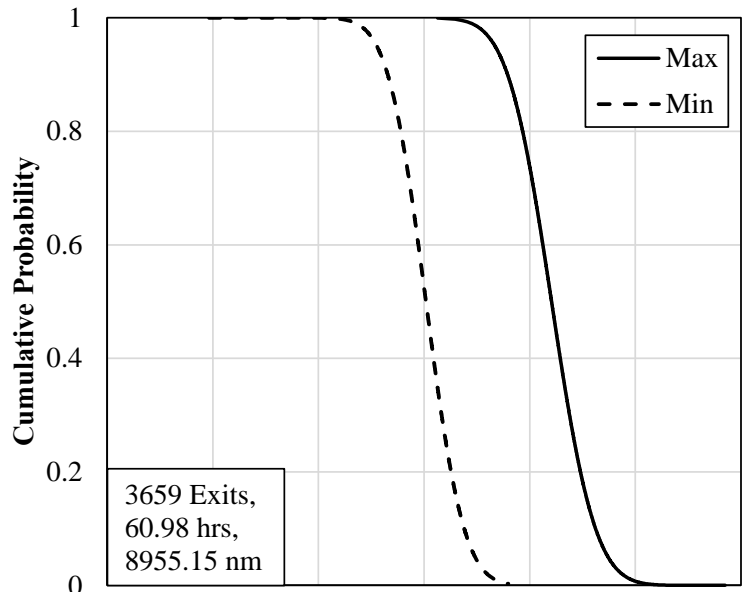


Figure 3.53: Cumulative Probability of Maximum and Minimum Roll Angle for Exit Phase

Figure 3.54 shows the  $V-n$  Diagram for the Exit phase. Since this phase typically

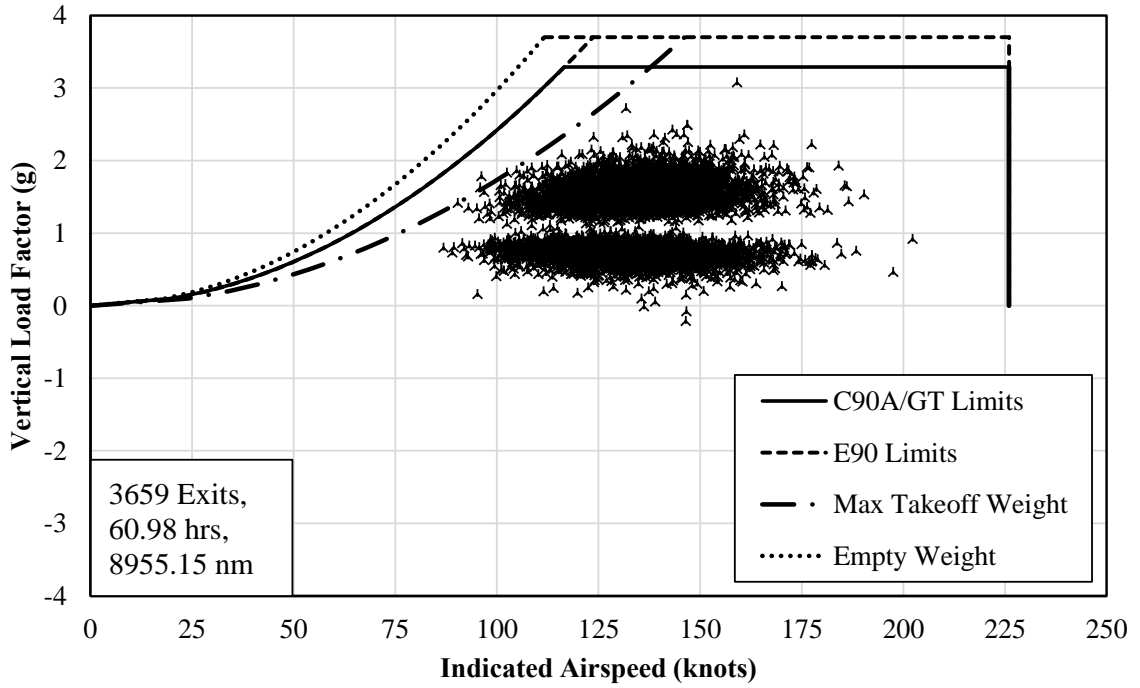


Figure 3.54:  $V-n$  Diagram for Exit Phase

## CHAPTER 4

### RESULTS AND DISCUSSION - AIRCRAFT LOADS

In this chapter, gust and maneuver loads for the overall flights as well as for each phase are examined. This includes a discussion of discrete gust velocities. The cumulative occurrences are presented in normalized form, per nautical mile as well as per 1000 hours. AGL altitude bands are used throughout.

#### 4.1 Overall Results

In this section, the vertical gust and maneuver loads and the discrete gust velocities are presented. The load factor cumulative occurrences were normalized per nautical mile as well as per 1000 hours. The cumulative occurrences of the loads are also presented for AGL altitude bands that were discussed in the previous chapter. The AGL altitude bands were chosen rather than MSL altitudes because of the better correlation of the data with the former. Figures 4.1 through 4.4 show the cumulative occurrence of the vertical gust and maneuver loads for complete flights in the entire data set. In case of the vertical gust loads, Figure 4.1 shows an inverse relationship between the load counts and the corresponding AGL altitude. Figure 4.2, which also represents the vertical gust loads, illustrates the results in terms of MSL altitudes. It is evident that here is no clear relationship between the MSL altitudes and the load counts. The same observation can be made from the cumulative occurrence plot of the vertical maneuver loads shown in Figures 4.3 and 4.4. The former contains the loads represented in the AGL altitude bands while the latter shows the data in MSL altitude bands. As the result of this comparison, the data in the remainder of this document is given in terms of AGL altitude bands.

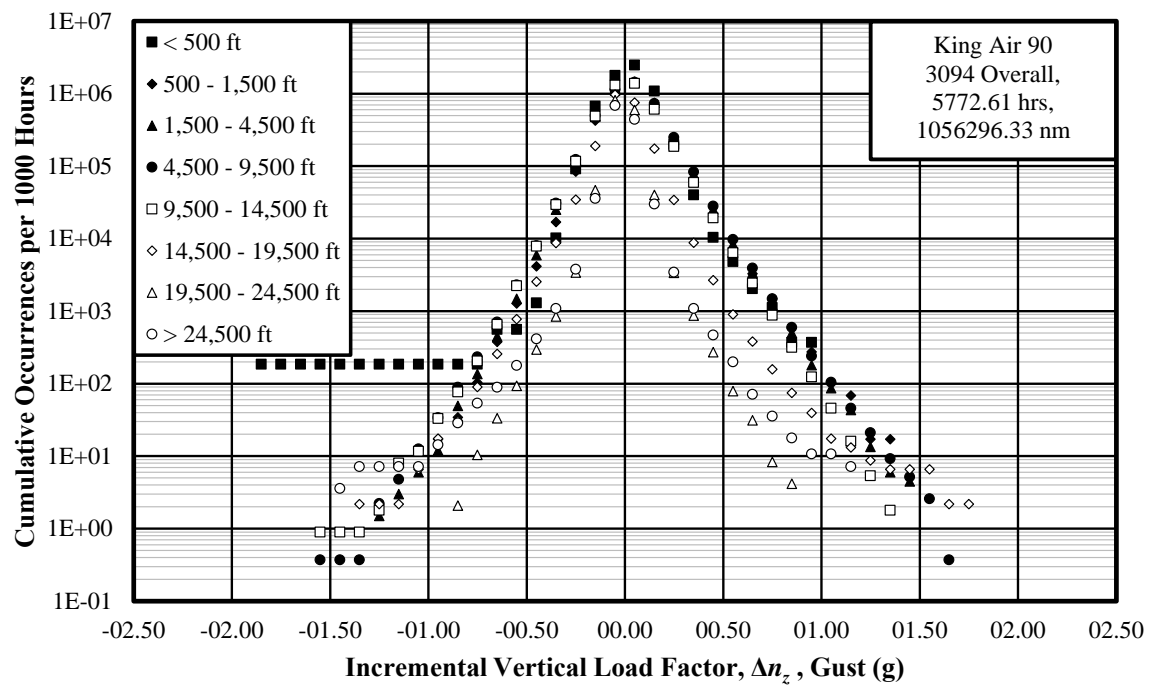
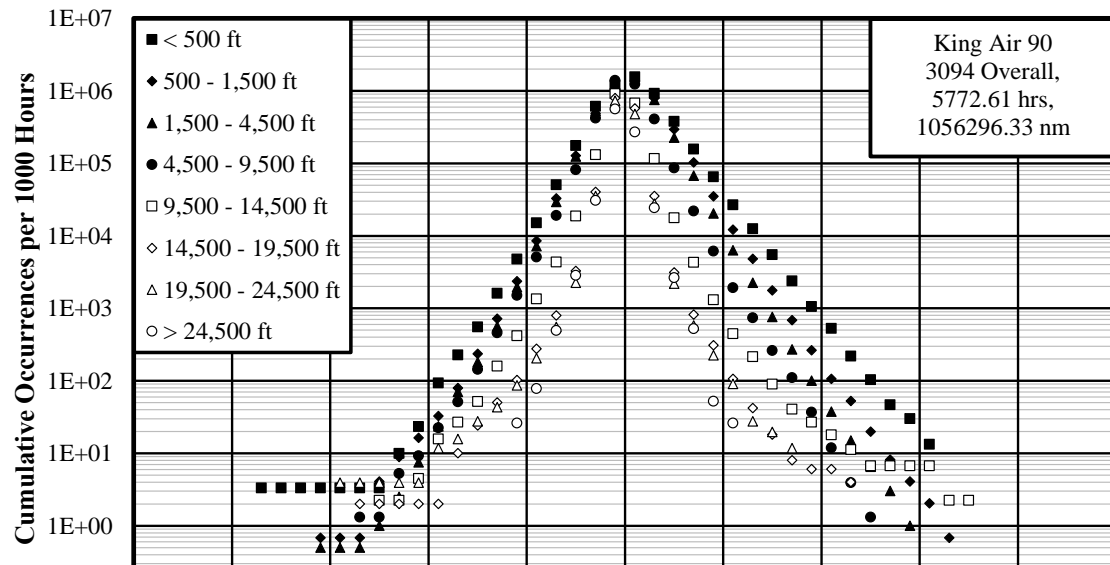


Figure 4.2: Cumulative Occurrences of Incremental Vertical Gust Load Factor per 1000 Hours - Overall (MSL Altitude)

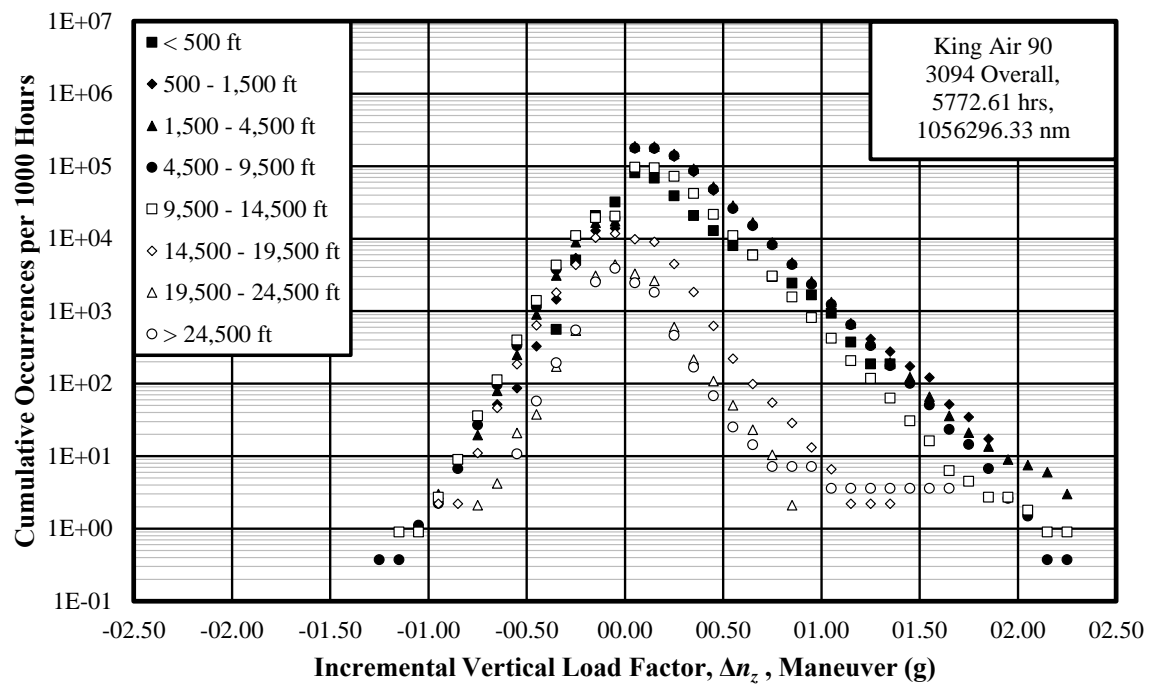
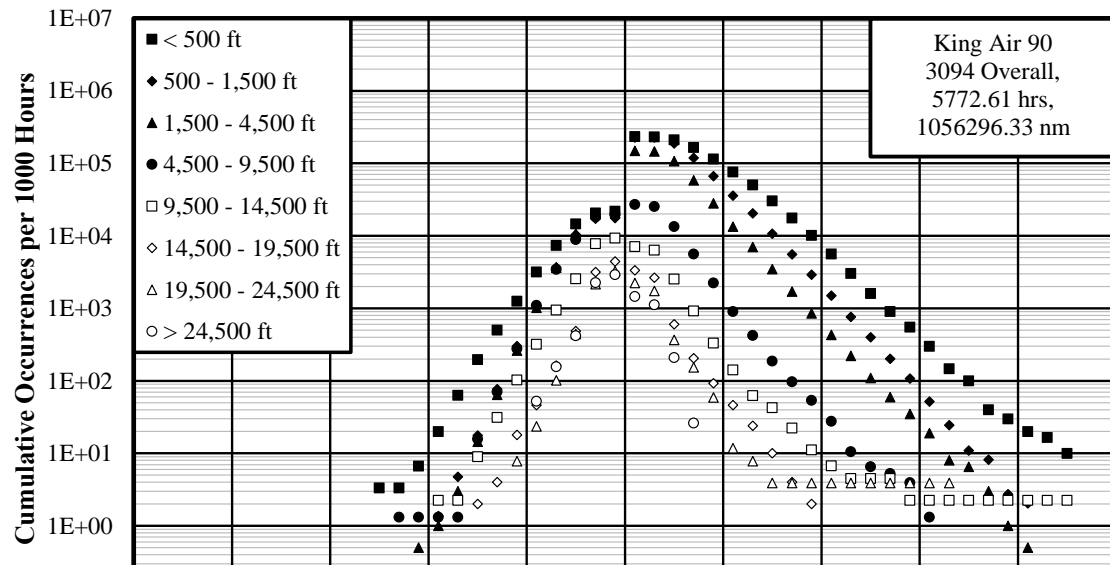


Figure 4.4: Cumulative Occurrences of Incremental Vertical Maneuver Load Factor per 1000 Hours - Overall (MSL Altitude)

For this section, flights were divided into three categories: 1) Extreme Attitudes, 2) Firefighting, and 3) Ferry missions. The Extreme Attitude flights were defined in Chapter 3 as those that exhibited unusually high pitch or roll angles. The Ferry flights were defined in Chapter 2 as those where the aircraft was flown from one location to another with an average speed of 150 knots or greater and did not have any Turn or Lead phases. The remaining flights were classified as Firefighting flights.

Table 4.1 lists the flight types and the time spent in each altitude band. It is clear that the Firefighting and Extreme Attitude flights took place mostly in the 500-4,500 feet altitude band whereas the Ferry flights were flown mostly at altitudes greater than 9,500 feet.

Table 4.1: Time in Altitude Band for Each Flight Type in Hours

<b>AGL Altitude /Phase</b>	<b>Time (hours)</b>			
	<b>Firefighting</b>	<b>Ferry</b>	<b>Extreme Attitude</b>	<b>Total</b>
< 500 ft.	249.35	27.79	24.47	301.61
500 – 1500 ft.	1276.60	56.16	135.66	1468.42
1500 – 4500 ft.	1654.49	186.89	158.22	1999.60
4500 – 9500 ft.	412.66	315.4	34.69	762.75
9500 – 14500 ft.	104.51	334.74	8.00	447.25
14500 – 19500 ft.	25.21	469.05	4.77	499.03
19500 – 24500 ft.	7.47	245.41	2.39	255.27
> 24500 ft.	0.61	37.76	0.02	38.39

Table 4.2 contains the distance flown in each altitude band by each of the flight types. Similar to the time spent in the altitude band, the Firefighting and Extreme Attitude flights were flown the most in the 500-4,500 feet altitude band. The Ferry flights were flown the most distance at altitudes greater than 9,500 feet.

Table 4.2: Distance Flown in Altitude Band for Each Flight Type in Nautical Miles

AGL Altitude /Phase	Distance (nm)			
	Firefighting	Ferry	Extreme Attitude	Total
< 500 ft.	36145.15	3335.41	3585.38	43065.94
500 – 1500 ft.	190826.78	8643.32	19672	219142.1
1500 – 4500 ft.	272720.46	35527.6	25478.7	333726.8
4500 – 9500 ft.	85208.34	68299	7475.47	160982.8
9500 – 14500 ft.	24704.36	78554.7	1897.14	105156.2
14500 – 19500 ft.	6140.89	114940	1165.66	122246.3
19500 – 24500 ft.	1844.79	60153.4	599.44	62597.59
> 24500 ft.	152.12	9150.99	5.83	9308.94

#### 4.1.1 Vertical Load Factor

The cumulative occurrences of the incremental vertical gust load factor per 1000 hours and per nautical mile for all altitude bands combined are shown in Figures 4.5 and 4.6. These figures provide a comparison of the Extreme Attitude, Firefighting, and Ferry flights. Despite the large vertical loads present in the Extreme Attitude flights, their trend agreed very closely with that of the Firefighting flights. In the case of Ferry flights, there was a noticeable difference in the cumulative occurrence. The difference was more significant over the positive load factors where the frequency of occurrence was nearly an order of magnitude lower than those of Firefighting flights. This outcome was expected because, ferry flights took place at higher altitudes.

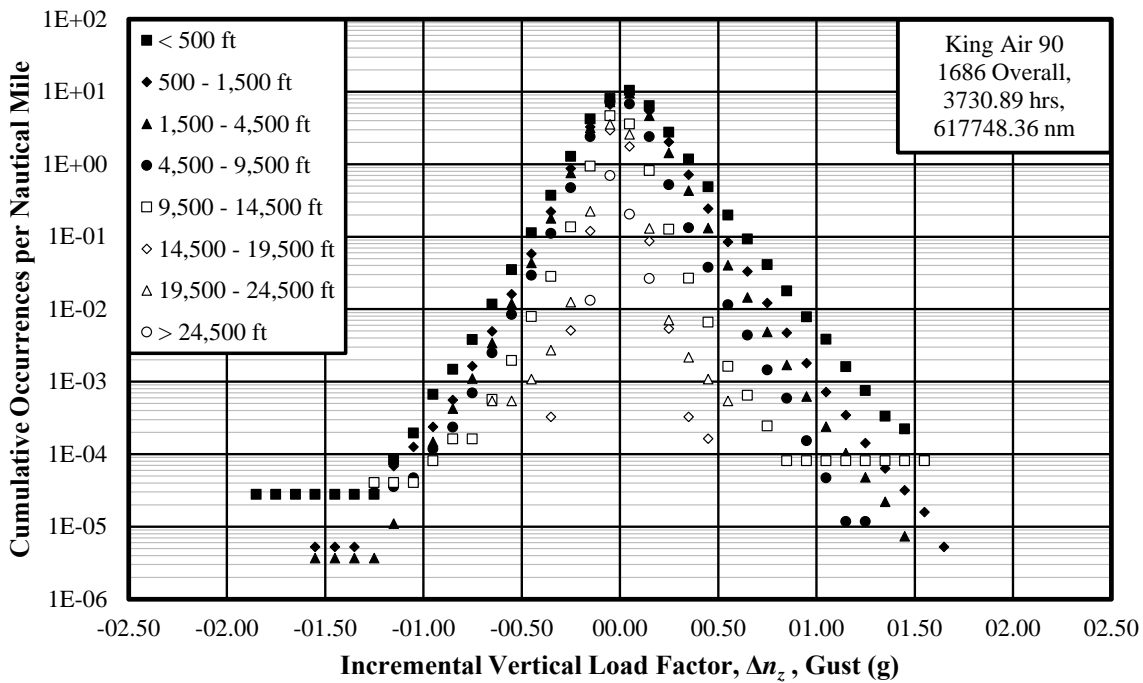
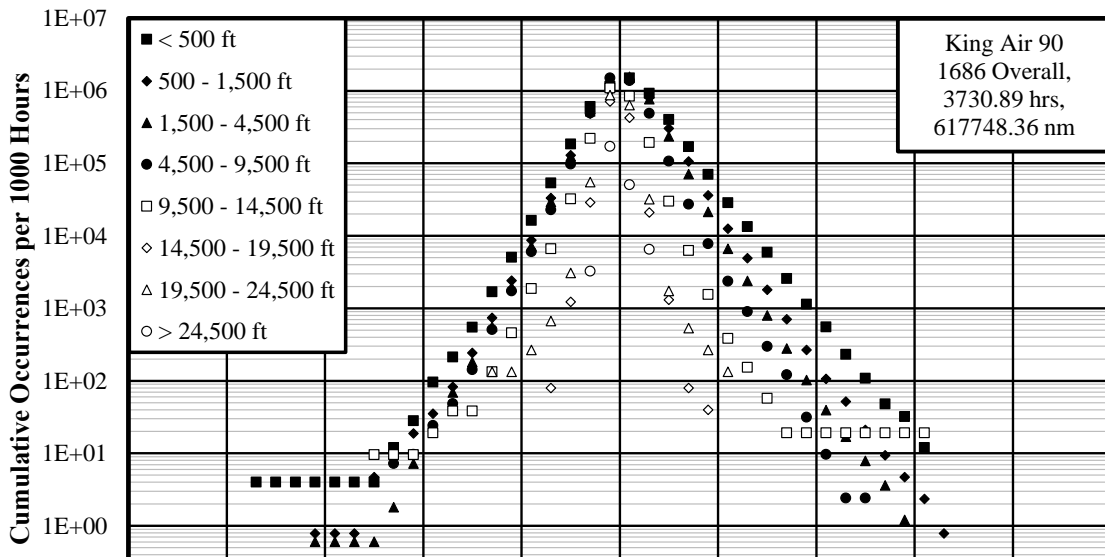


Figure 4.6: Cumulative Occurrences of Incremental Vertical Gust Load Factor per Nautical Mile

Figures 4.7 and 4.8 show the cumulative occurrences of the incremental vertical maneuver load factor per 1000 hours and per nautical mile for all the altitude bands combined. These figures show that the Firefighting and Extreme Attitudes flights had nearly identical

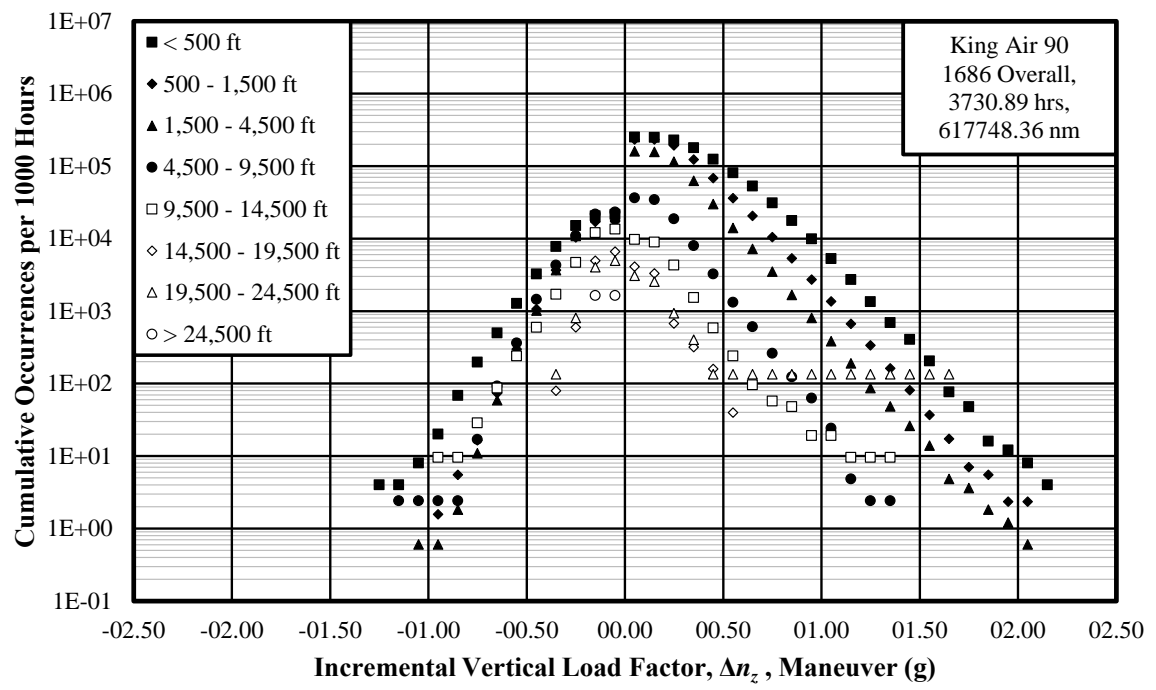


Figure 4.7: Cumulative Occurrences of Incremental Vertical Maneuver Load Factor per 1000 Hours

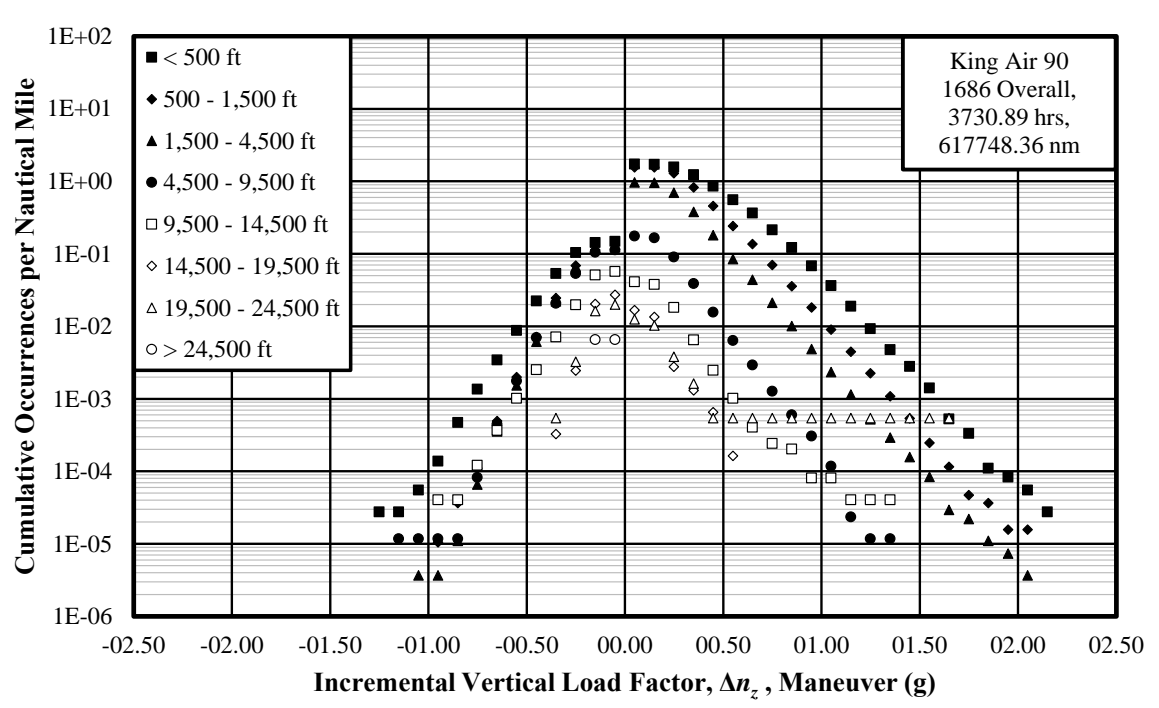


Figure 4.8: Cumulative Occurrences of Incremental Vertical Maneuver Load Factor per Nautical Mile

Figures 4.9 through 4.14 show the cumulative occurrences of the incremental vertical gust load factor by altitude bands for Extreme Attitudes, Firefighting, and Ferry flights respectively. These plots clearly show an inverse relationship between the AGL altitude and the cumulative occurrence of the vertical gust load factor. In the case of Ferry flights, the occurrences of vertical gust load factor greater than 1g was relatively low.

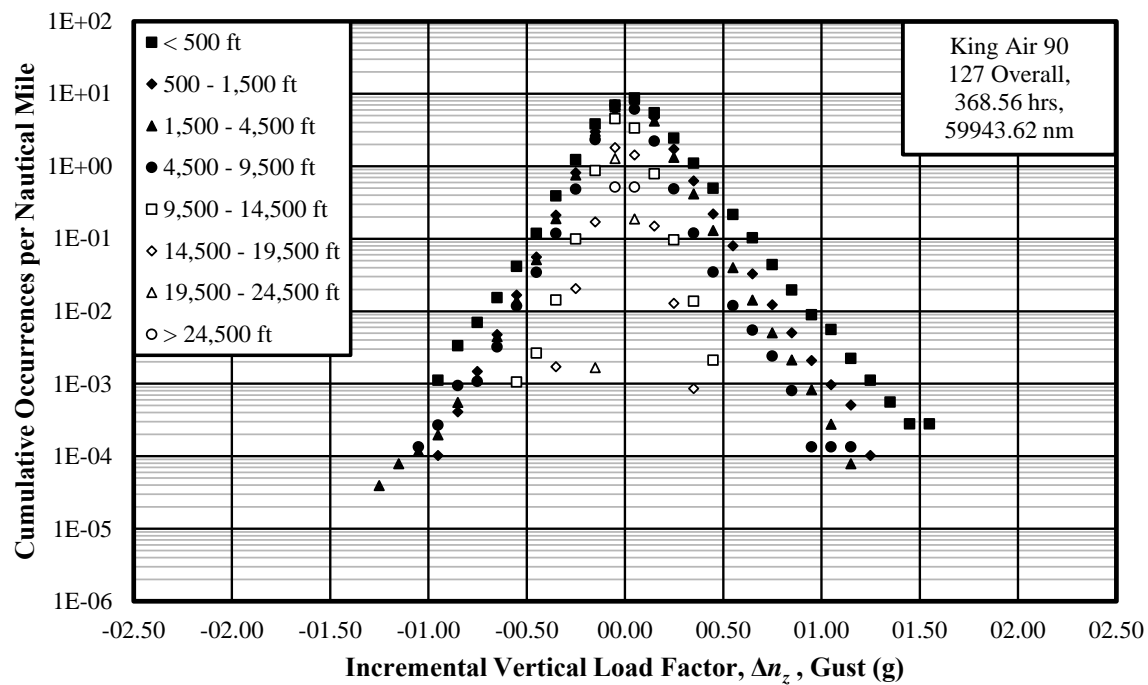
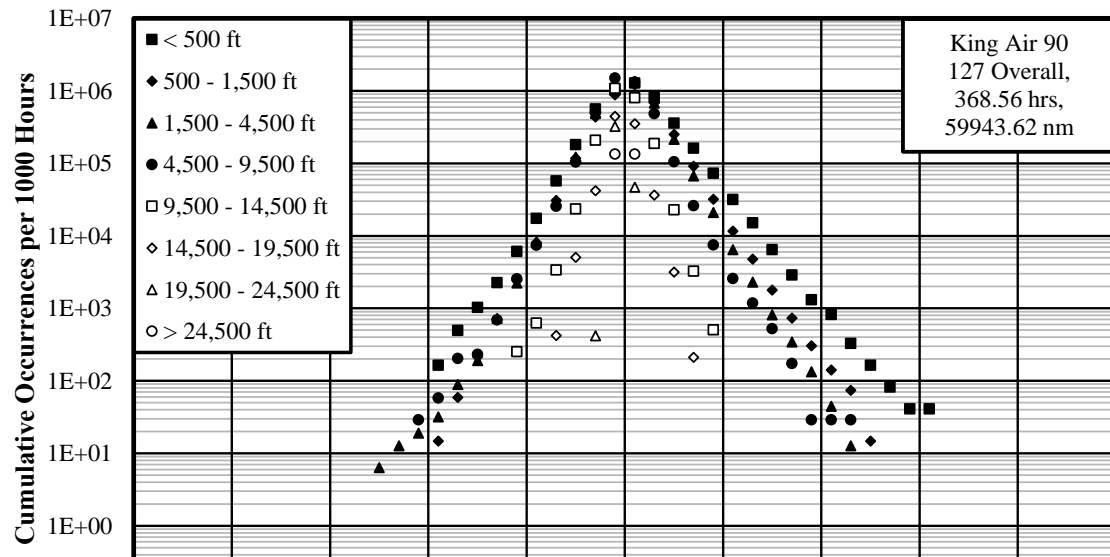


Figure 4.10: Cumulative Occurrences of Incremental Vertical Gust Load Factor per Nautical Mile - Extreme Attitudes

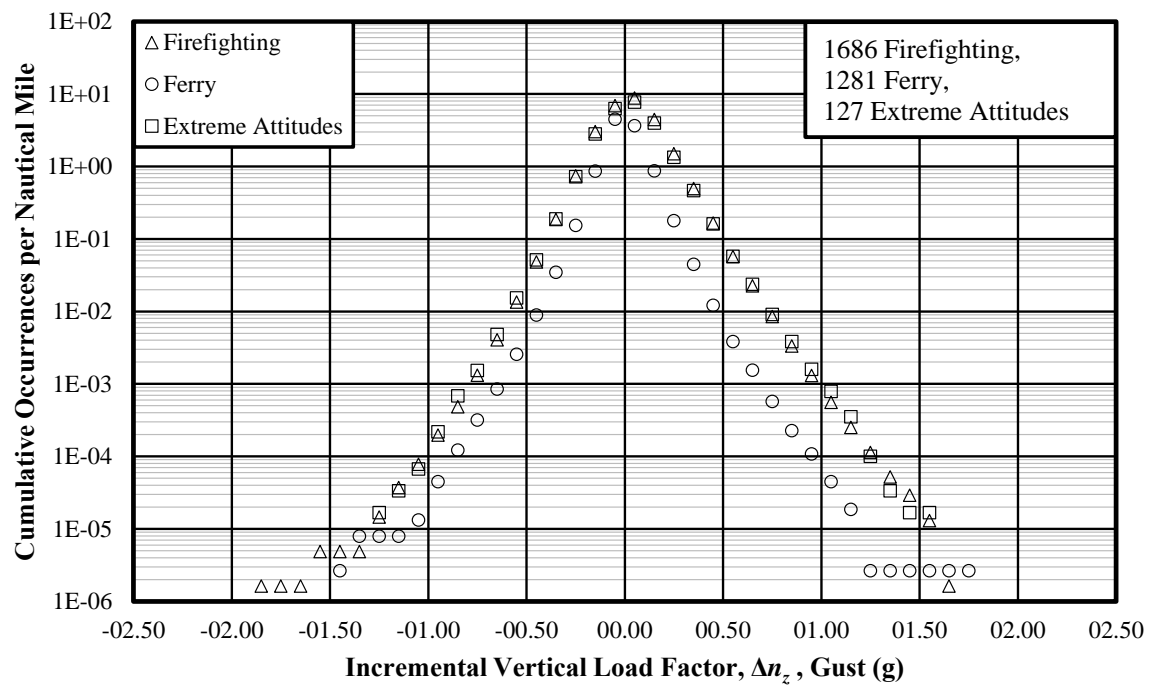
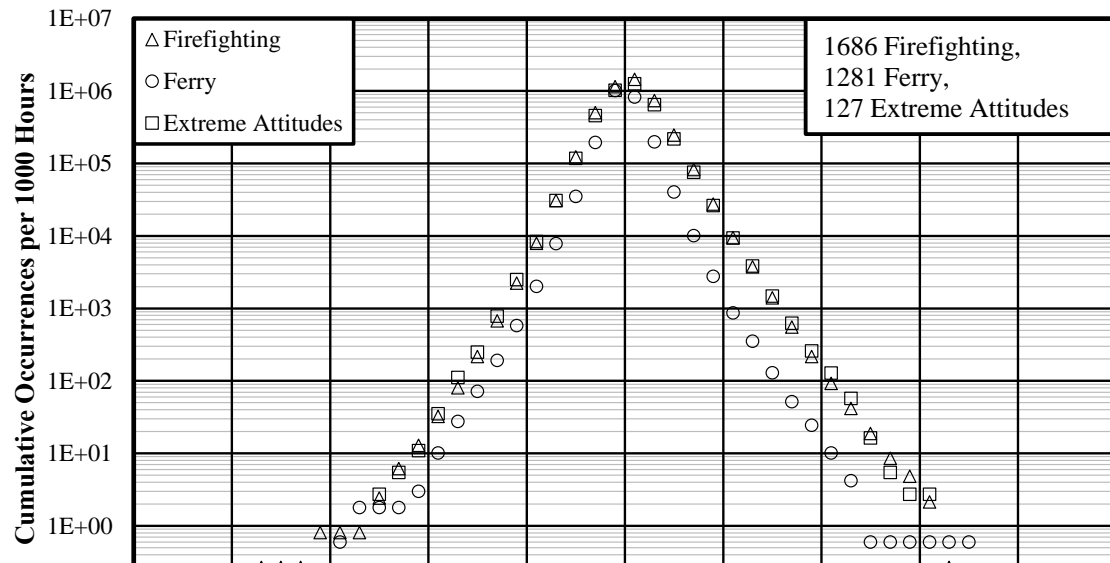


Figure 4.12: Cumulative Occurrences of Incremental Vertical Gust Load Factor per Nautical Mile - Firefighting

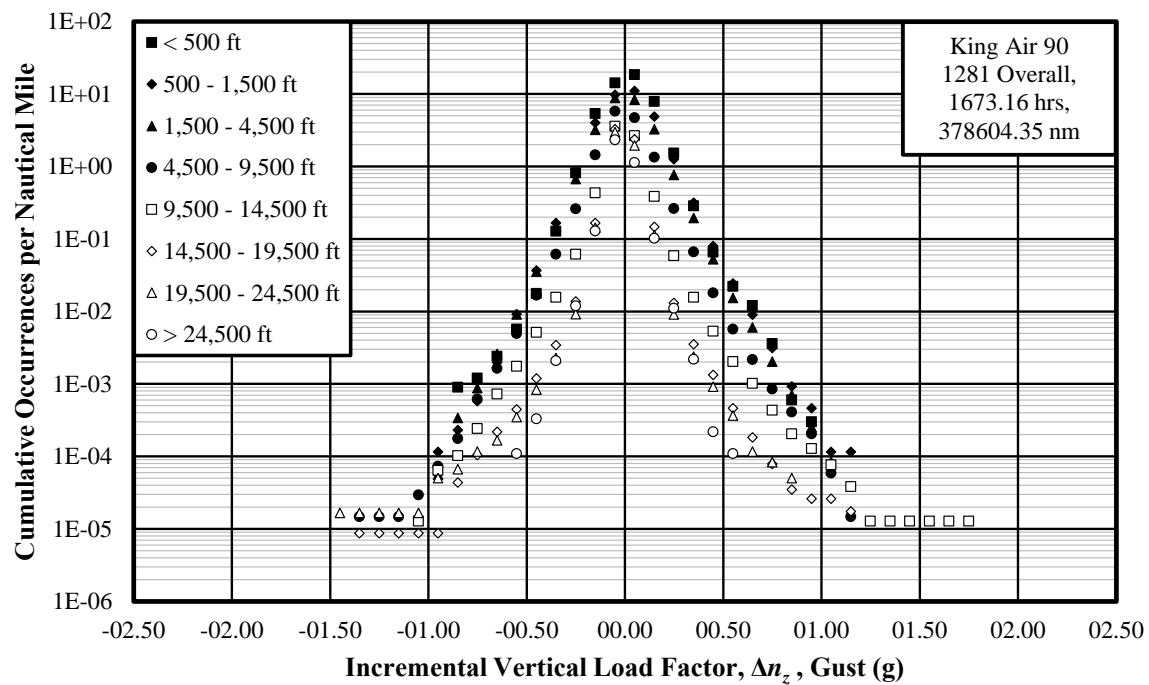
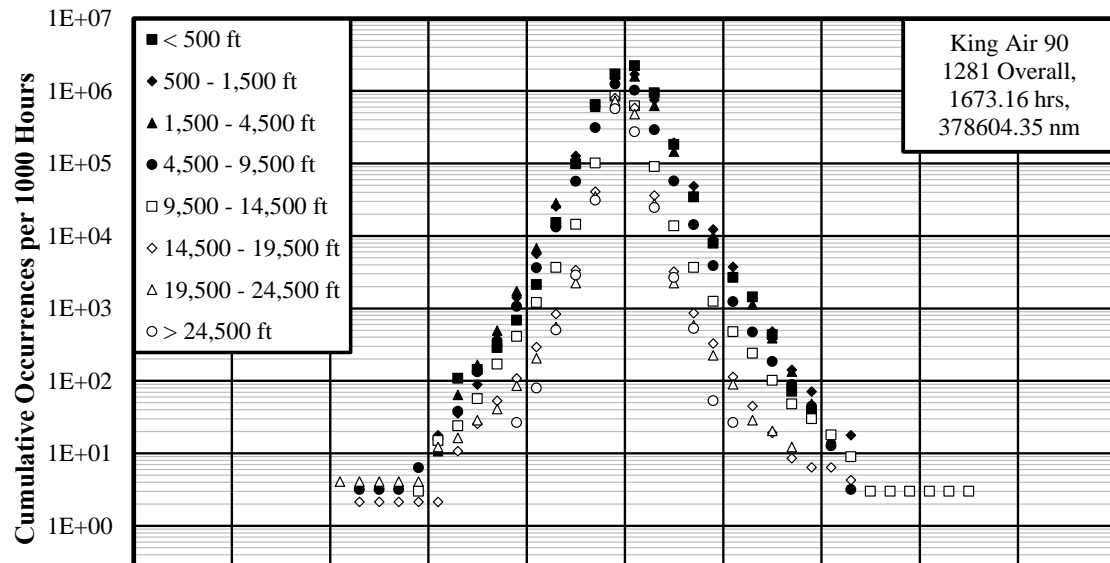


Figure 4.14: Cumulative Occurrences of Incremental Vertical Gust Load Factor per Nautical Mile - Ferry

The cumulative occurrences of the incremental vertical maneuver load factor by altitude bands for Extreme Attitudes, Firefighting, and Ferry flights is shown in Figures 4.15 through 4.20. The inverse relationship between the AGL altitude and the cumulative occurrence of the load factors can be seen clearly in these figures. In general, there was not

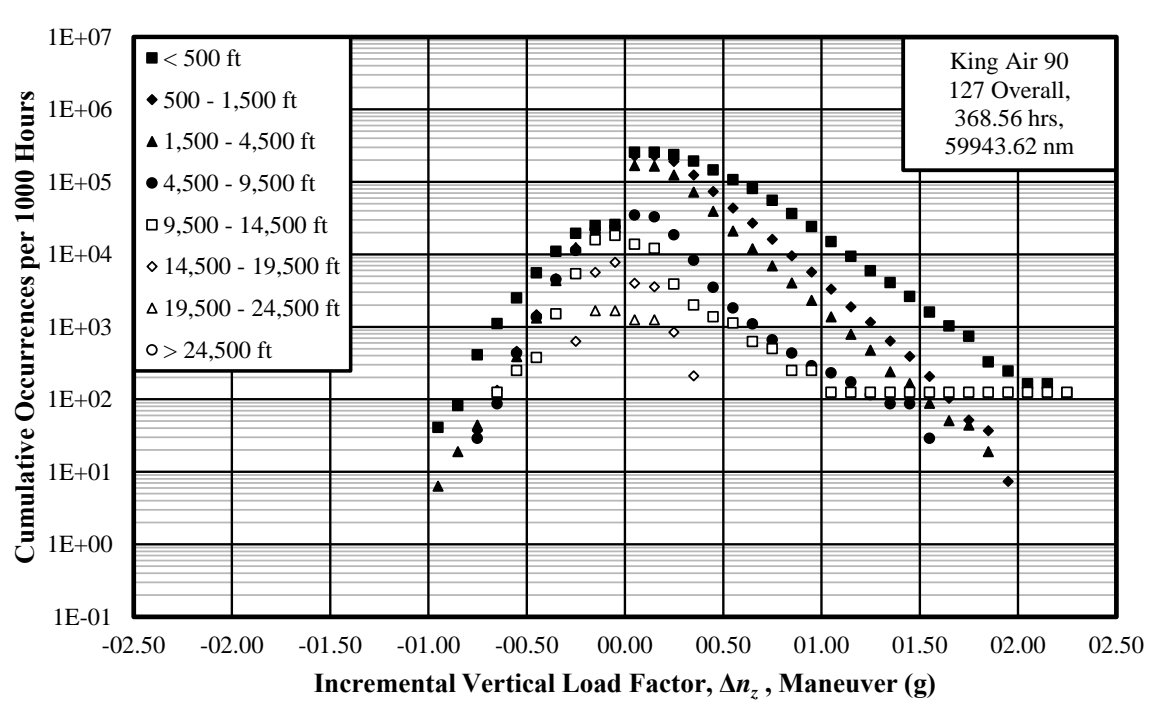


Figure 4.15: Cumulative Occurrences of Incremental Vertical Maneuver Load Factor per 1000 Hours - Extreme Attitudes

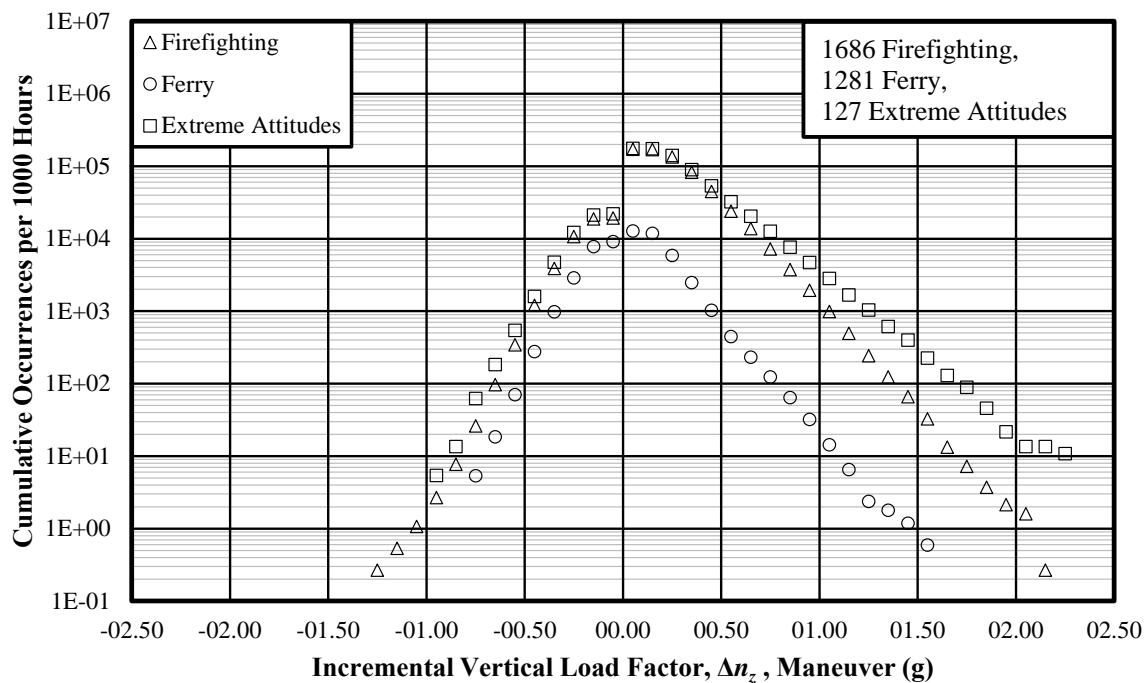
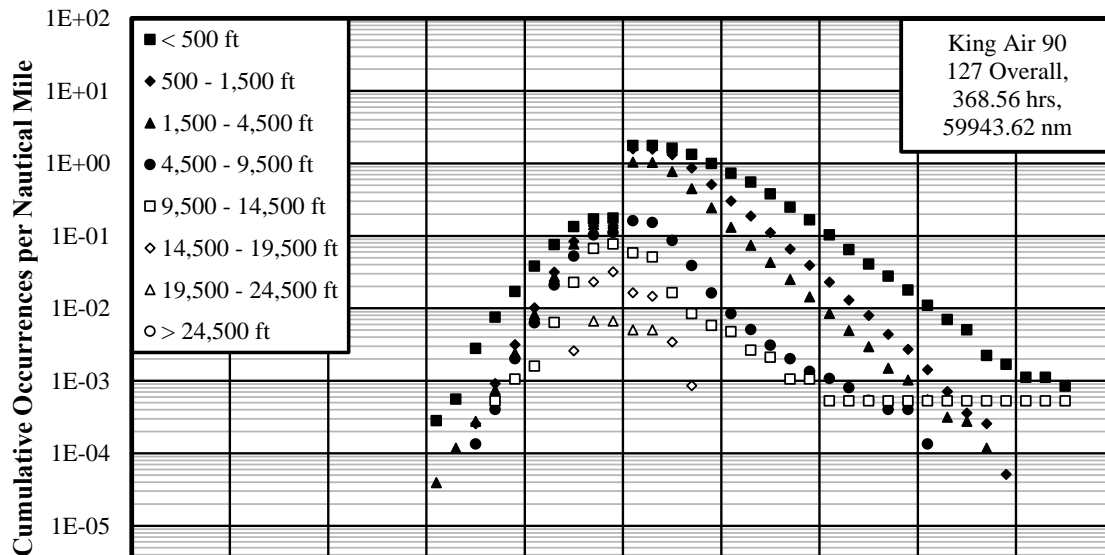


Figure 4.17: Cumulative Occurrences of Incremental Vertical Maneuver Load Factor per 1000 Hours - Firefighting

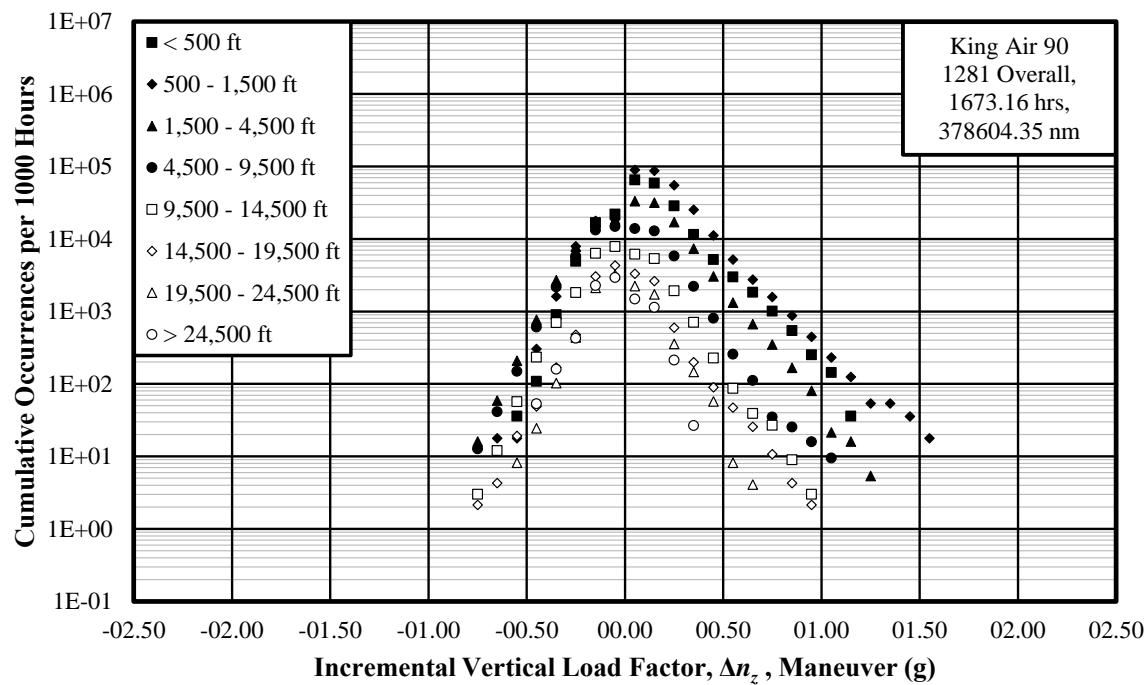
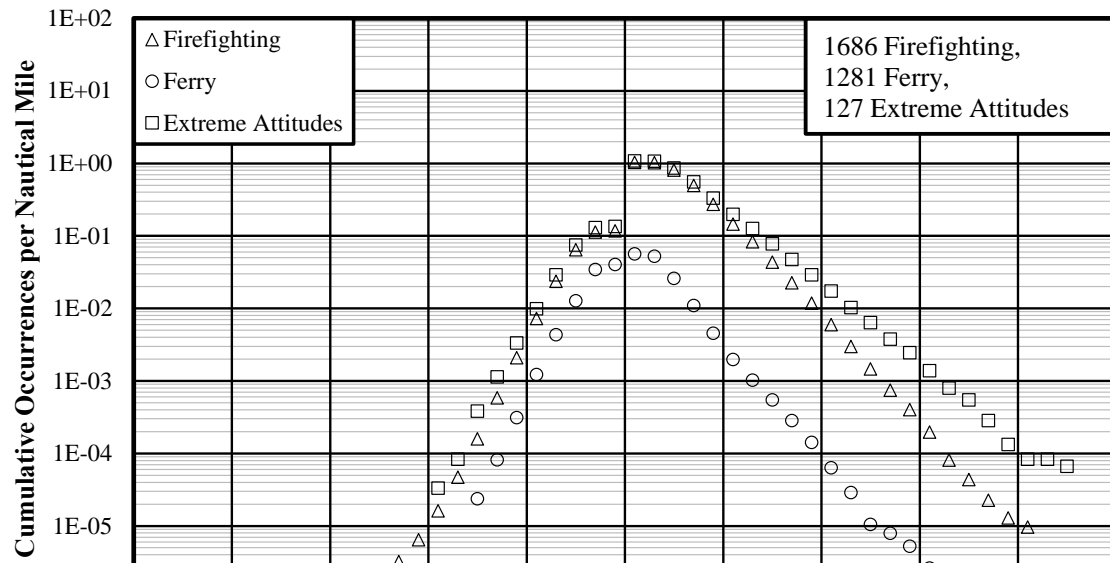


Figure 4.19: Cumulative Occurrences of Incremental Vertical Maneuver Load Factor per 1000 Hours - Ferry

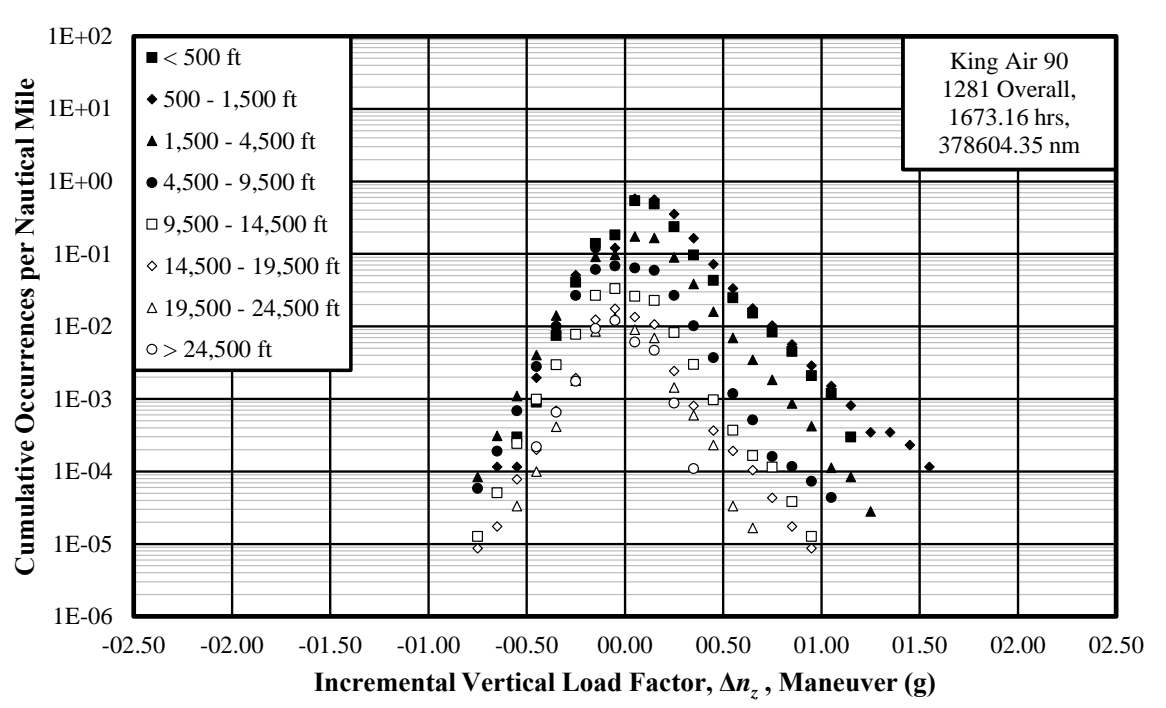


Figure 4.20: Cumulative Occurrences of Incremental Vertical Maneuver Load Factor per Nautical Mile - Ferry

#### 4.1.2 Discrete Gust Velocities

The discrete gust velocities were obtained from the vertical gust load factors as described in Section 2.8. The cumulative occurrences of the derived gust velocity per 1000 hours and per nautical mile for all the altitude bands are shown in Figures 4.21 and 4.22 for various missions. Similar to the vertical gust load factor, the occurrences of derived gust velocity from Extreme Attitude flights agreed very closely with those of the Firefighting flights. The Ferry flights once again showed a lower frequency of occurrences as compared to others, mostly due to the higher altitudes at which these flights took place.

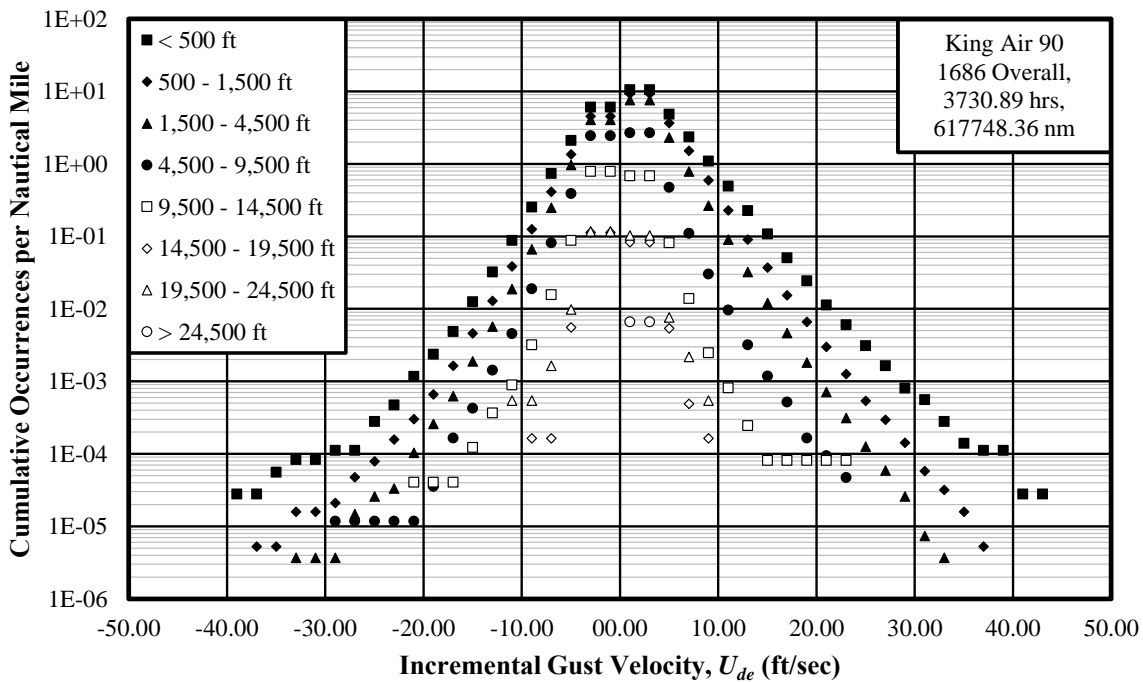
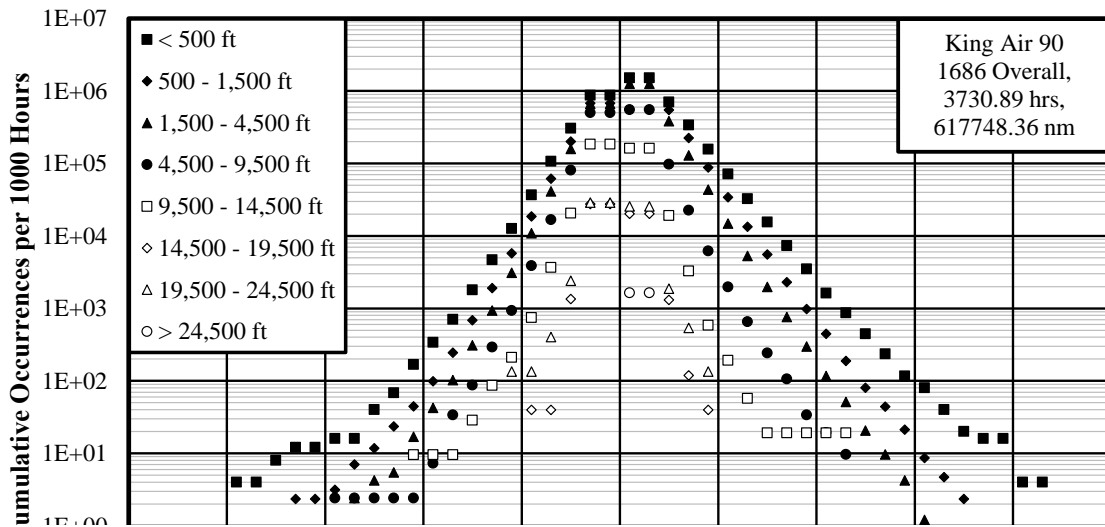


Figure 4.22: Cumulative Occurrences of Derived Gust Velocity per Nautical Mile

Figures 4.23 through 4.28 show the cumulative occurrences of the derived gust velocity for different missions by altitude bands. As expected, these figures also show the inverse relationship between the AGL altitude and cumulative occurrences of the gust velocity. In addition, all cases showed the positive gust velocities as being slightly more frequent than the negative gust velocities. Since atmospheric turbulence is mostly isotropic, this behavior could only be attributed to the shortcomings of the method of separating gust and maneuver loads.

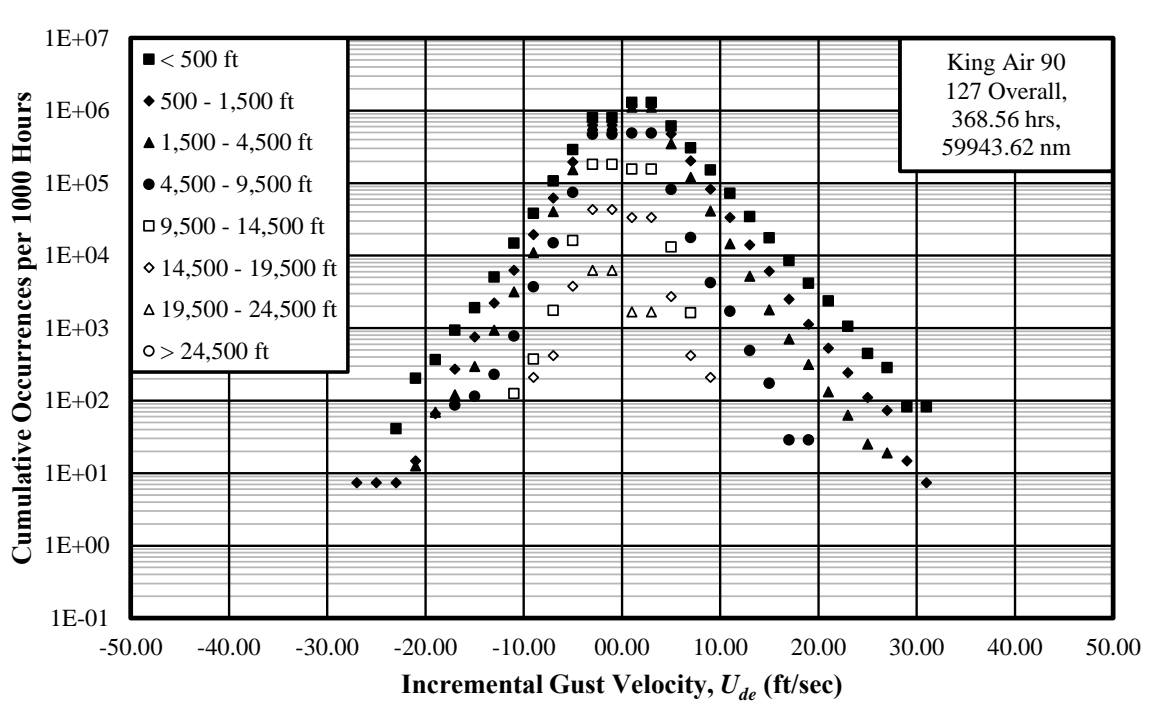


Figure 4.23: Cumulative Occurrences of Derived Gust Velocity per 1000 Hours - Extreme Attitudes

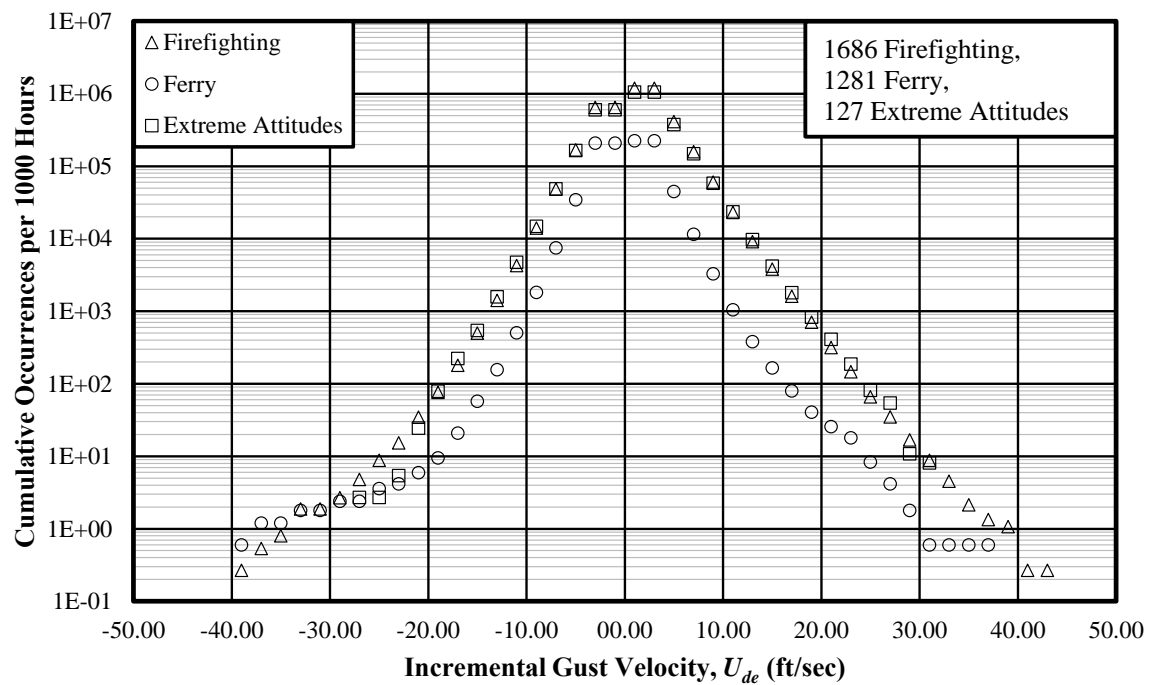
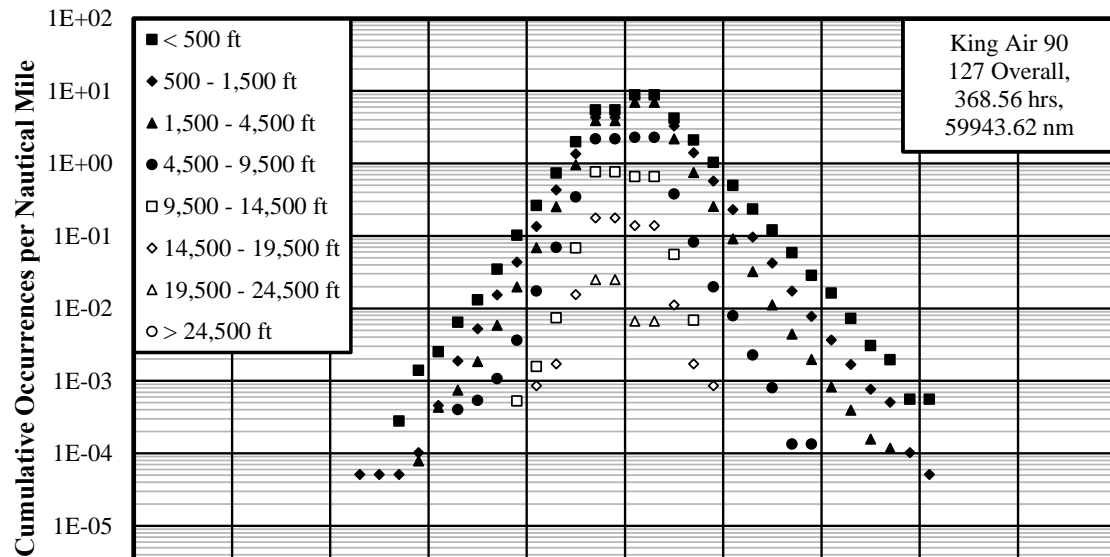


Figure 4.25: Cumulative Occurrences of Derived Gust Velocity per 1000 Hours - Firefighting

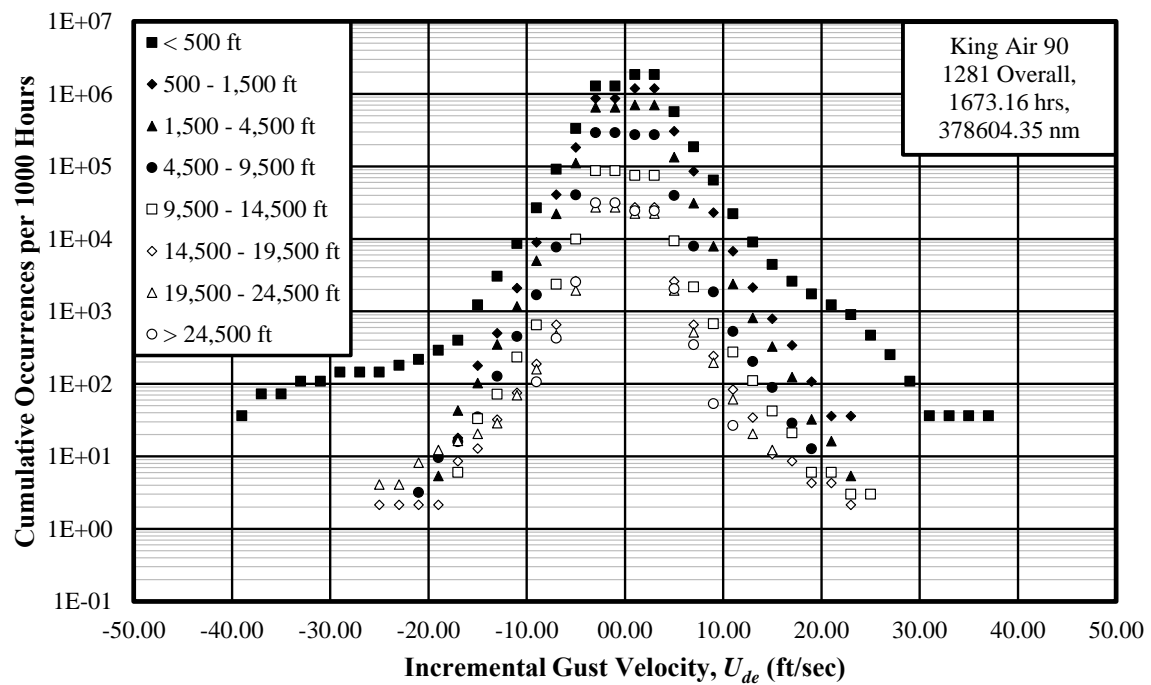
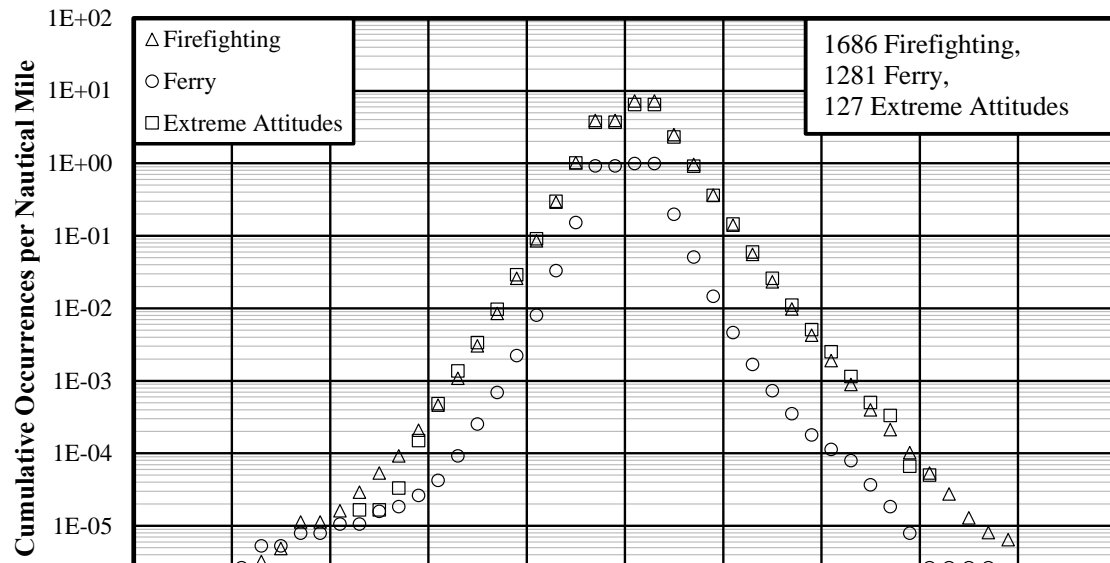


Figure 4.27: Cumulative Occurrences of Derived Gust Velocity per 1000 Hours - Ferry

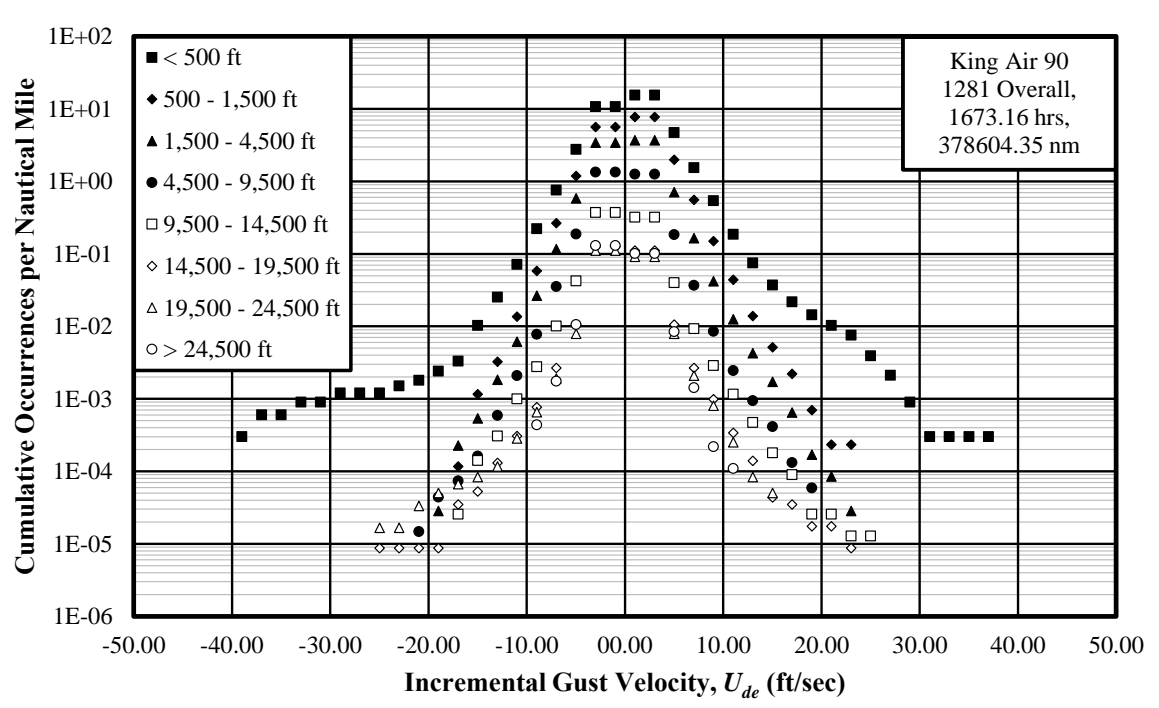


Figure 4.28: Cumulative Occurrences of Derived Gust Velocity per Nautical Mile - Ferry

#### 4.2 Phase-Specific Results

The phase-specific loads are relevant only for the firefighting missions because Ferry and Extreme Attitude flights were not divided into phases. The phases of a firefighting mission, as detailed in Chapter 2, were Cruise-1, Cruise-2, Entry, Lead, Exit, and Turns. The objective of this analysis was to determine the phase of a firefighting mission during which the aircraft was subjected to the largest and the most frequent loads.

Flight time spent in each of the phases in each of the altitude bands are listed in Table 4.3. Cruise-1 and Cruise-2 phases were conducted more often in the 1,500-9,500-foot AGL altitude band. As expected, the aircraft, during the Entry and Exit phases, was flown the most time at AGL altitudes less than 1,500 feet whereas during the Lead phase, it was flown most of the time in altitudes less than 500 feet. The Turns phase conducted the majority of its maneuvers at AGL altitudes between 500 and 4,500 feet.

Table 4.3: Time in Altitude Band for Each Phase in Hours

<b>Band/Phase</b>	<b>Cruise-1</b>	<b>Cruise-2</b>	<b>Entry</b>	<b>Lead</b>	<b>Exit</b>	<b>Turns</b>
< 500 ft.	17.93	25.50	24.21	10.14	18.44	35.09
500 – 1500 ft.	67.44	107.26	33.60	3.23	37.85	371.89
1500 – 4500 ft.	237.09	284.49	3.30	0.18	4.82	397.03
4500 – 9500 ft.	204.13	107.35	0.00	0.00	0.00	11.56
9500 – 14500 ft.	67.34	24.90	0.00	0.00	0.00	0.10
14500 – 19500 ft.	19.63	3.99	0.00	0.00	0.00	0.00
19500 – 24500 ft.	3.49	1.96	0.00	0.00	0.00	0.00
> 24500 ft.	0.00	0.61	0.00	0.00	0.00	0.00

Table 4.4 shows the distance travelled by the aircraft during each phase in the specified altitude bands. The observations for the time spent by the aircraft in the altitude bands are identical to those for the distance.

Table 4.4: Distance Flown in Altitude Band for Each Phase in Nautical Miles

<b>Band/Phase</b>	<b>Cruise-1</b>	<b>Cruise-2</b>	<b>Entry</b>	<b>Lead</b>	<b>Exit</b>	<b>Turns</b>
< 500 ft.	2518.36	3268.99	3504.41	1494.91	2688.79	5118.03
500 – 1500 ft.	11059.13	16733.58	4868.01	472.37	5547.47	53772.68
1500 – 4500 ft.	43969.85	51904.56	490.94	27.43	718.94	60380.49
4500 – 9500 ft.	43959.54	22917.23	0.22	0.00	0.00	1897.17
9500 – 14500 ft.	15995.67	5894.69	0.00	0.00	0.00	19.62
14500 – 19500 ft.	4821.30	967.59	0.00	0.00	0.00	0.00
19500 – 24500 ft.	874.81	488.65	0.00	0.00	0.00	0.00
> 24500 ft.	0.00	152.12	0.00	0.00	0.00	0.00

#### 4.2.1 Vertical Acceleration

The cumulative occurrence of the incremental vertical gust load factor for all phases over all altitude bands is shown in Figures 4.29 and 4.30. Also included in these plots are the results for the overall flights. These plots indicate that during the Lead phase, the occurrences of positive vertical loads were the highest. This may be due to the fact the lead phases were flown at the lowest altitudes, where atmospheric turbulence was the most severe.

The next largest occurrences for positive vertical gust loads were for the Exit followed by the Entry phase.

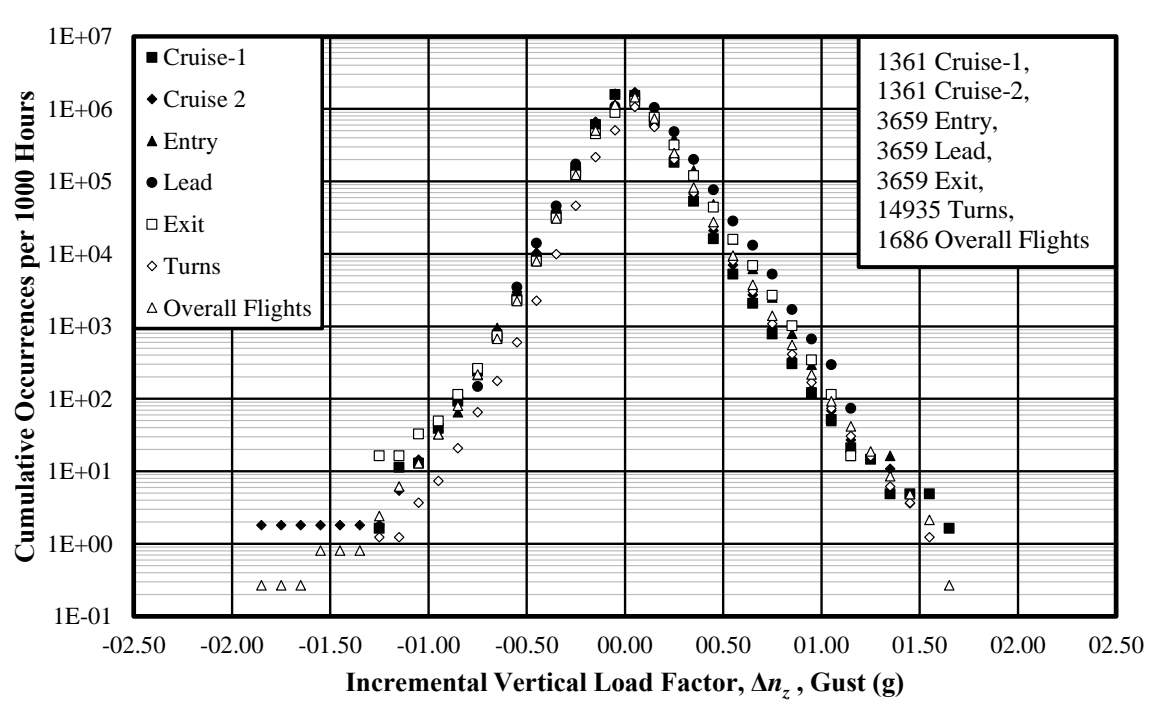


Figure 4.29: Cumulative Occurrences of Incremental Vertical Gust Load Factor per 1000 Hours - All Phases

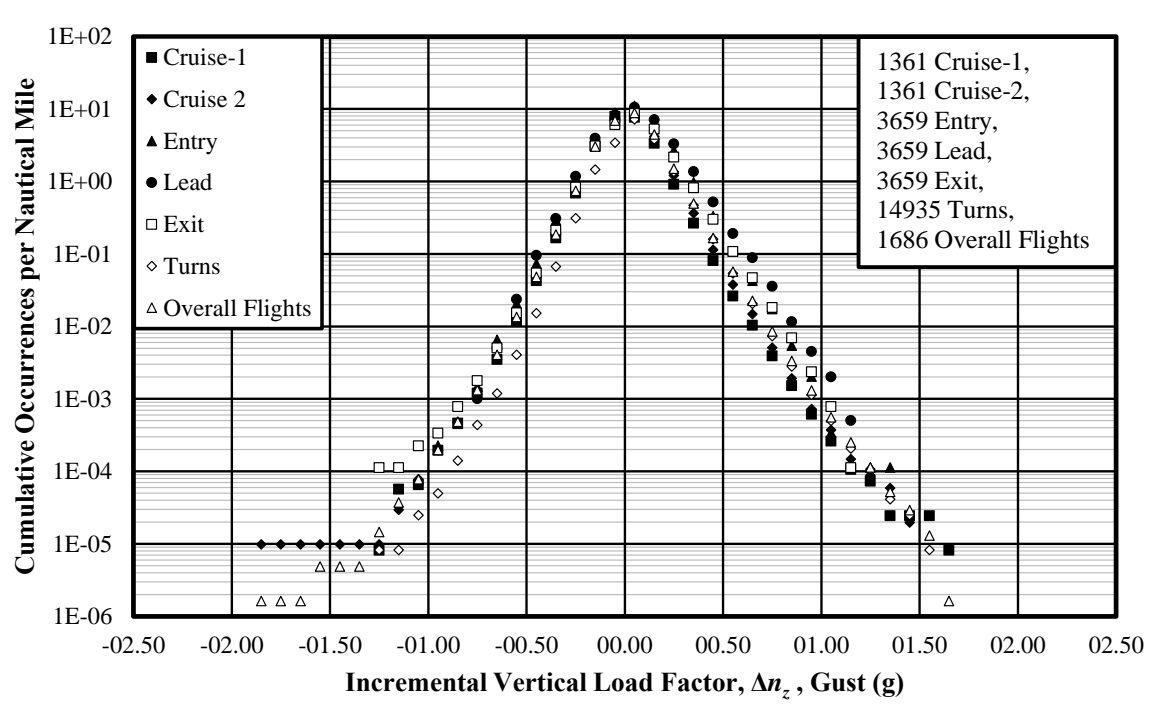


Figure 4.30: Cumulative Occurrences of Incremental Vertical Gust Load Factor per Nautical Mile - All Phases

Cumulative occurrence of vertical gust load factor for individual phases separated by altitude bands is shown in Figures 4.31 through 4.42. Since the largest amount of data was associated with Cruise-1 and Cruise-2 phases, their associated load factors spanned over the widest range. Consequently, the largest load factors were detected during these phases. It can also be seen from these figures that the largest positive load were associated with the lowest altitudes.

For the Entry, Lead, and Exit phases, the frequencies of occurrence of gust load factors were slightly higher than those of the other phases. Furthermore, since these phases occurred most frequently at the lowest altitude bands, there was not sufficient data for meaningful representation of the results at altitudes above 4500 feet AGL. The Turn phase incremental vertical gust loads were generally less than  $\pm 1.5$  g. The only significant incidents of incremental load factors greater than 1.5 g occurred at altitude less than 500 feet.

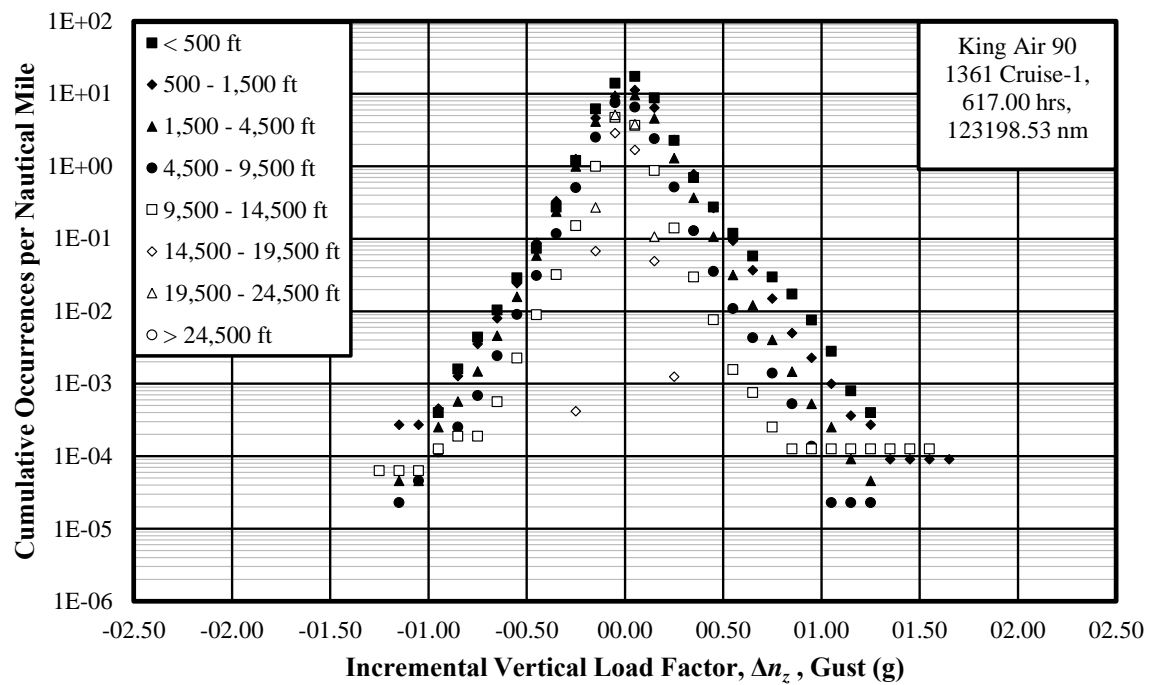
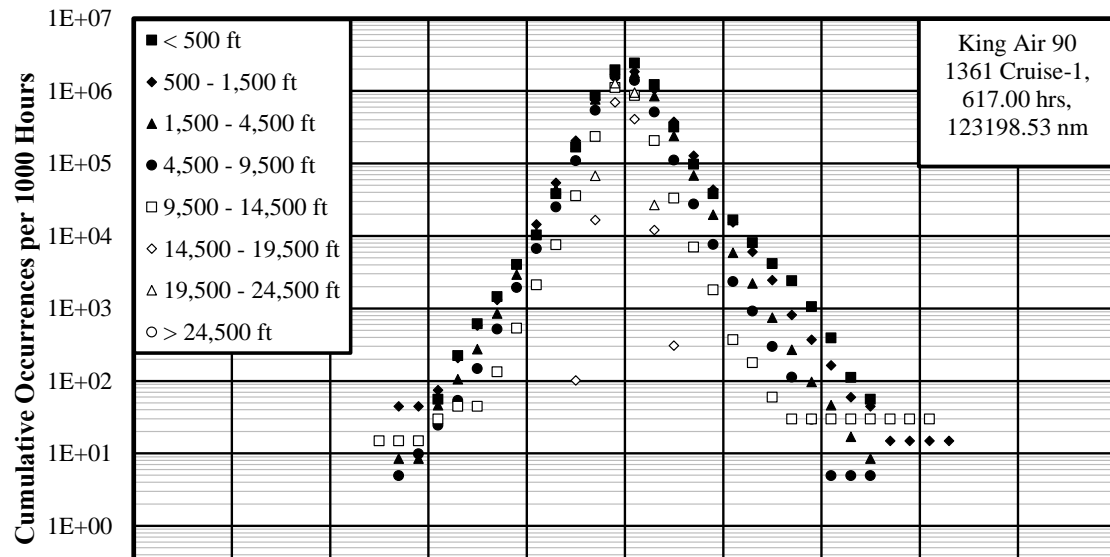


Figure 4.32: Cumulative Occurrences of Incremental Vertical Gust Load Factor per Nautical Mile - Cruise-1 Phase

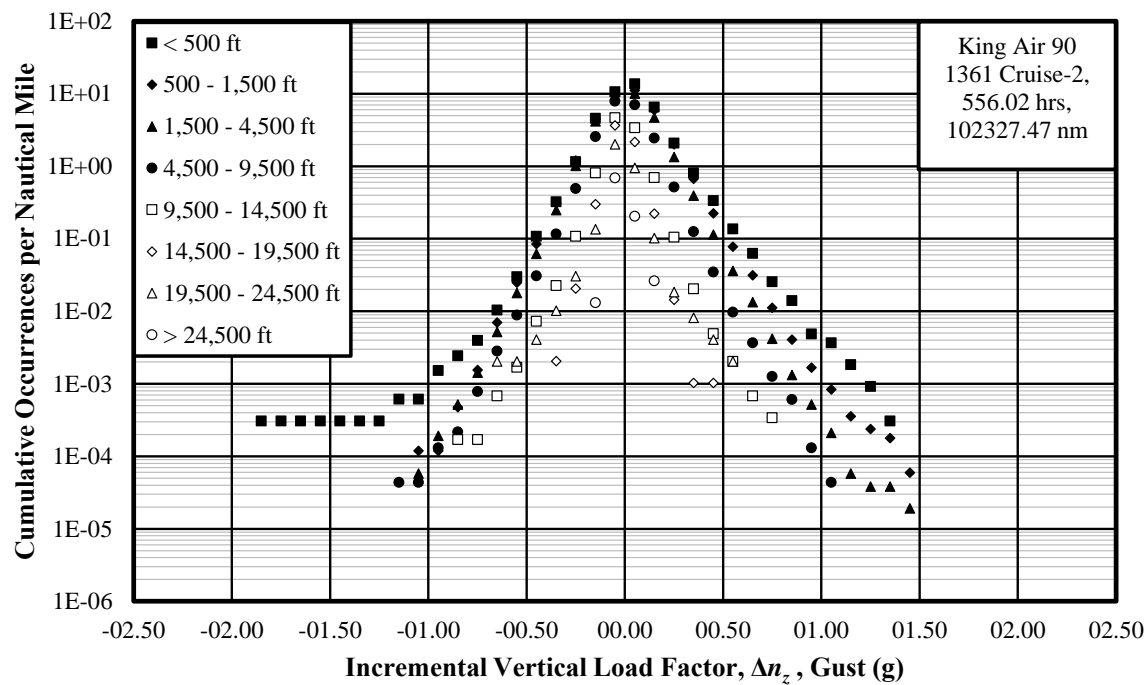
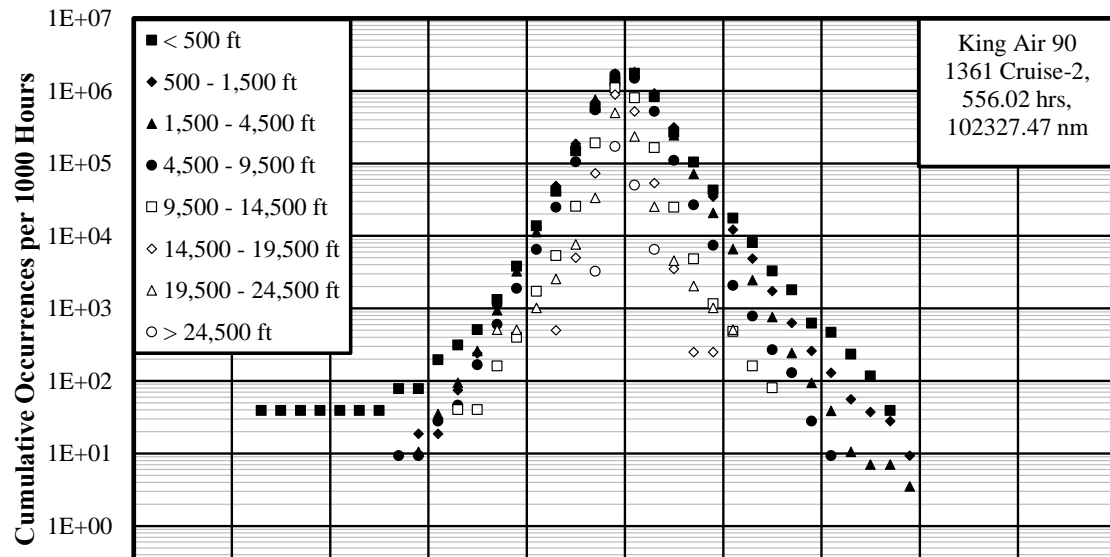


Figure 4.34: Cumulative Occurrences of Incremental Vertical Gust Load Factor per Nautical Mile - Cruise-2 Phase

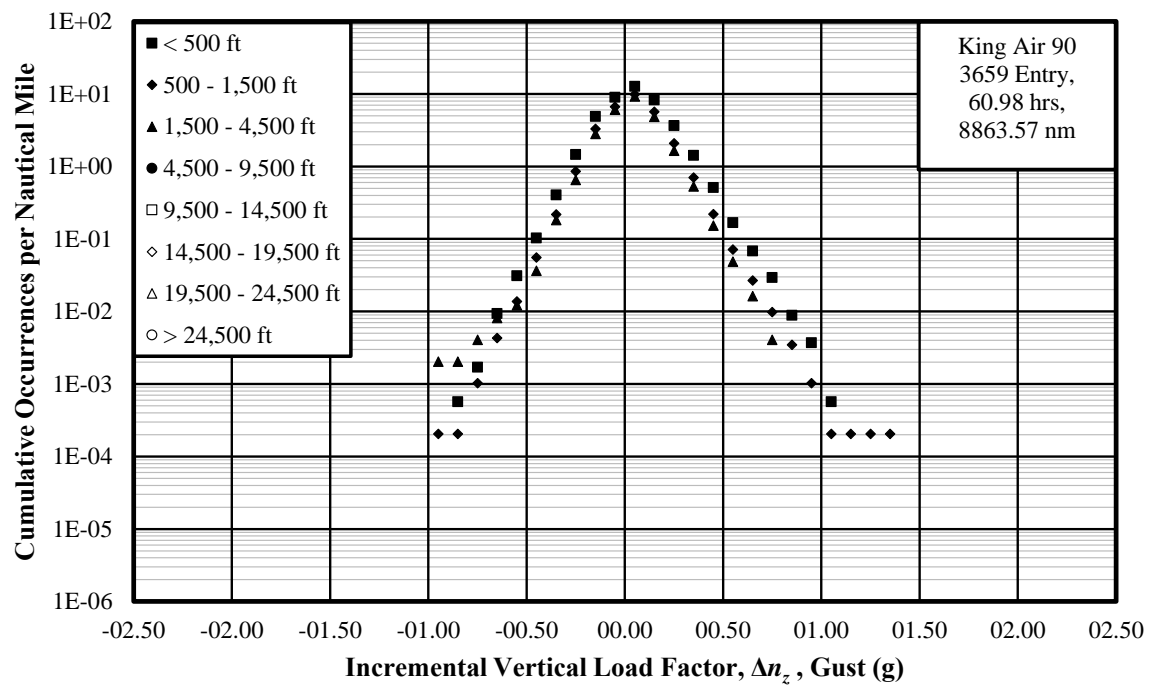
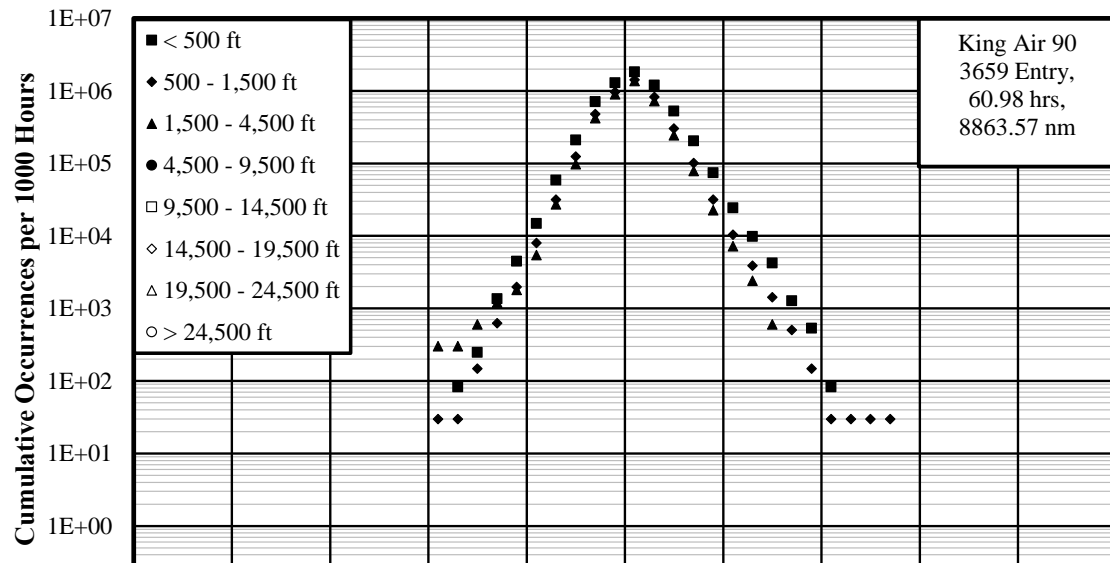


Figure 4.36: Cumulative Occurrences of Incremental Vertical Gust Load Factor per Nautical Mile - Entry Phase

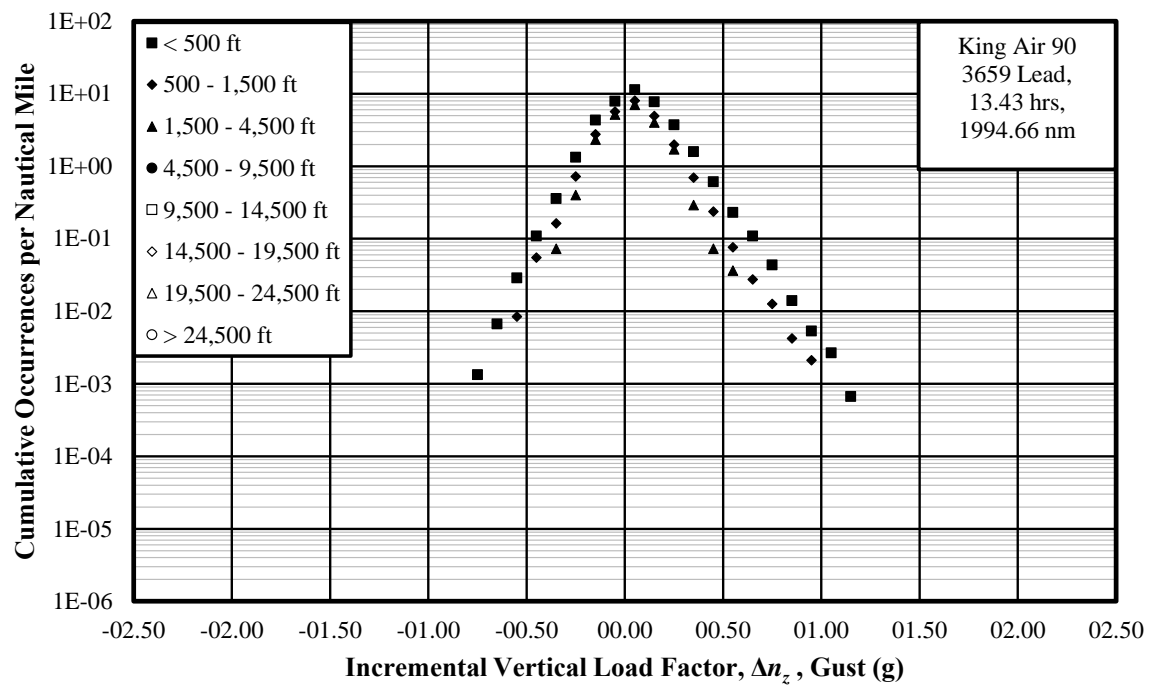
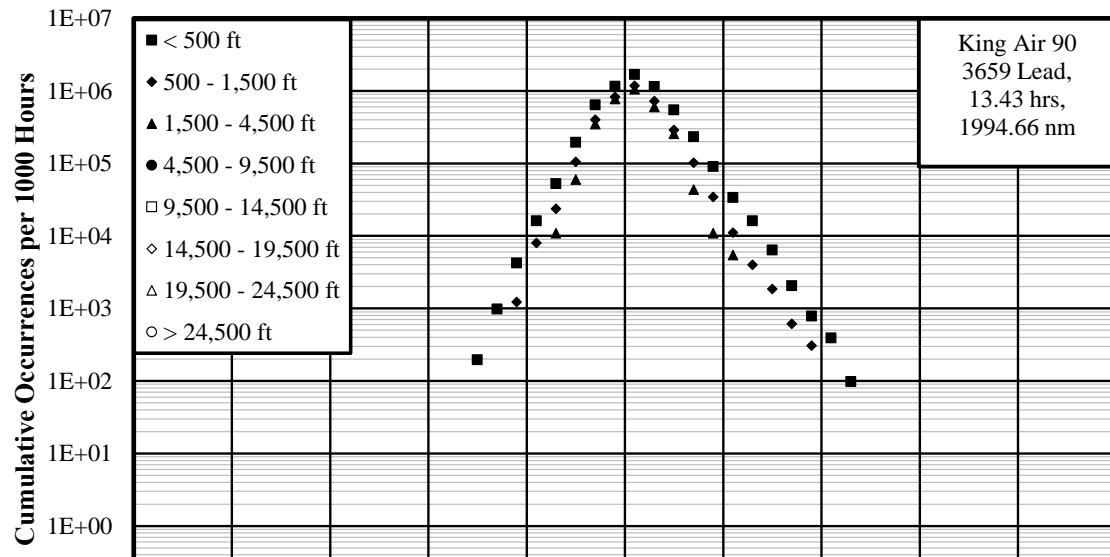


Figure 4.38: Cumulative Occurrences of Incremental Vertical Gust Load Factor per Nautical Mile - Lead Phase

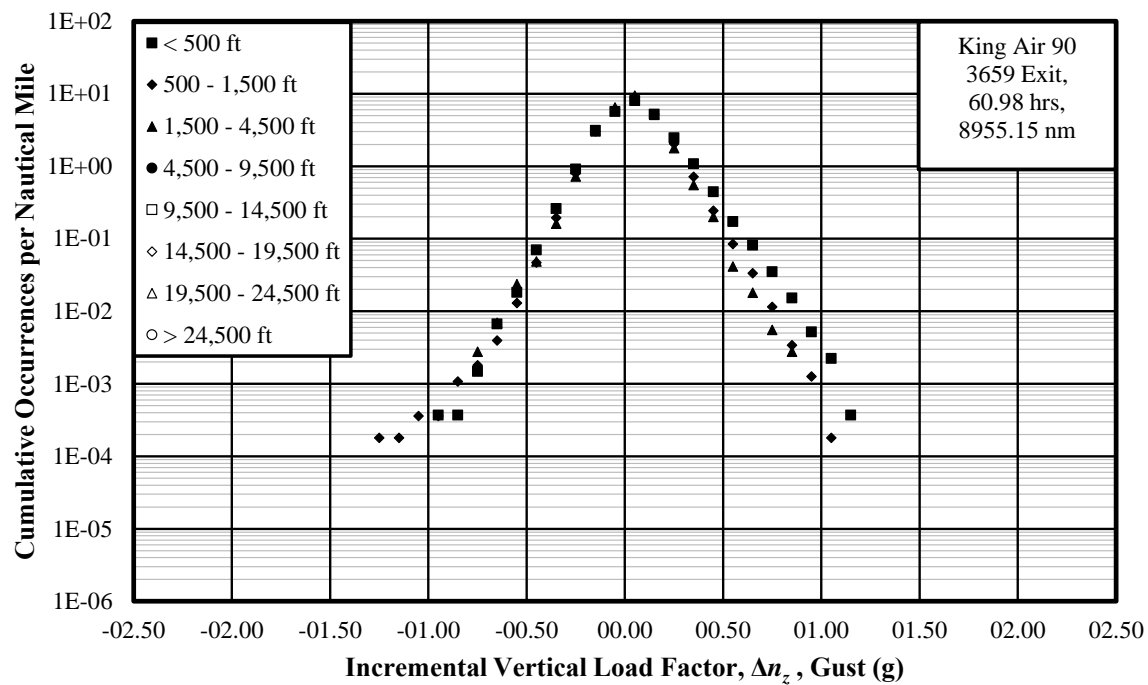
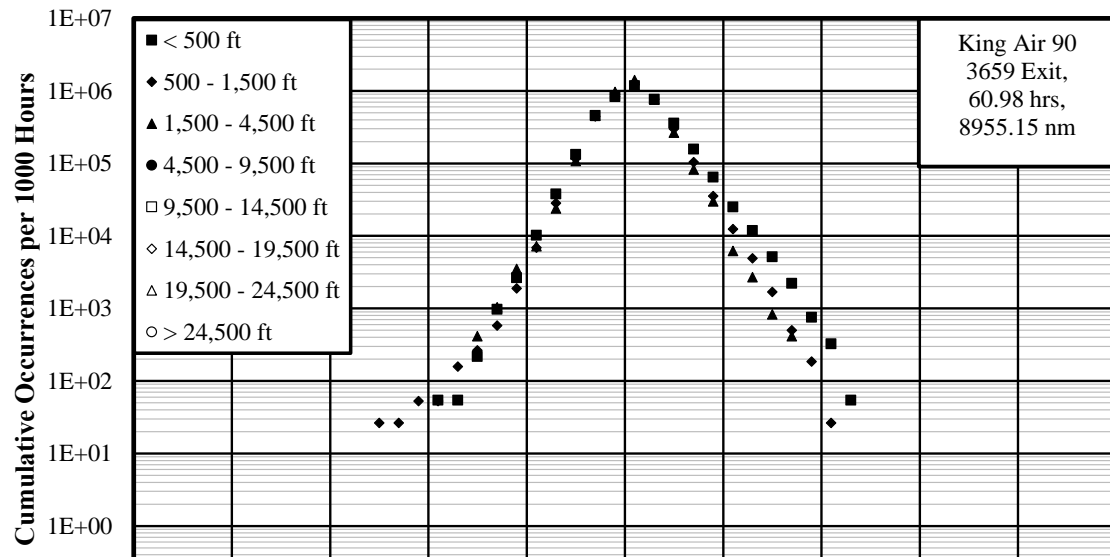


Figure 4.40: Cumulative Occurrences of Incremental Vertical Gust Load Factor per Nautical Mile - Exit Phase

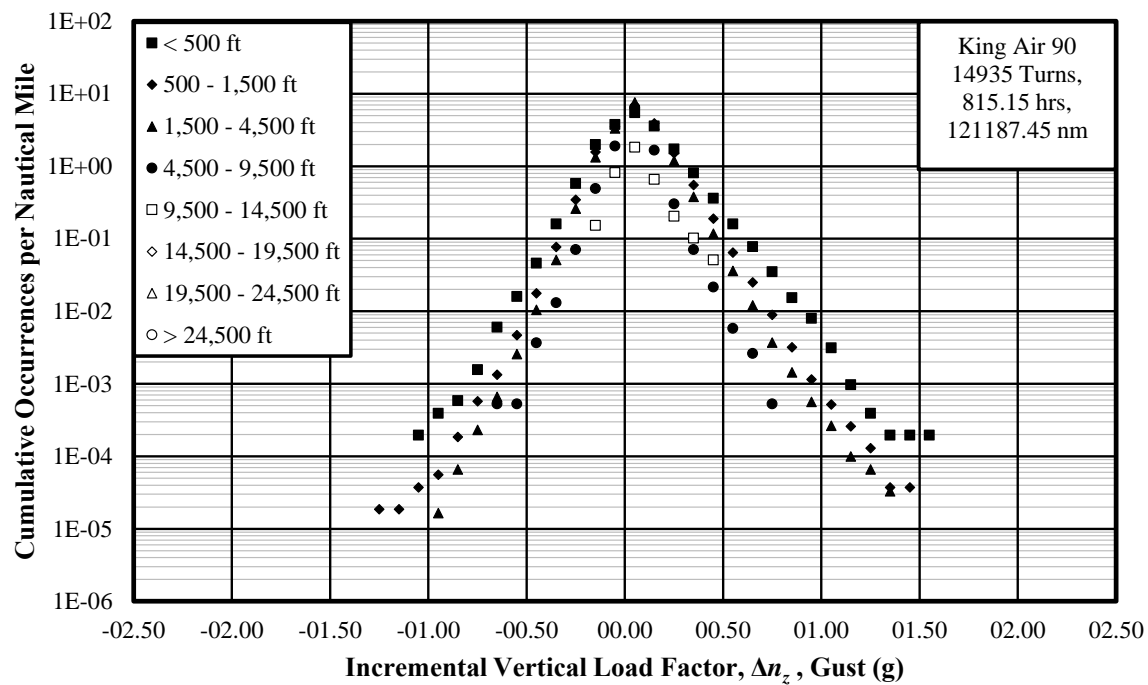
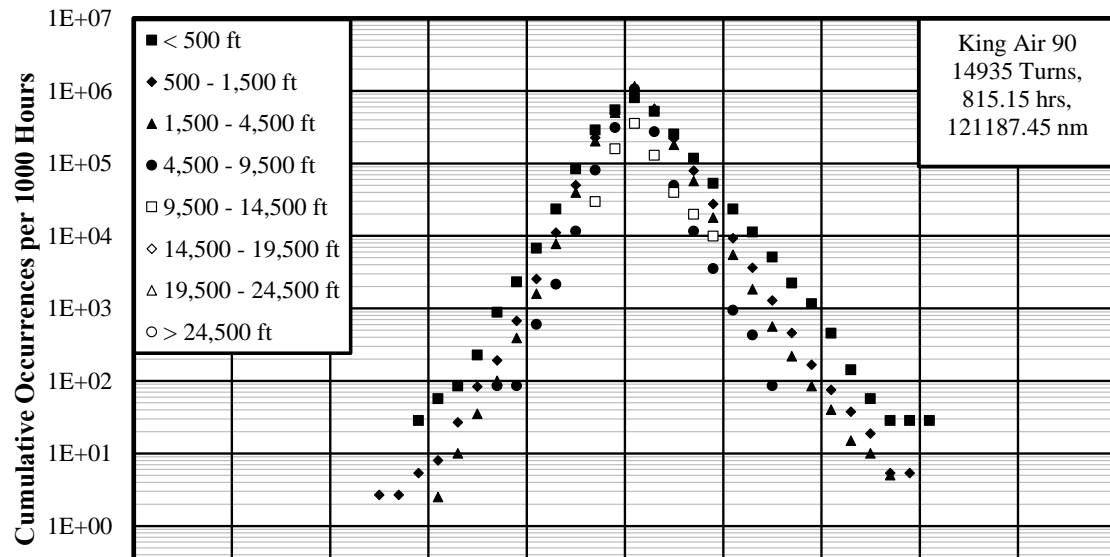


Figure 4.42: Cumulative Occurrences of Incremental Vertical Gust Load Factor per Nautical Mile - Turns Phase

Figures 4.43 and 4.44 show the cumulative occurrences of the incremental vertical maneuver load for all phases over all altitude bands. These figures show that for load factors less than +1 g, the largest number of occurrences occurred during the Lead followed by the Exit phases. Following them were the Turns and the Entry. However, larger load factors occurred more frequently during the Turns phase. The Exit and Turns phases had a wide range of loads with the Exit phase being the one with higher frequency of occurrence for all

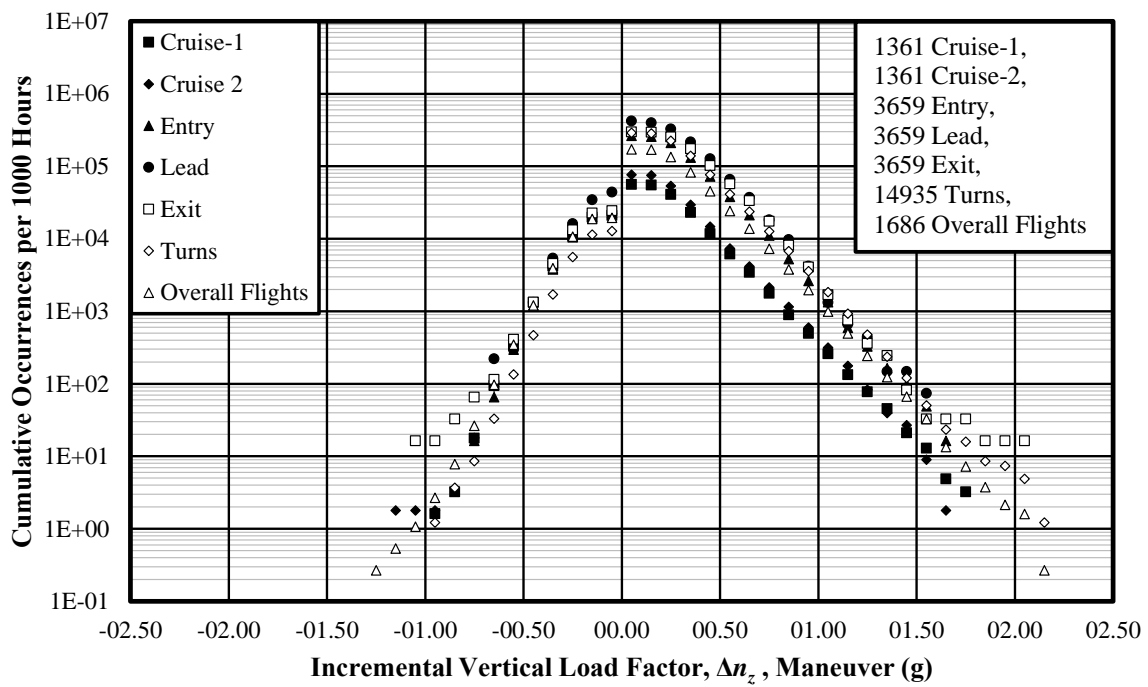


Figure 4.43: Cumulative Occurrences of Incremental Vertical Maneuver Load Factor per 1000 Hours - All Phases

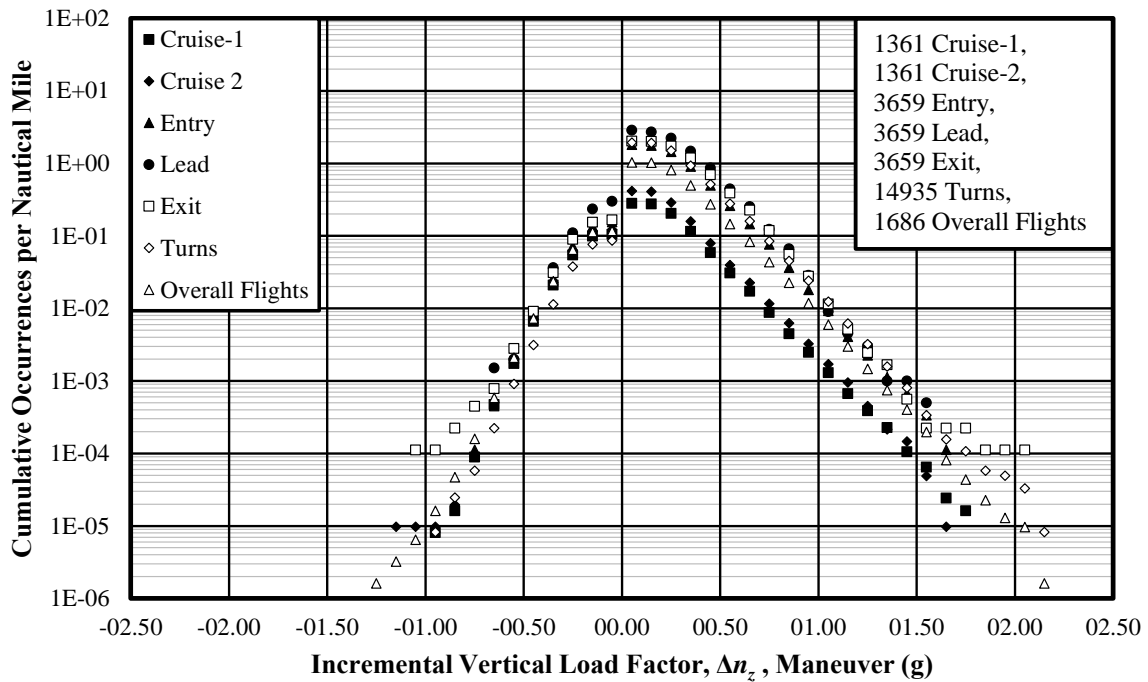


Figure 4.44: Cumulative Occurrences of Incremental Vertical Maneuver Load Factor per Nautical Mile - All Phases

The cumulative occurrences of the incremental vertical maneuver load factor by altitude bands for each phase are shown in Figures 4.45 through 4.56. In the Cruise-1 phase, there was a single incident of incremental load factor of  $\pm 1.65$  g in the 19,500-24,500-foot AGL altitude band. Upon inspection of the flight file, it was determined that this large load factor was caused by pull-up maneuver conducted at nearly 24,000 feet AGL altitude. The negative maneuver load for Cruise-1 was never less than  $-1$  g.

Cruise-2 phase had a rare occurrence of  $-1.15$  g maneuver load factor besides which the negative load factor never exceeded  $-1$  g. In the case of Cruise-1 and Cruise-2 phases, the frequency of occurrences of the maneuver loads were noticeably higher for lower altitudes as well as at lower incremental load factors.

The frequency of occurrence of maneuver vertical load factors was higher for the Entry phase than for cruise phases. The presence of the higher altitude bands in this case was due to the inclusion of some other phases during phase identification as mentioned earlier. The

Exit phase had the highest positive maneuver load of 2.05 g occurring in the 500-1,500-foot altitude band.

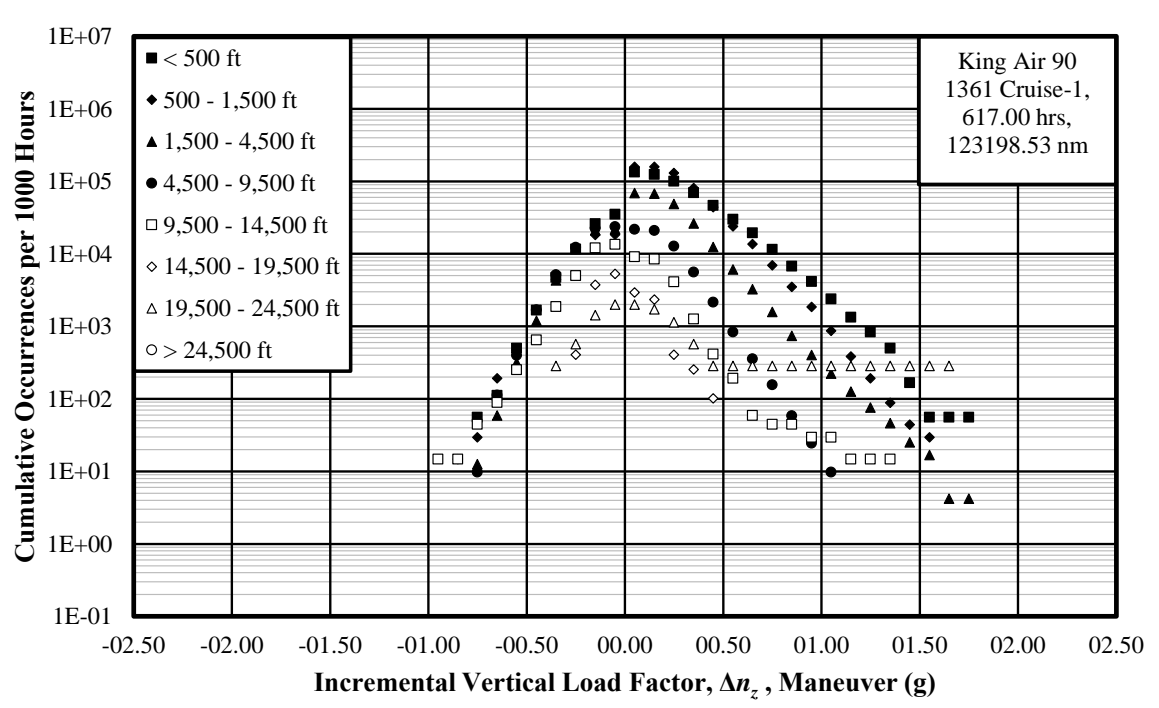


Figure 4.45: Cumulative Occurrences of Incremental Vertical Maneuver Load Factor per 1000 Hours - Cruise-1 Phase

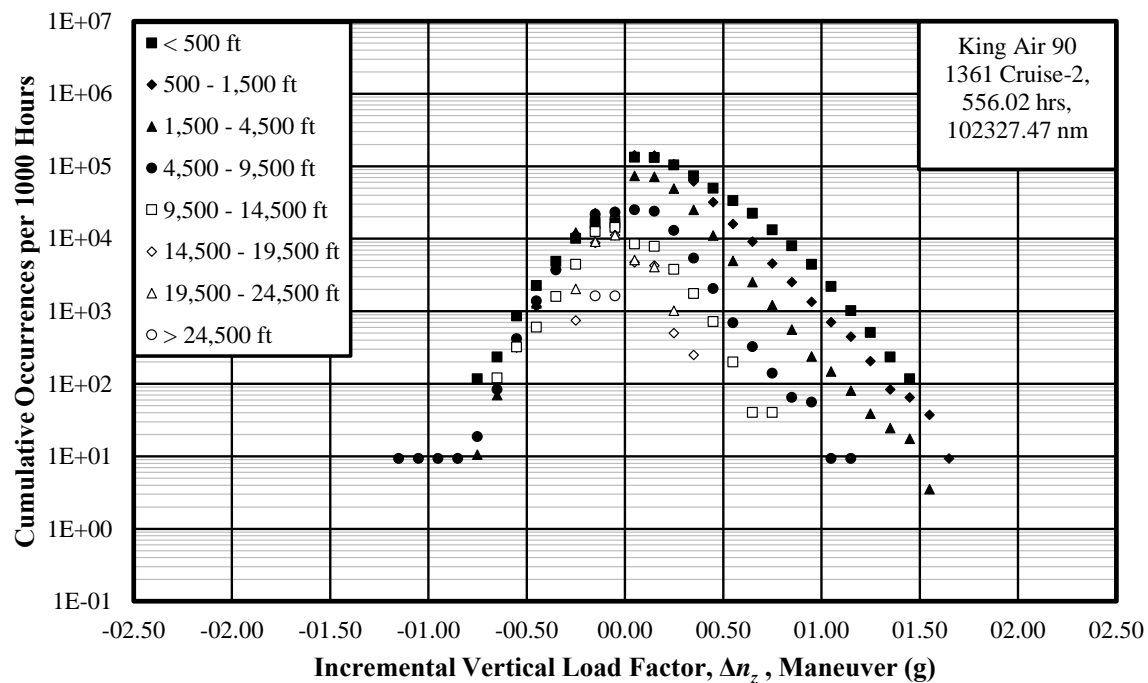
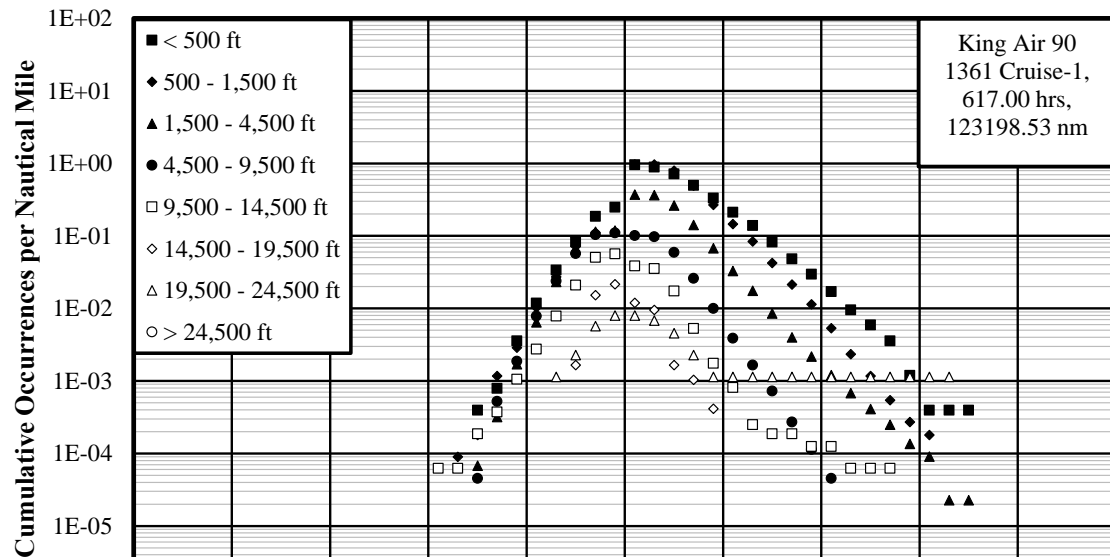


Figure 4.47: Cumulative Occurrences of Incremental Vertical Maneuver Load Factor per 1000 Hours - Cruise-2 Phase

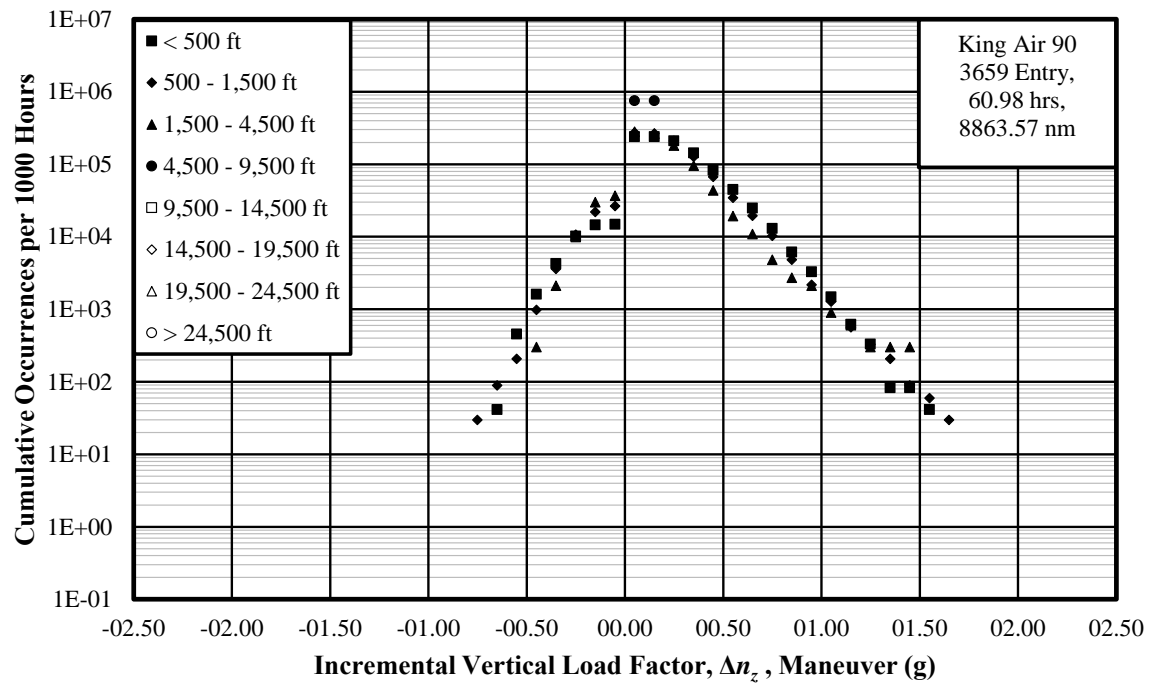
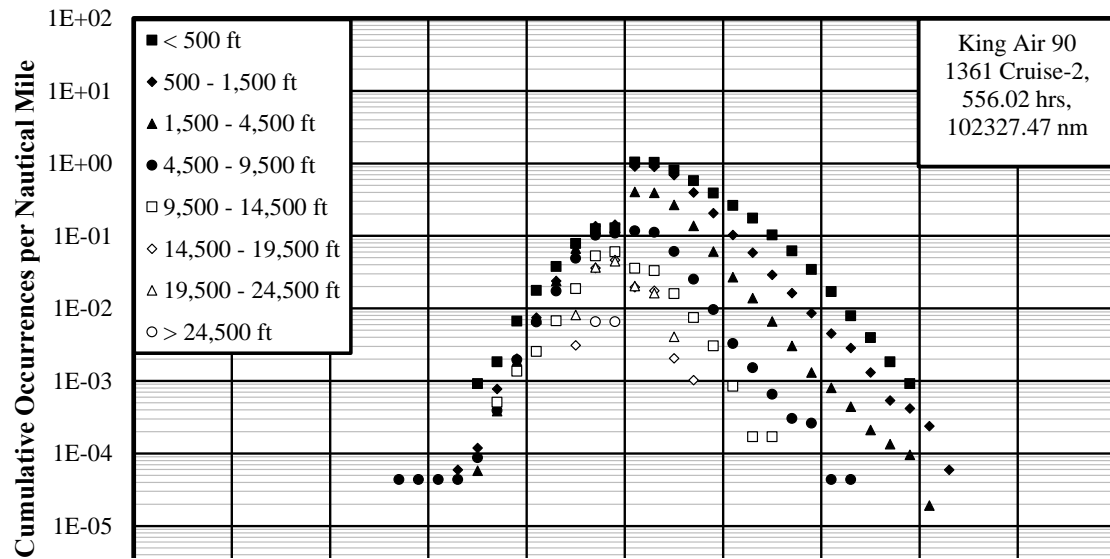


Figure 4.49: Cumulative Occurrences of Incremental Vertical Maneuver Load Factor per 1000 Hours - Entry Phase

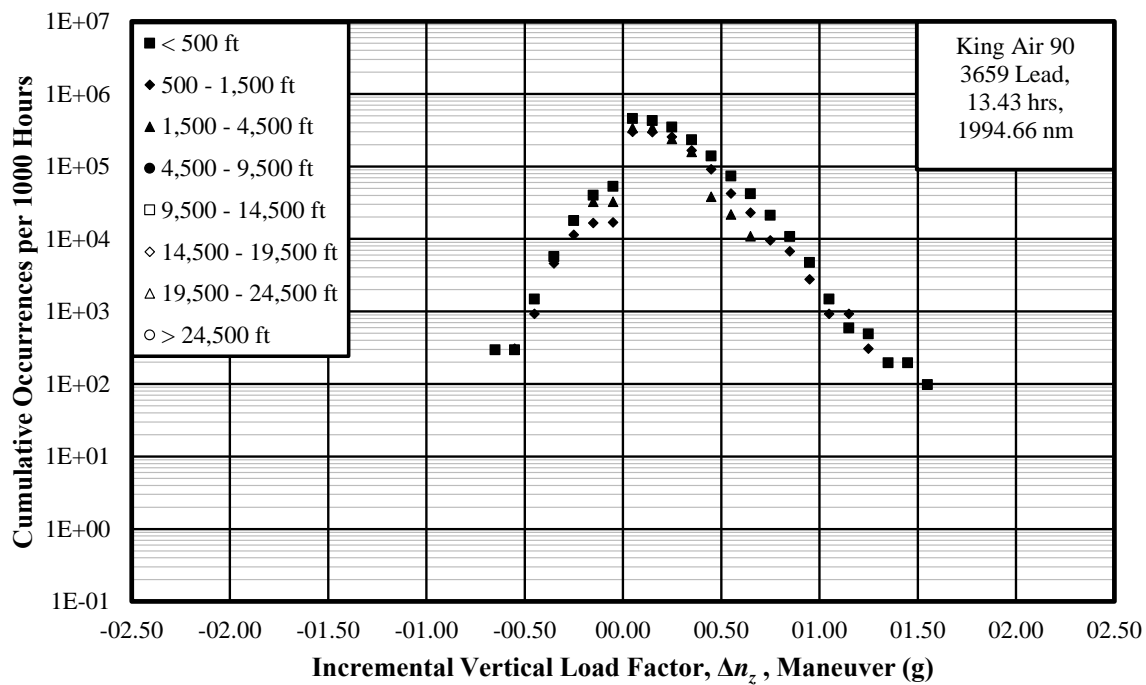
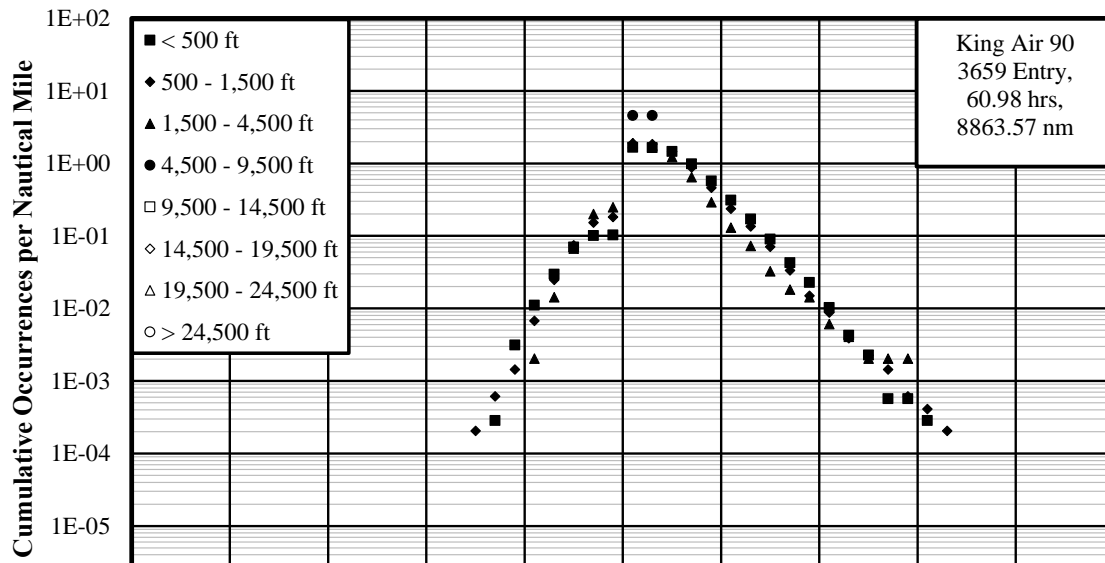


Figure 4.51: Cumulative Occurrences of Incremental Vertical Maneuver Load Factor per 1000 Hours - Lead Phase

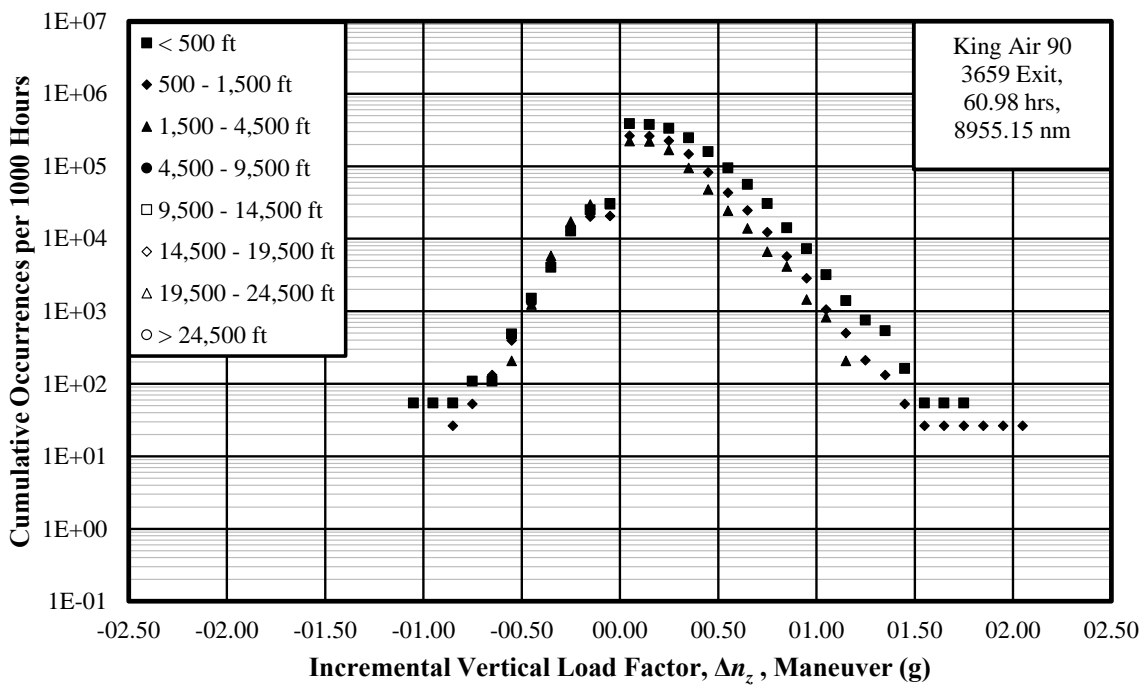
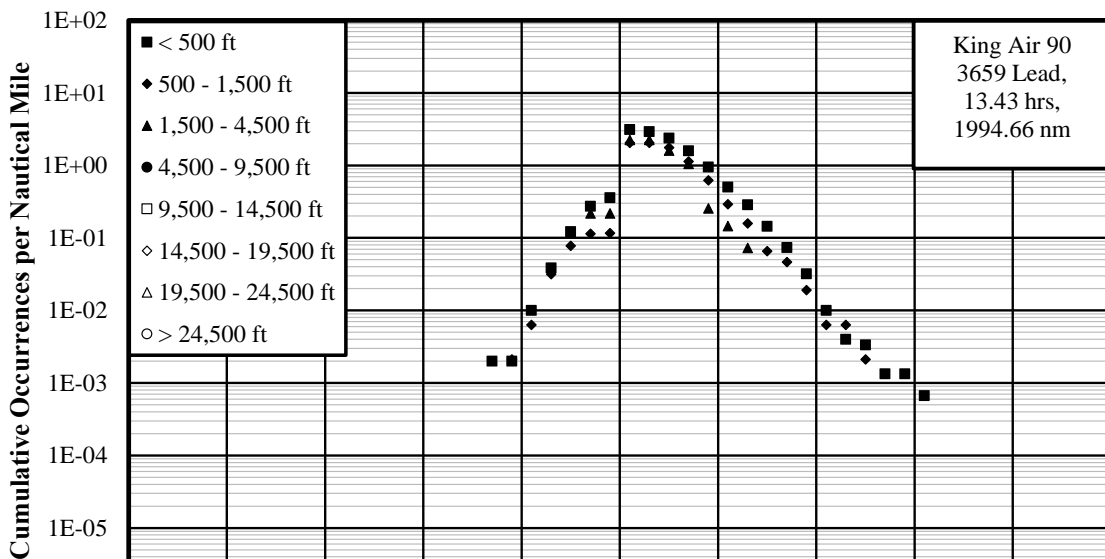


Figure 4.53: Cumulative Occurrences of Incremental Vertical Maneuver Load Factor per 1000 Hours - Exit Phase

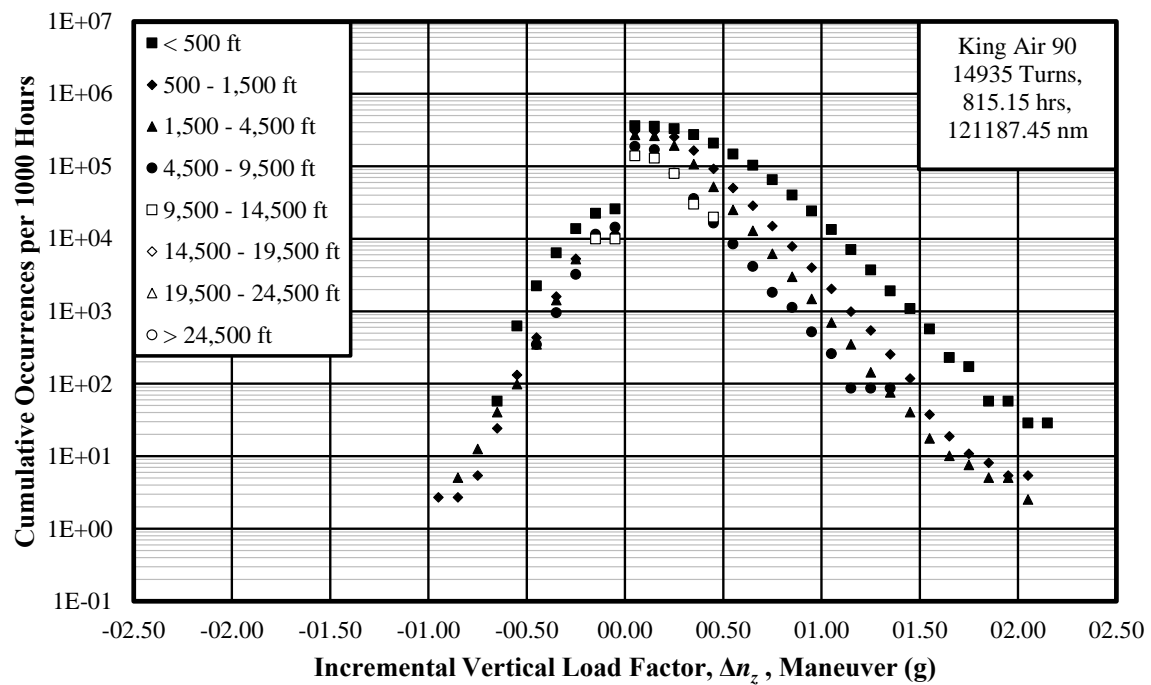
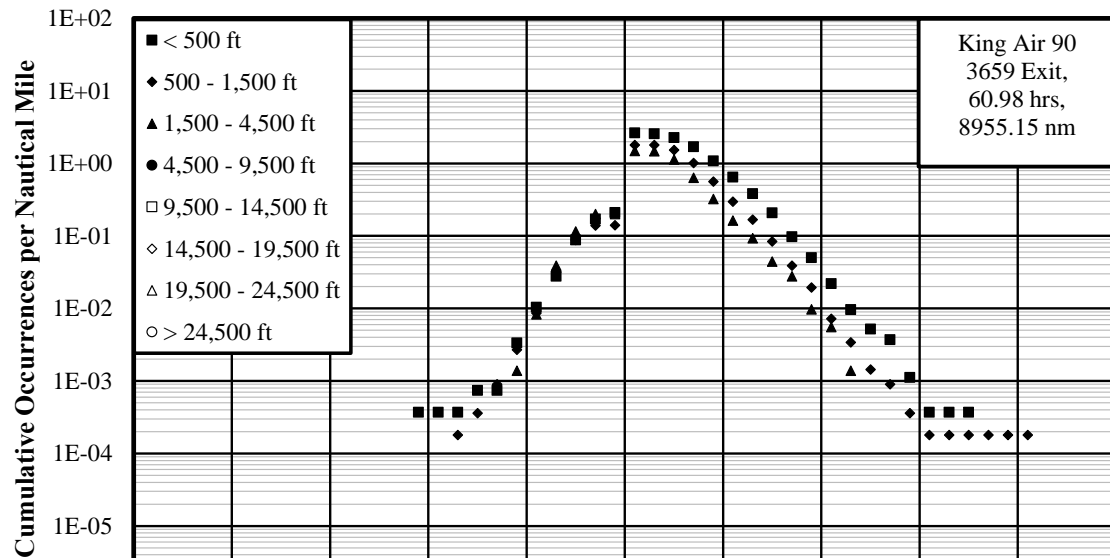


Figure 4.55: Cumulative Occurrences of Incremental Vertical Maneuver Load Factor per 1000 Hours - Turns Phase

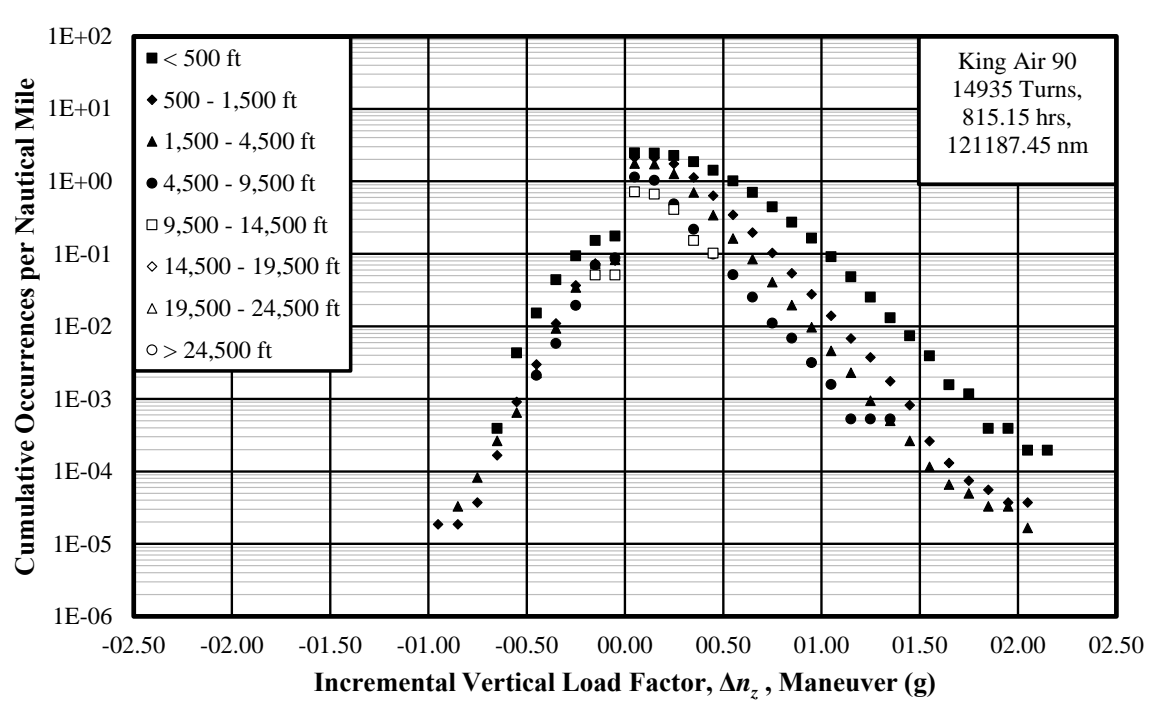


Figure 4.56: Cumulative Occurrences of Incremental Vertical Maneuver Load Factor per Nautical Mile - Turns Phase

#### 4.2.2 Discrete Gust Velocities

The cumulative occurrences of the derived gust velocity for all the altitude bands and all phases are shown in Figures 4.57 and 4.58. From these figure it can be inferred that the Entry and Exit phases had nearly identical frequencies of occurrence of gust velocities. This was expected in that both these phases are flown at comparable altitudes. The cumulative occurrence of the discrete gust velocities for the Lead phase was the highest for smaller gusts velocities whereas those of the Entry and Exit phases were higher at larger velocities.

Figures 4.59 through 4.70 are the cumulative occurrences of the derived gust velocity for each phase over individual altitude bands. The frequency of occurrence for low altitude was the highest for the entire range of gust velocities for all phases. Entry phase was an exception where the altitude band of 500-1,500 feet AGL presented the highest, but insignificant, frequency for the largest gust velocity. In no case did the gust velocity exceed a magnitude of 40 feet/second.

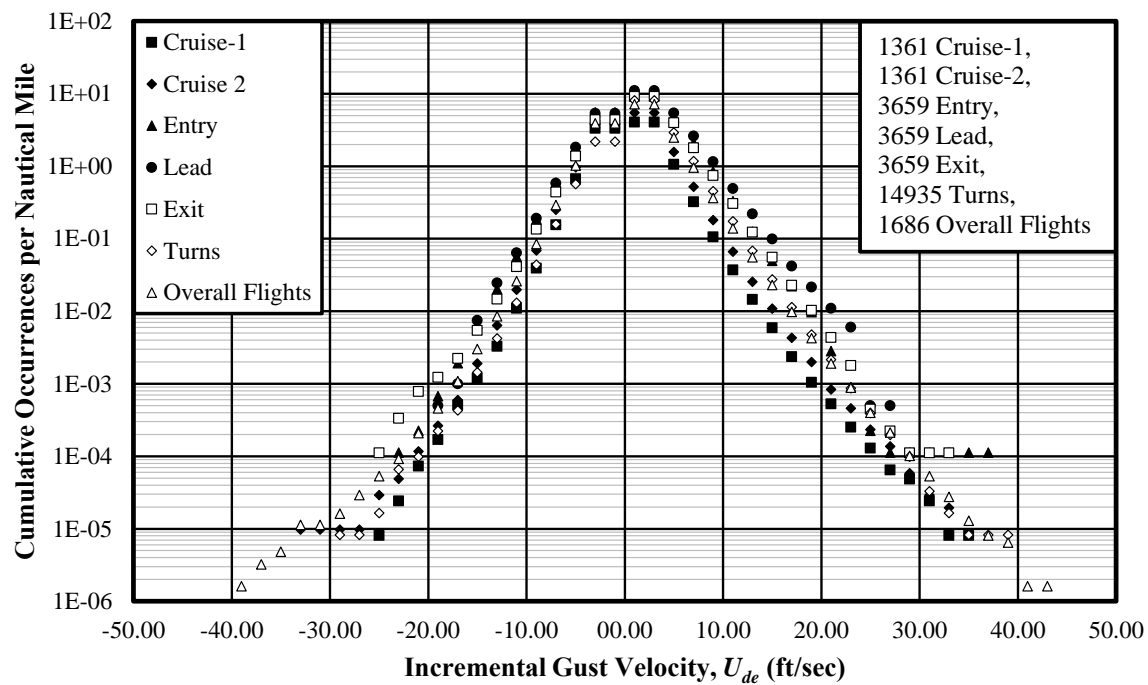
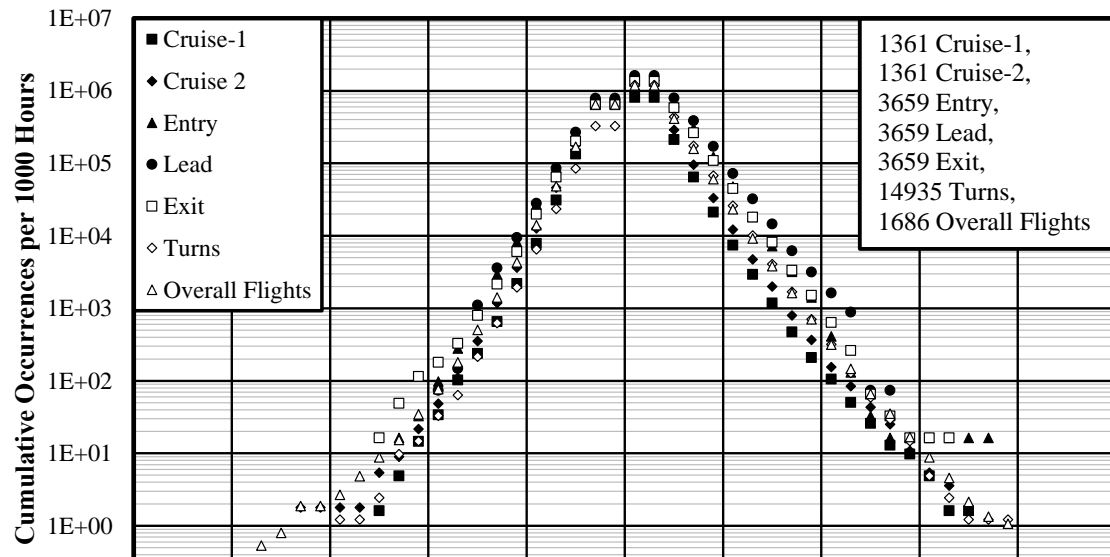


Figure 4.58: Cumulative Occurrences of Incremental Gust Velocity per Nautical Mile - All Phases

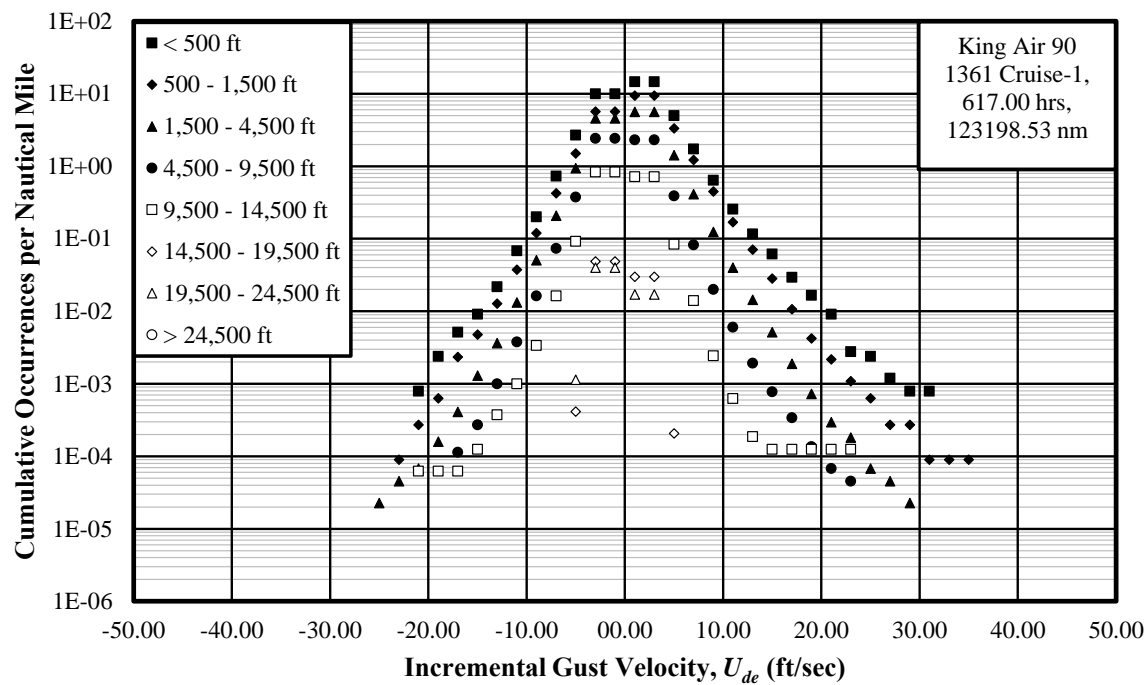
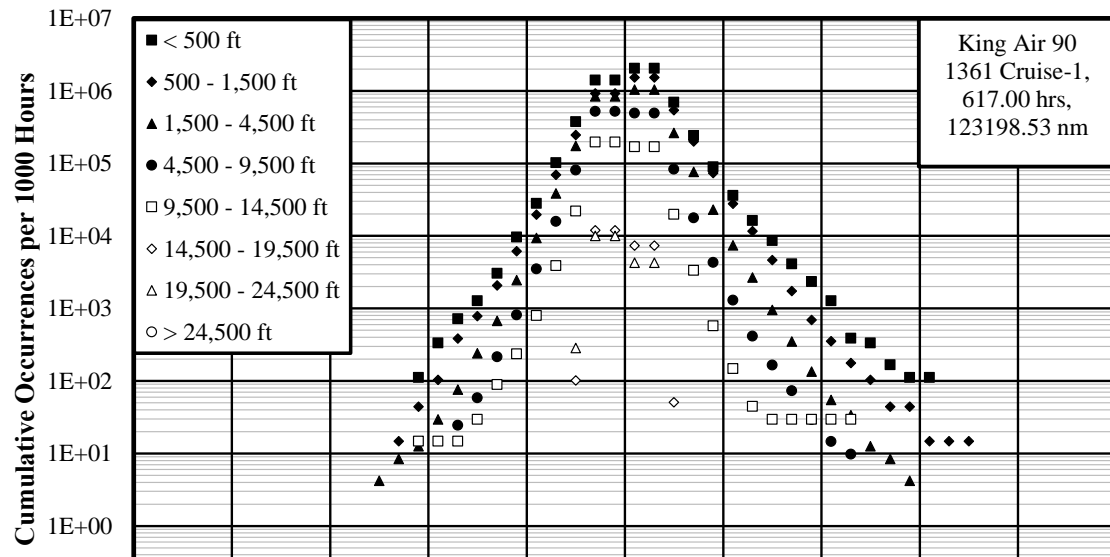


Figure 4.60: Cumulative Occurrences of Incremental Gust Velocity per Nautical Mile - Cruise-1 Phase

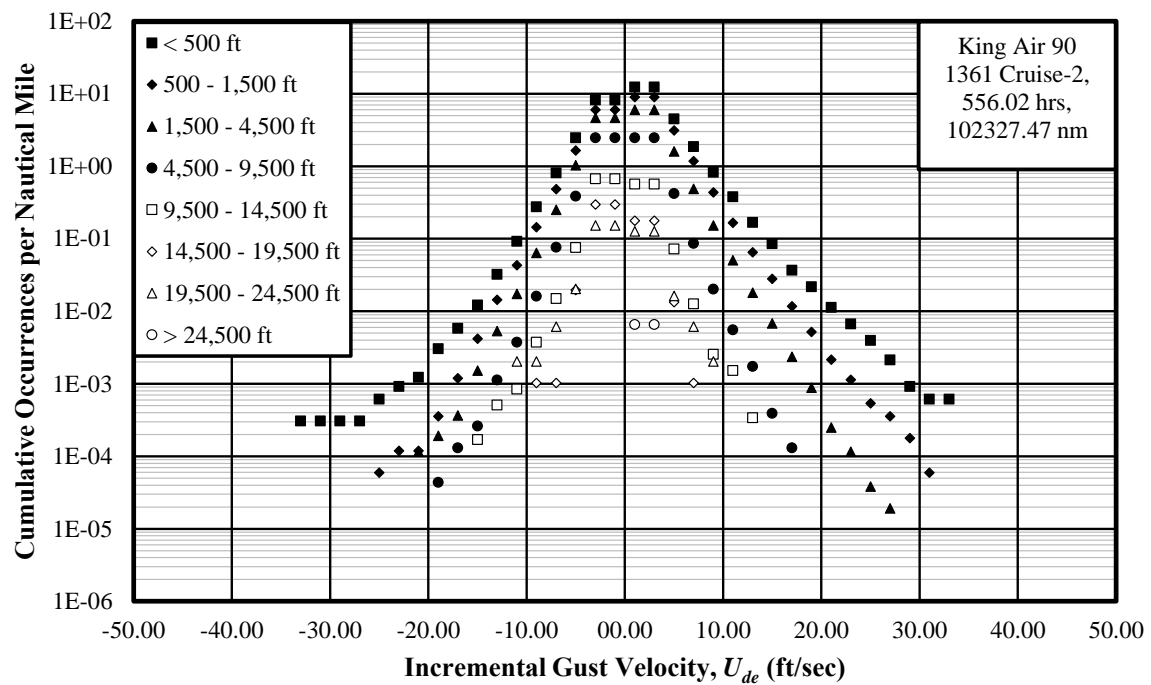
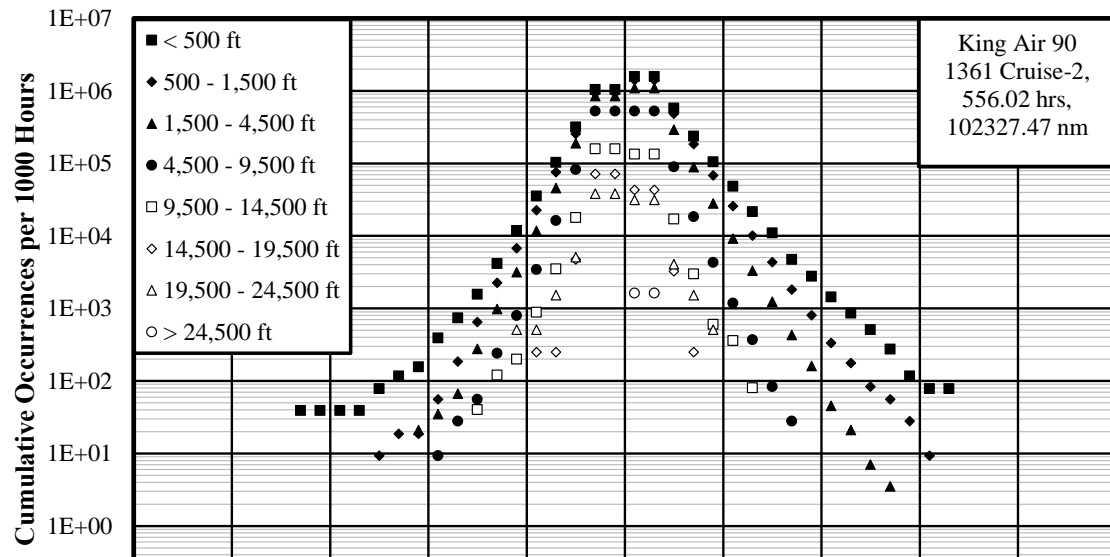


Figure 4.62: Cumulative Occurrences of Incremental Gust Velocity per Nautical Mile - Cruise-2 Phase

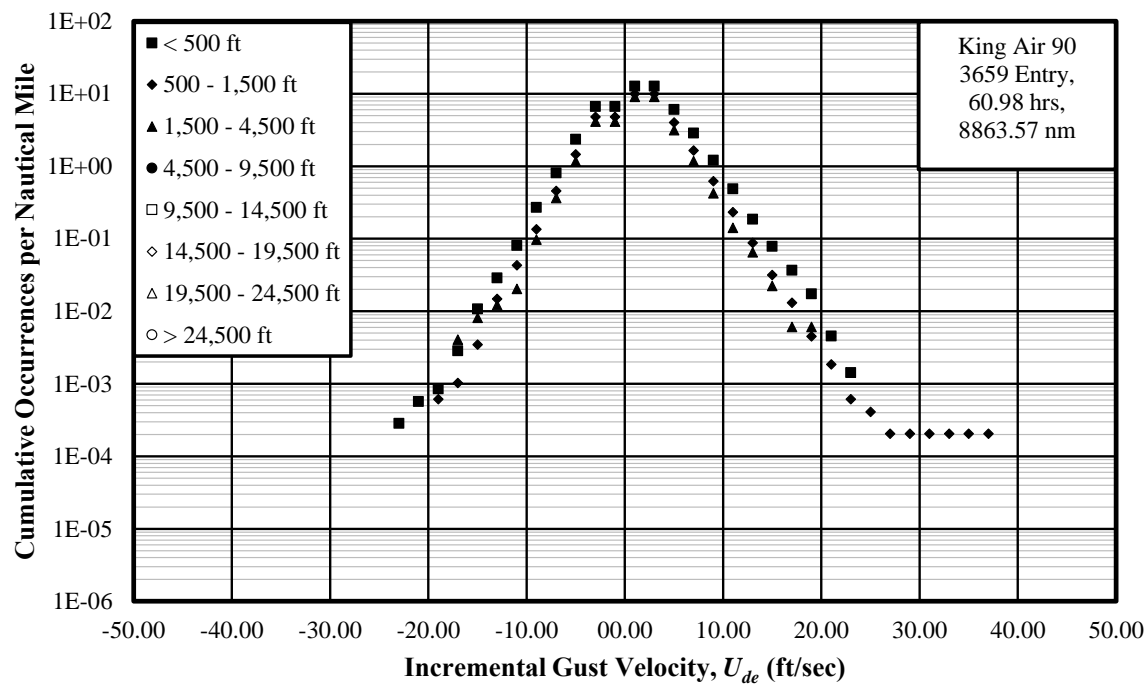
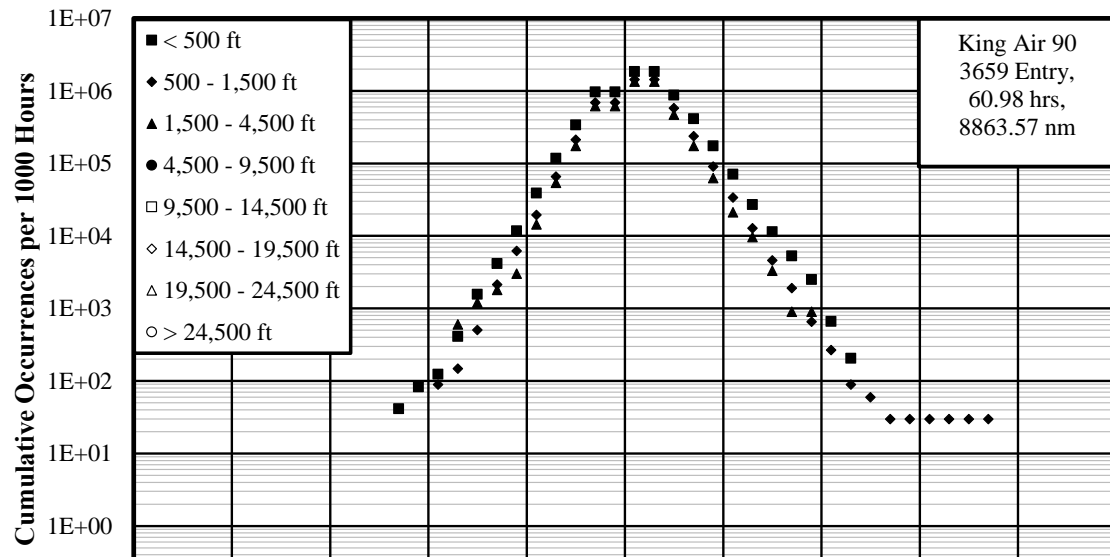


Figure 4.64: Cumulative Occurrences of Incremental Gust Velocity per Nautical Mile - Entry Phase

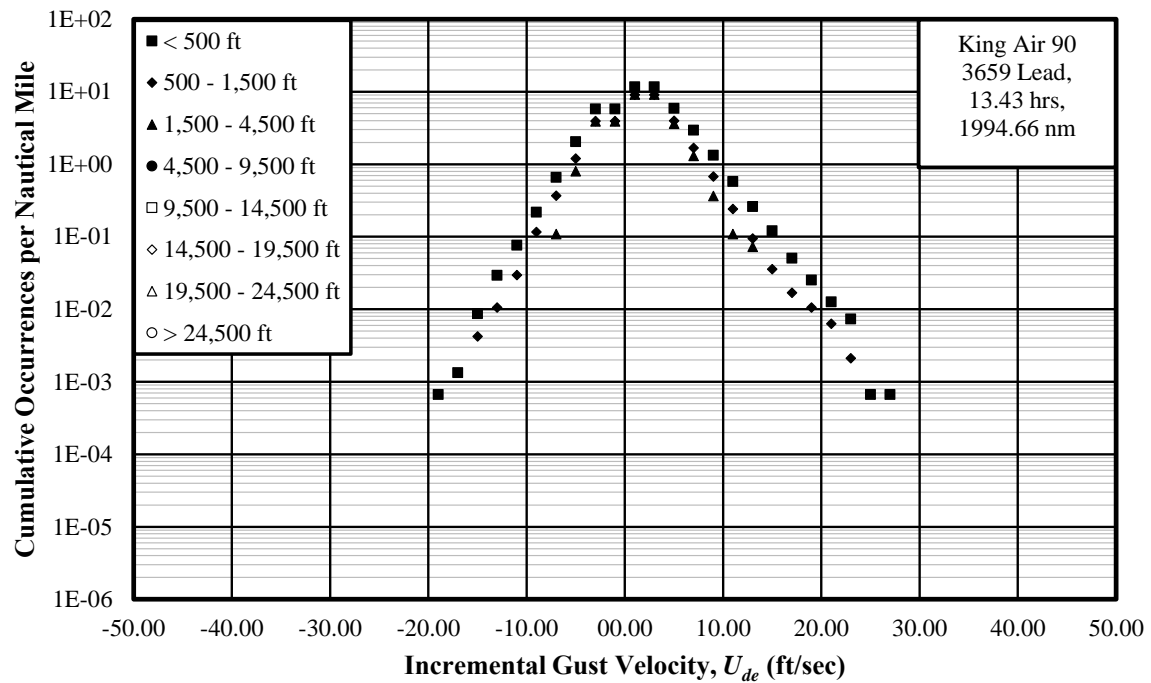
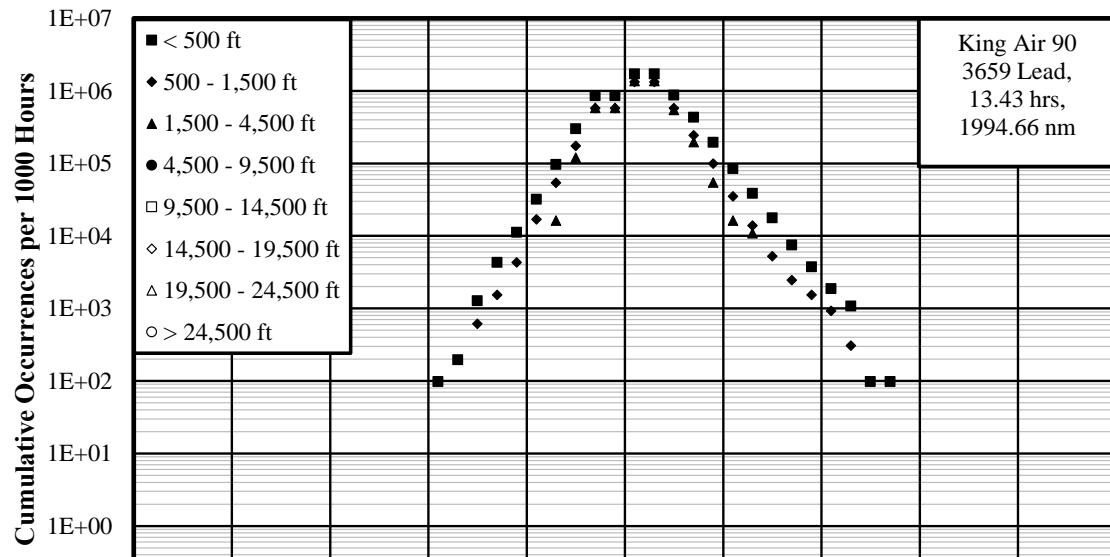


Figure 4.66: Cumulative Occurrences of Incremental Gust Velocity per Nautical Mile - Lead Phase

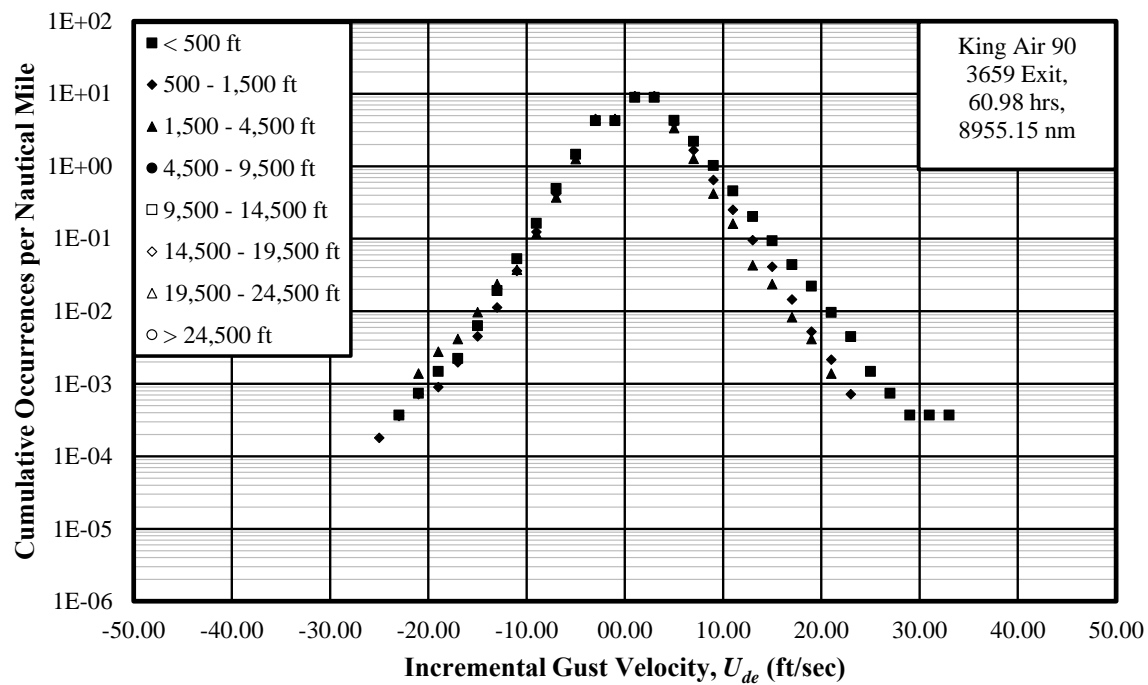
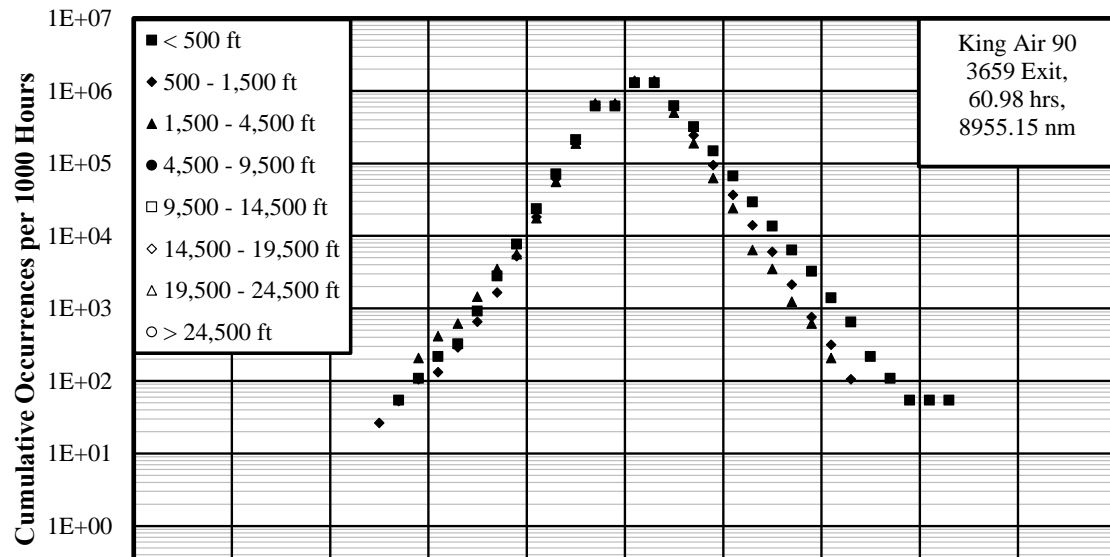


Figure 4.68: Cumulative Occurrences of Incremental Gust Velocity per Nautical Mile - Exit Phase

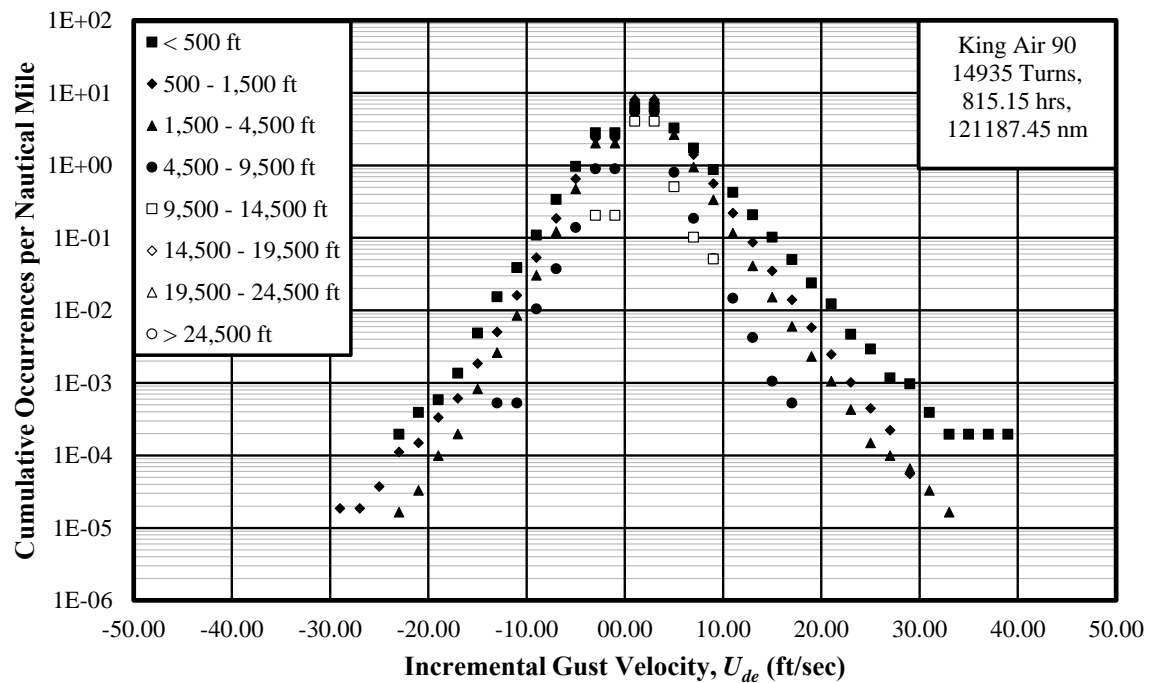
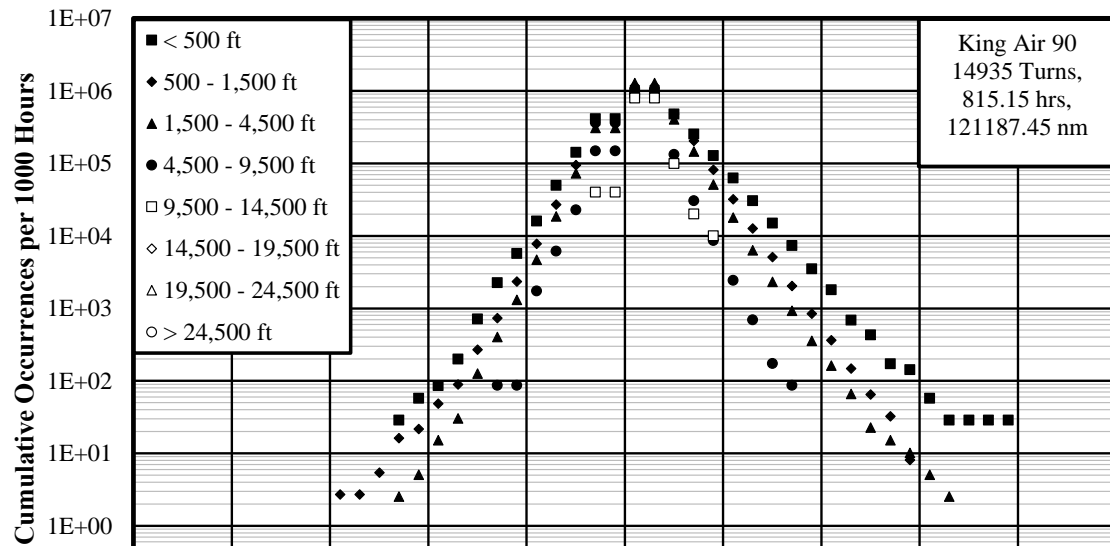


Figure 4.70: Cumulative Occurrences of Incremental Gust Velocity per Nautical Mile - Turns Phase

## CHAPTER 5

### CONCLUSION

The flight data from three Beechcraft King Air models, flown as lead planes for aerial firefighting, were used to extract the operational usage, loads and gust velocities. Since the role of these aircraft included maneuvers and flying conditions for which they were not designed, it was necessary to analyze the operational data. Of the 4074 files obtained from the USFS central depository, 3094 complete flights were identified for the 2009 through 2013 fire seasons.

These flights were categorized as Extreme Attitude, Firefighting and Ferry flights. The flights in which the aircraft were flown with roll angles in excess of 80 degrees or pitch angles of 30 degrees were classified as Extreme Attitudes, which encompassed four percent of total flights. Flights in which the aircraft was flown from one airport to another without going through Turns or Leads were classified as Ferry. Ferry flights accounted for approximately 41 percent of all flights. All other flights were called Firefighting, which was 54.5 percent of total flights.

Extreme Attitude and Firefighting flight gust loads and discrete gust velocity exceedance charts showed very close agreement over the entire range of values. As expected, there was a higher frequency of occurrence of maneuver loads at higher load factors. During Ferry flights, the aircraft was flown most of the time at AGL altitude greater than 9,500 feet. The gust and maneuver load exceedance spectra, showed significantly lower frequency of occurrence throughout the range of values.

Firefighting flights were split into Cruise-1, Cruise-2, Entry, Lead, Exit, and Turns phase. It was found that during Cruise-1 and Cruise-2 phases, aircraft were mostly flown at AGL altitudes 1,500 through 9,500 feet. Typical of the Entry, Lead, and Exit phases, the majority of the flight time was spent at AGL altitudes less than 1,500 feet. Turn phase consisted of the aircraft making repetitive turns at AGL altitude between 500 and 4,500 feet.

The highest occurrences of gust and maneuver loads were during the Lead phase followed by the Exit and Entry phases. At larger vertical load factors, the frequency of occurrence was the highest for the Turn phase and were associated with low altitude turns conducted at AGL altitude less than 500 feet. In these altitudes, the frequencies of occurrence were more than an order of magnitude larger than the next higher altitude band. The discrete gust velocity exceedance charts for individual phases revealed similar results as those from the gust loads. The largest frequency of occurrence belonged to the Lead, followed by Exit and Entry phases.

The goal of the analysis was to understand the severity of the loads experienced by these aircraft during the demanding ASM/Lead missions.

## BIBLIOGRAPHY

## BIBLIOGRAPHY

- [1] Moore, J. "Simulated attack - Firefighting pilots sharpen skills in simulaiton," [online]. 2014. URL: <http://www.aopa.org/News-and-Video/All-News/2014/September/03/Simulated-attack> [cited 5 January 2015].
- [2] Jewel, Jr, J. W., Morris, G. J., and Avery, D. E., "Operating Experiences of Retardant Bombers During Firefighting Operations," Technical Memorandum NASA TM-X-72622, NASA, Langley Research Center, Hampton VA 23681-2199, USA, 1974.
- [3] George, C., "An update on the Operational Retardant Effectiveness (ORE) program. In The Art and Science of Fire Management," Proceedings of the First Interior West Fire Council Annual Meeting and Workshop, 1988, pp. 24–27.
- [4] Blue Ribbon Panel, "Federal Aerial Firefighting: Assessing Safety and Effectiveness," Report, U.S. Dept. of Agriculture, Forest Service, U.S. Dept. of the Interior, Bureau of Land Management, Dec. 2002.
- [5] Press, H., Meadows, M. T., and Hadlock, I., "A Reeevaluaion of Data on Atmospheric Turbulence and Airplane Gust Loads for Application in Spectral Calculations," Technical Report NACA-TR-1272, NACA, Langley Aeronautical Lab, Langley Field, VA, 1956.
- [6] Press, H., Meadows, M. T., and Hadlock, I., "Estimates of Probability Distribution of Root-Mean-Square Gust Velocity of Atmospheric Turbulence from Operational Gust-Load Data by Random-Process Theory," Technical Notes NACA-TN-3362, NACA, Langley Aeronautical Lab, Langley Field, VA, 1955.
- [7] Barnes, T. J., "The FAA Operational Loads Monitoring Program - Achievements and Problems," *22nd Congress of International Council of the Aeronautical Sciences*, Paper ICAS 2000-4.3.3, Harrogate, UK, 2000.
- [8] Rustenburg, J. W., Skinn, D. A., and Tipps, D. O., "An Evaluation of Methods to Separate Maneuver and Gust Load Factors From Measured Acceleration Time Histories," FAA Report DOT/FAA/AR-99/14, University of Dayton Research Institute, Dayton, OH, 1999.
- [9] Beechcraft, *Beechcraft King Air C90B (Model C90A) POH/AFM*, Raytheon Aircraft Company, 2002.
- [10] Beechcraft, *Beechcraft King Air C90GT POH/AFM*, Raytheon Aircraft Company, 2007.
- [11] Beechcraft, *Beechcraft King Air E90 Pilot's Operating Manual*, Raytheon Aircraft Company, 1977.
- [12] Evans, G., "National Elevation Dataset - Release Notes," USGS, EROS Center, Feb. 2014.

- [13] Rustenburg, J. W., Skinn, D. A., Tipps, D. O., and Jones, T., “Statistical Loads Data for the Embraer-145XR Aircraft in Commercial Operations,” FAA Report DOT/FAA/AR-07/61, University of Dayton Research Institute, Dayton, OH, Nov. 2007.
- [14] National Wildfire Coordinating Group, *Interagency Aerial Supervision Guide*, PMS 505, NWCG National Interagency Aviation Committee, Jan. 2014, p. 90.
- [15] Gesch, D. B. and Oimoen Michael J, Evans, G. A., “Gesch, D.B., Oimoen, M.J., and Evans, G.A., 2014, Accuracy assessment of the U.S. Geological Survey National Elevation Dataset, and comparison with other large-area elevation datasets - SRTM and ASTER,” 2014, pp. 5.

## APPENDICES

## APPENDIX A

### NATIONAL ELEVATION DATASET

Table A.1 [15] shows the vertical accuracy of the control points across the United States. The errors are given in meters. The largest root mean square error was 2.57 meters (8.4 feet) for Barren Land and the lowest was 1.02 meters (3.34 feet) for Cultivated Crops. This suggests that the largest vertical error in the AGL altitude obtained from NED would be 8.4 feet.

Table A.1: National Elevation Dataset (NED) absolute vertical accuracy for the conterminous United States as measured against reference geodetic control points

Land cover class	Number of reference points	Minimum	Maximum	Mean	Standard deviation	RMSE
Developed, Open Space	8,247	-24.64	15.57	-0.15	1.31	1.32
Developed, Low Intensity	6,680	-14.91	13.92	-0.27	1.48	1.5
Developed, Medium Intensity	3,081	-15.12	7.88	-0.54	1.8	1.88
Developed, High Intensity	695	-21.43	6.62	-0.79	2.32	2.45
Barren Land	246	-19.88	7.79	-0.86	2.42	2.57
Deciduous Forest	356	-11.8	3.57	-0.33	1.48	1.52
Evergreen Forest	197	-13.09	5.17	-0.62	2.22	2.3
Mixed Forest	83	-9.82	3.66	-0.88	2.2	2.36
Shrub/Scrub	878	-17.84	8.87	-0.51	2.17	2.22
Grassland/ Herbaceous	856	-11.82	7.34	-0.33	1.55	1.58
Pasture/Hay	1,295	-8.82	5.77	-0.18	1.18	1.19
Cultivated Crops	1,889	-11.48	5.77	-0.14	1.01	1.02
Woody Wetlands	414	-15.68	8.91	-0.42	1.59	1.64
Emergent Herbaceous Wetlands	393	-10.1	3.17	-0.51	1.5	1.59
All	25,310	-24.64	15.57	-0.29	1.52	1.55

Figure A.1 [12] shows the available resolutions and their coverage area as of February 2014. It is evident that the availability of 1/9-arc-second data is sparse but the 1/3-arc-second data is available for the majority of the United States. There are also very small regions within the United States where the best resolution available is just 1-arc-second.

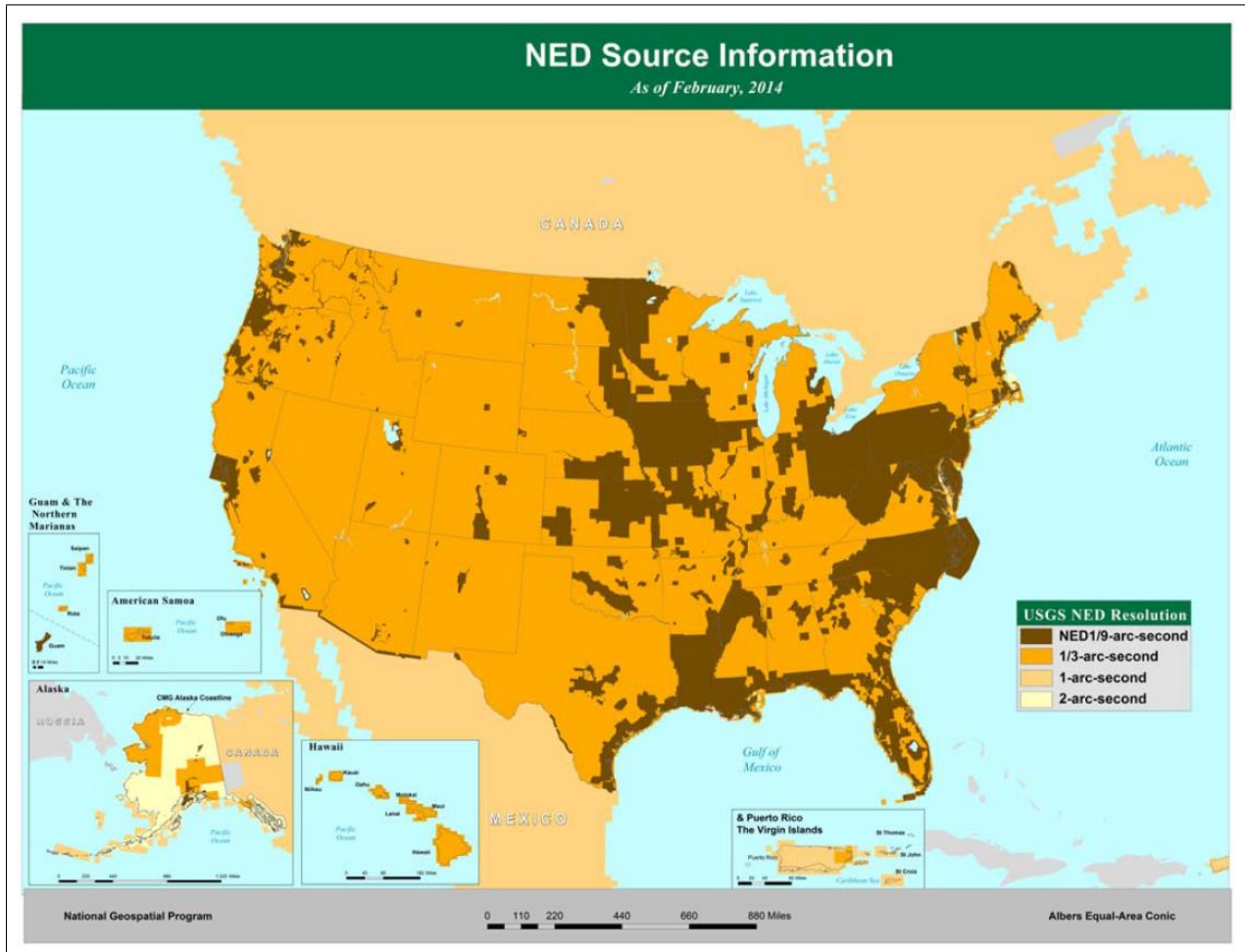


Figure A.1: Composite of source data by resolution - February, 2014